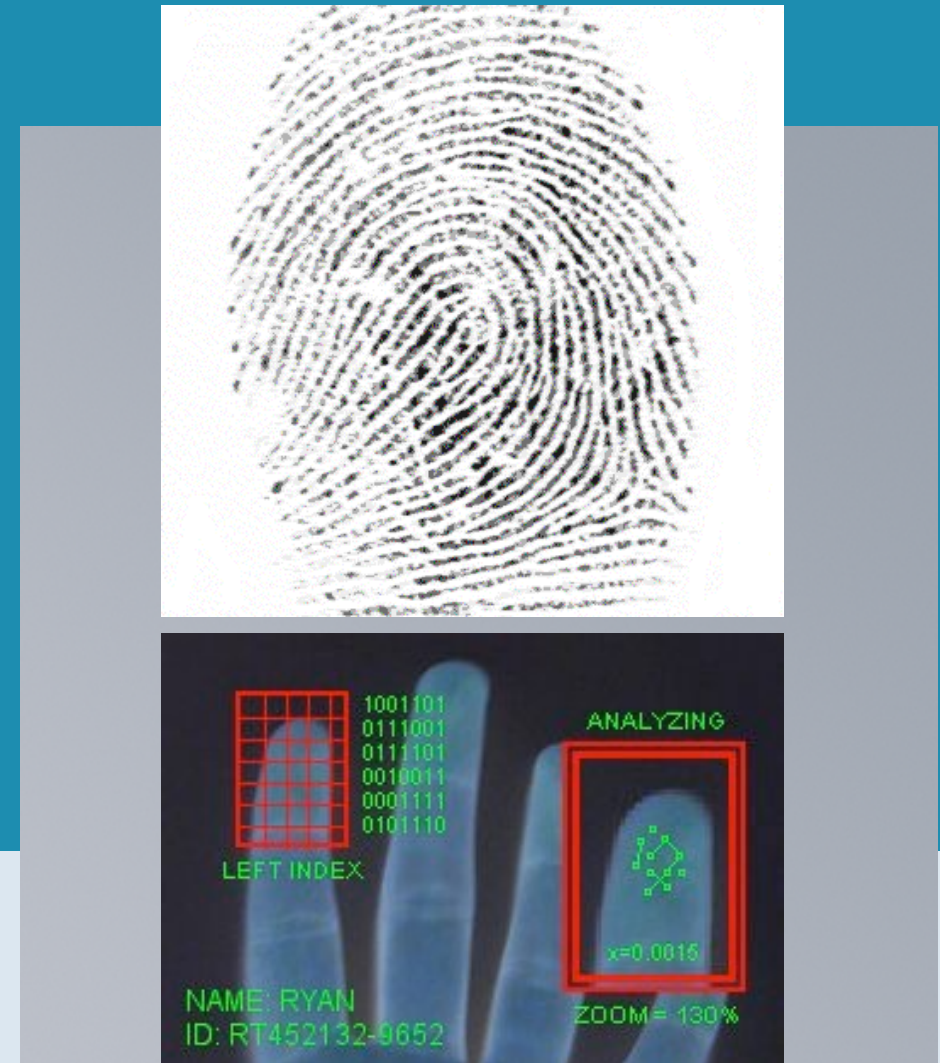


Fingerprint Recognition



Definition

Biometrics: identifying/authenticating an individual in an automated, reliable and fast way using unique physiological or behavioral characteristics

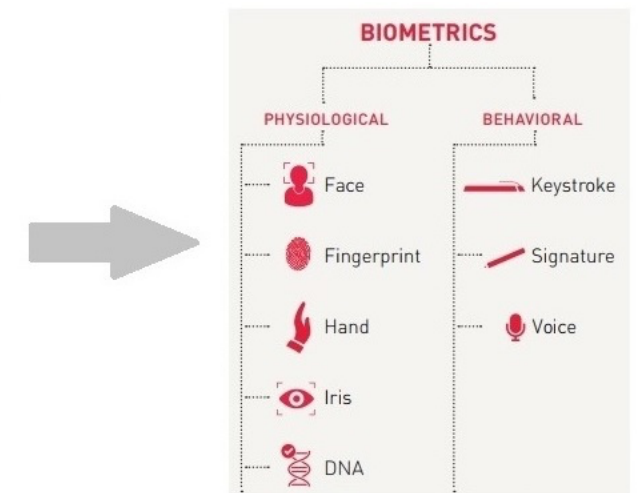
Physiological: static

morphometric (shape): face

biological: DNA

Behavioral: dynamic

the way we walk, speak, write



Biometrics Syllabus

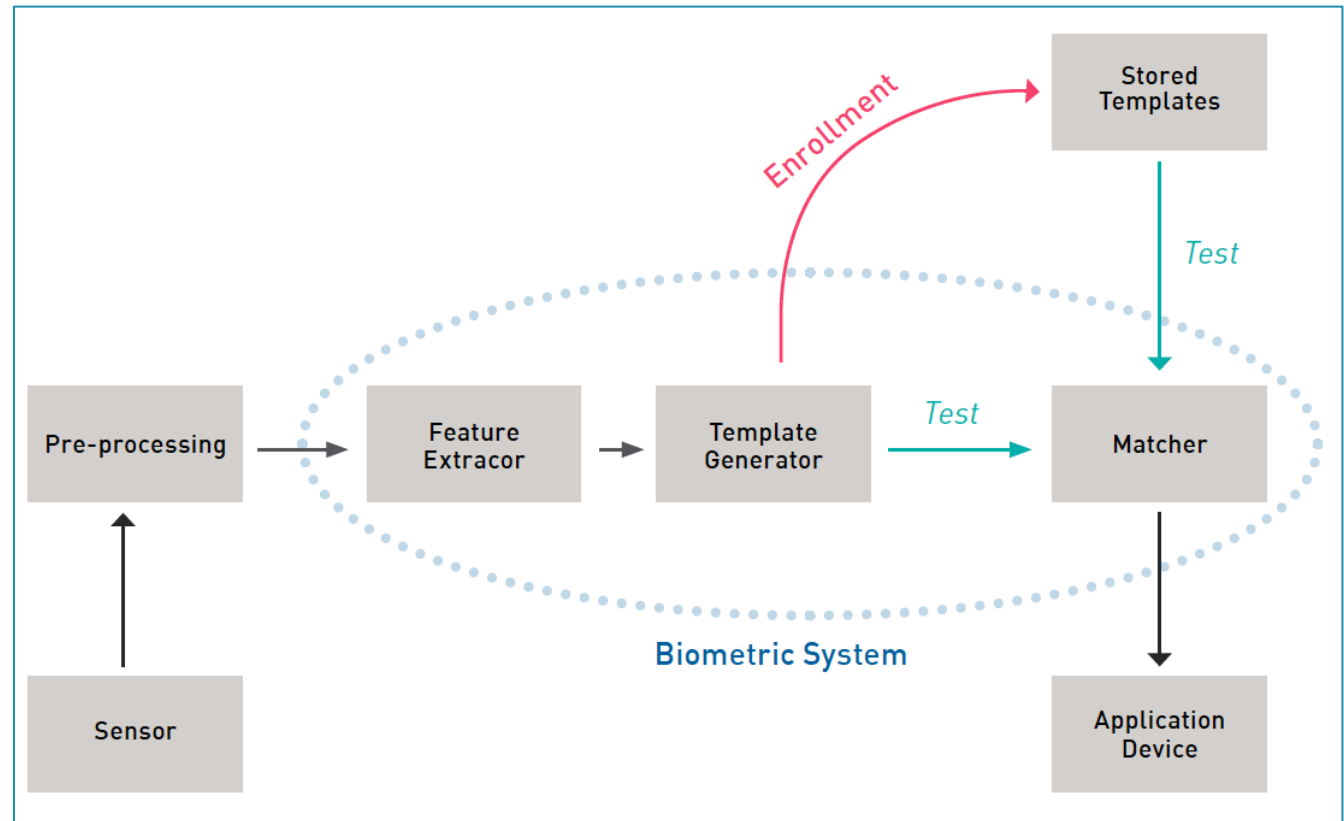
PART I BACKGROUND

- Introduction
- Basic pattern recognition aspects

Part II APPLICATIONS

- **fingerprints**
- **facial recognition**
- **iris scanning**
- retina scanning
- hand geometry
- voice verification
- signature verification
- Others (ear biometrics)
- Multi-modal biometrics

Part III Implementation and security issues



Fingerprint: what



- Fingerprint = pattern of flow-like ridges and valleys on the surface of a fingertip
- Fingerprint shape is determined during fetal period, depending on the initial conditions of the embryonic mesoderm.
- Fingerprints of identical twins are different
- No (detail) correlation between prints of different fingers of the same individual

Ancient fingerprints

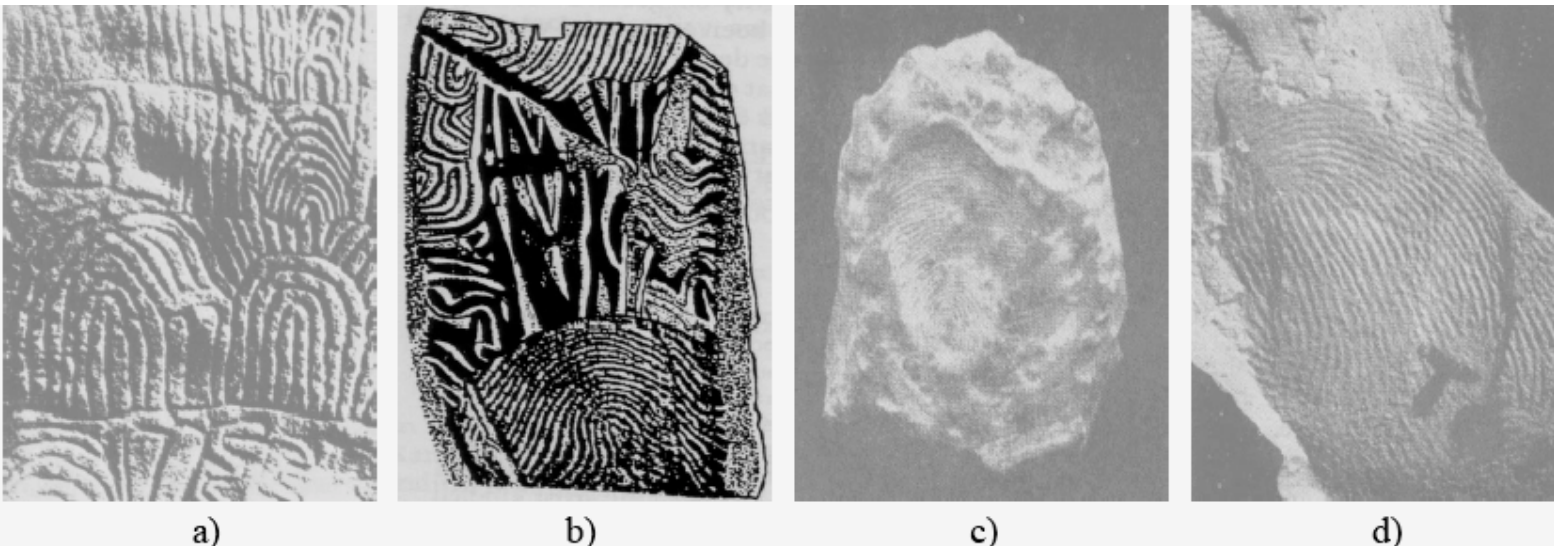


Figure 1.8. Examples of archaeological fingerprint carvings and historic fingerprint impressions: a) Neolithic carvings (Gavrinis Island) (Moenssens, 1971); b) standing stone (Goat Island, 2000 B.C.) (Lee and Gaensslen, 2001); c) a Chinese clay seal (300 B.C.) (Lee and Gaensslen, 2001); d) an impression on a Palestinian lamp (400 A.D.) (Moenssens, 1971). Although impressions on the Neolithic carvings and the Goat Island standing stones might not be used to indicate identity, there is sufficient evidence to suggest that the Chinese clay seal and impressions on the Palestinian lamp were used to indicate the identity of the providers. Figures courtesy of A. Moenssens, R. Gaensslen, and J. Berry.

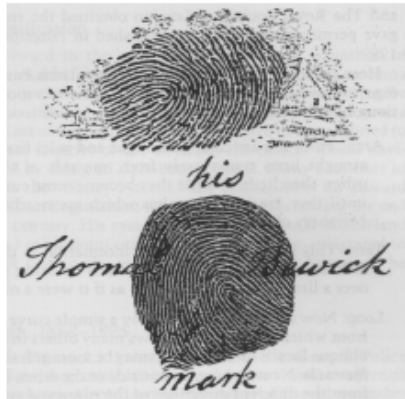
Scientific Fingerprint studies



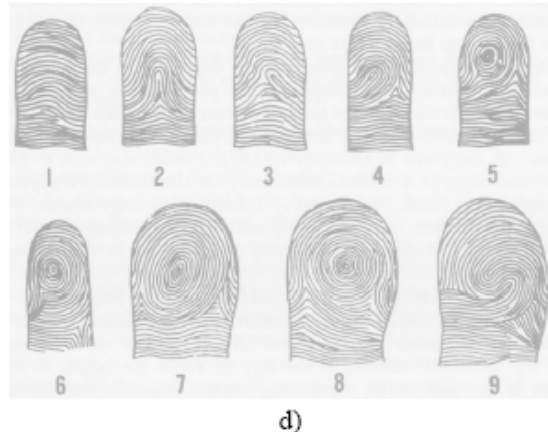
a)



b)



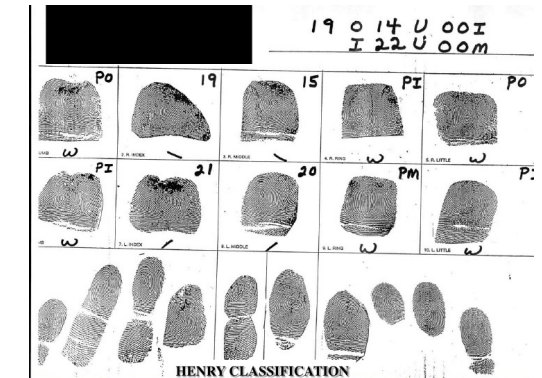
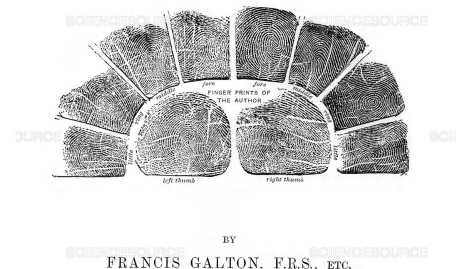
c)



d)

- a. Dermatoglyphics drawn by Grew (1684);
- b. Mayer's drawings of fingerprints (1788);
- c. Trademark of Thomas Bewick (1806);
- d. The nine patterns illustrated in Purkinje's thesis (1823);
- e. Sir Francis **Galton**: minutiae (1892);
- f. Edward Henry: **Henry** classification (1899)

FINGER PRINTS



Fingerprint characteristics

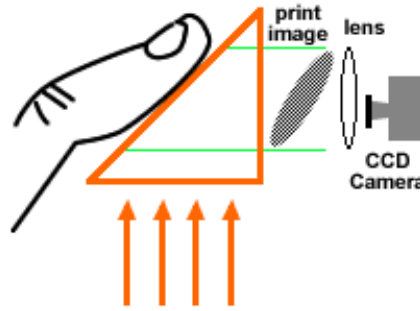
- The first legally accepted, readily automated and mature biometric technique
- Most understood and studied biometric
- Used for a long time : identification studies started late 19th century (FBI 1924: 810K FP cards)
- Validity well-established ((FBI, 1995): 200 million FP cards (10 fingers))
- Daily requests (10K/day) for FPR necessitate automation
- AFIS (Automatic Fingerprint Identification Systems) installed (since 1960s) in law enforcing agencies worldwide, continued to IAFIS (Integrated AFIS) maintained by FBI
- The success of AFIS led to incorporation in civilian applications
- With solid state sensors => incorporation in many applications
- Acceptability? Because of association with criminal investigations

Fingerprint Recognition System

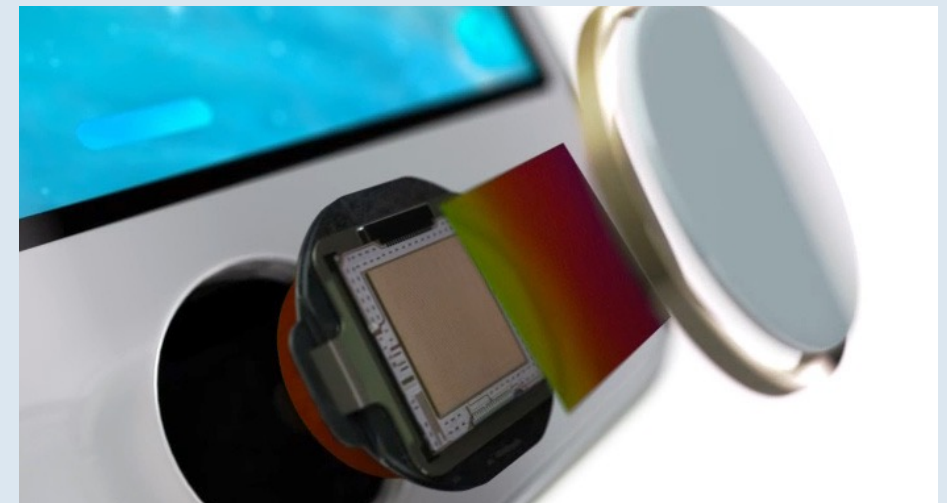


Overall Design of Fingerprint Recognition Systems

- Acquisition
- Enhancement
- Representation/feature extraction
- Feature matching



Fingerprint Acquisition



Acquisition of Fingerprints

- Inked fingerprints (off-line).
 - Impression of inked finger on paper.
 - Image scanned (using flat bed scanner).
 - Cumbersome.
 - Infeasible and socially unacceptable for identity verification.
- Latent fingerprints on crime scenes.
- Live scan (ink-less).
 - Image directly obtained without paper impression.



Fingerprint Examples



a)



b)



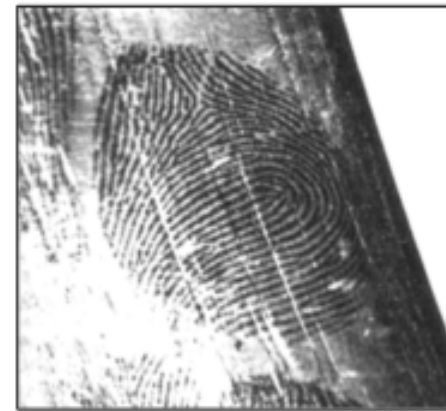
c)



d)



e)



f)

- a. Live-scan optical scanner
- b. Live-scan capacitive scanner
- c. Live-scan piezoelectric scanner
- d. Live-scan thermal scanner
- e. Off-line (rolled) inked impression
- f. Latent fingerprint

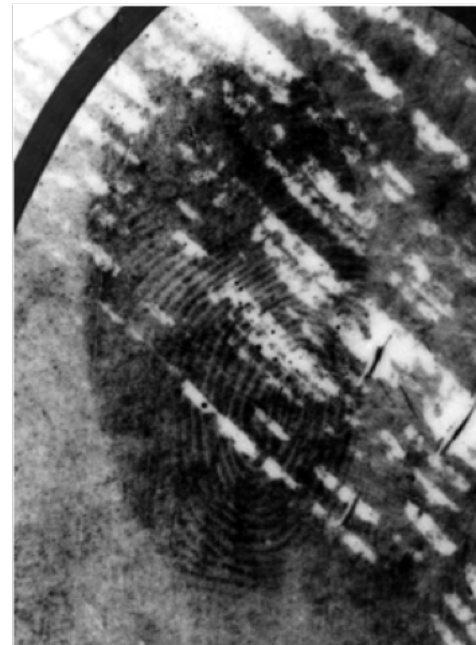
Same finger, different FP



(a)



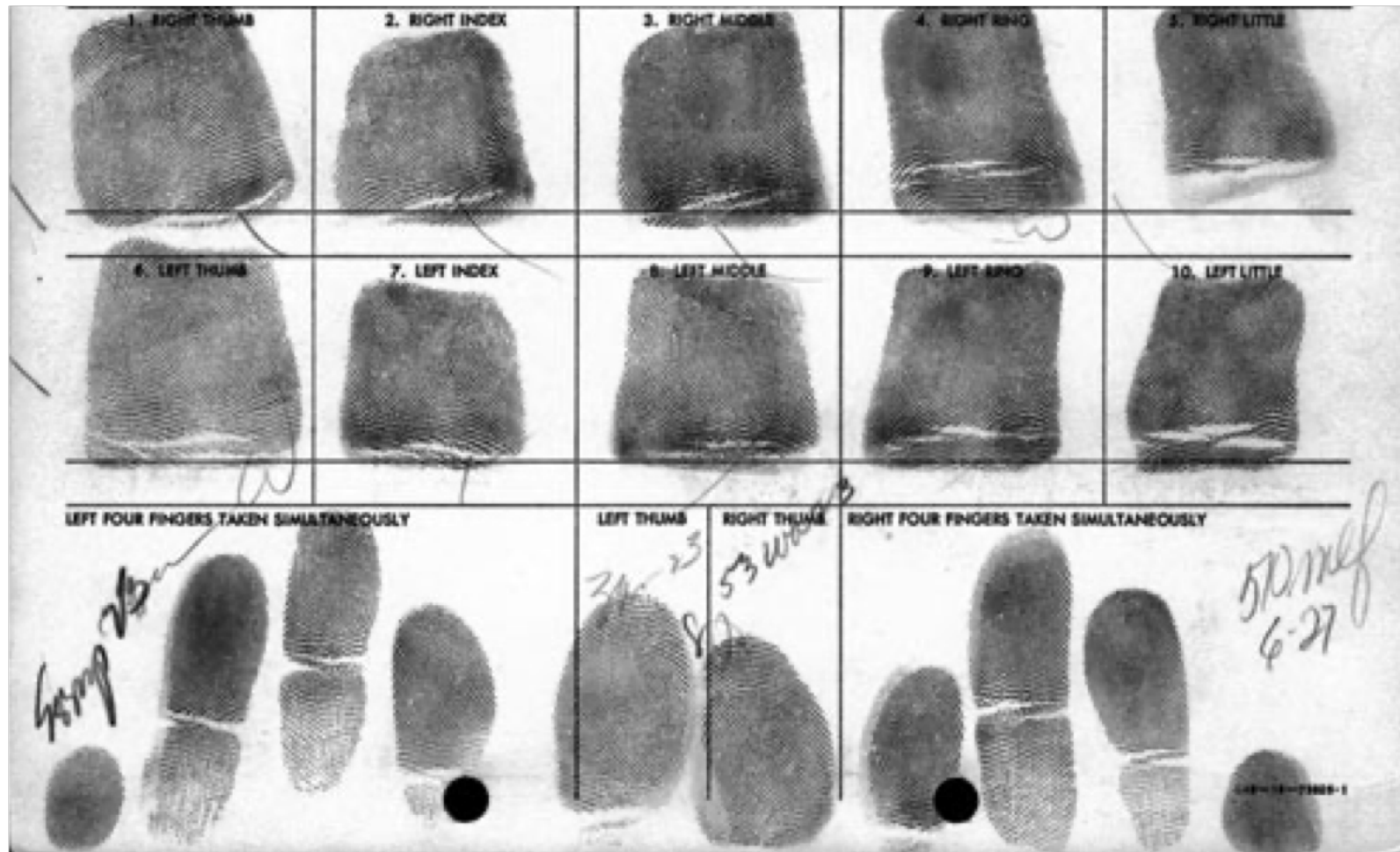
(b)



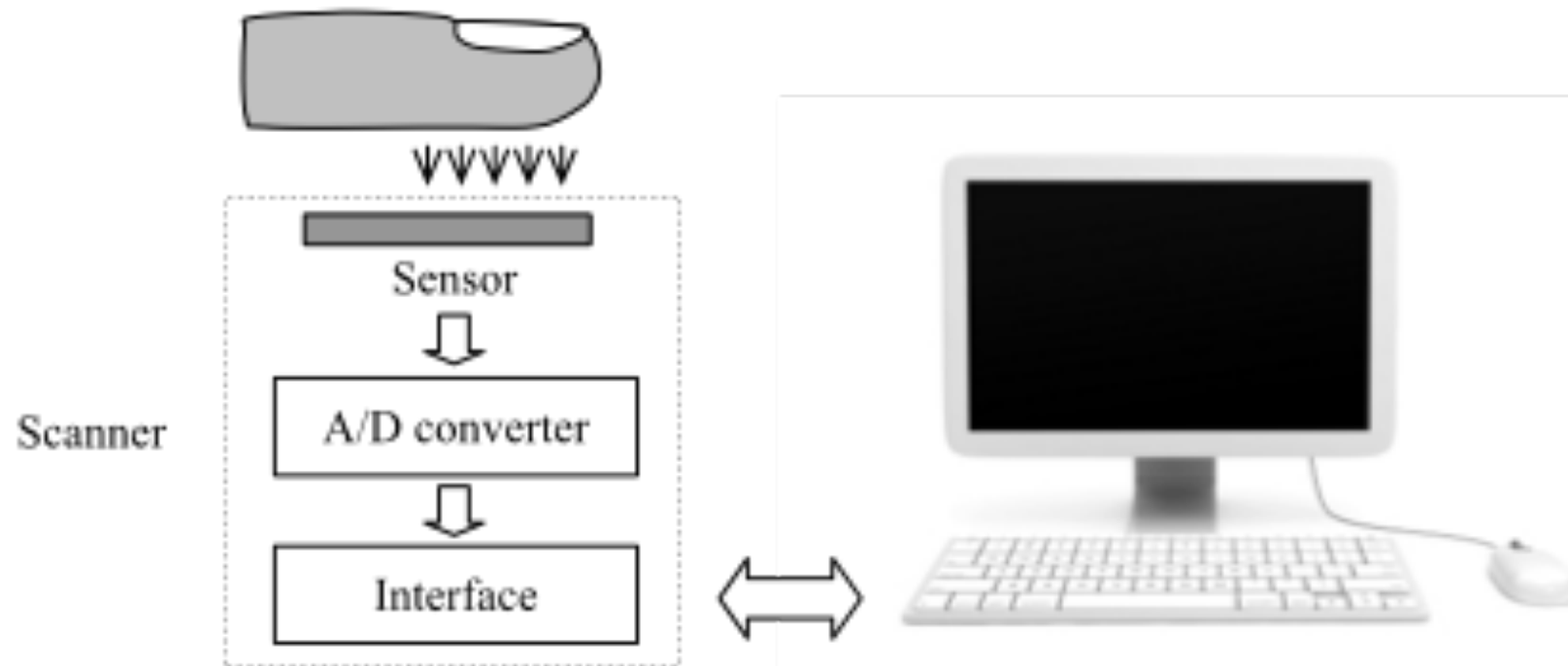
(c)

Fig. 2.3 Three different fingerprint impressions of the same finger. (a) Rolled fingerprint, (b) plain fingerprint, and (c) latent fingerprint.

Inked fingerprints



General structure of FP live-scan device



Multi-finger and single-finger acquisition

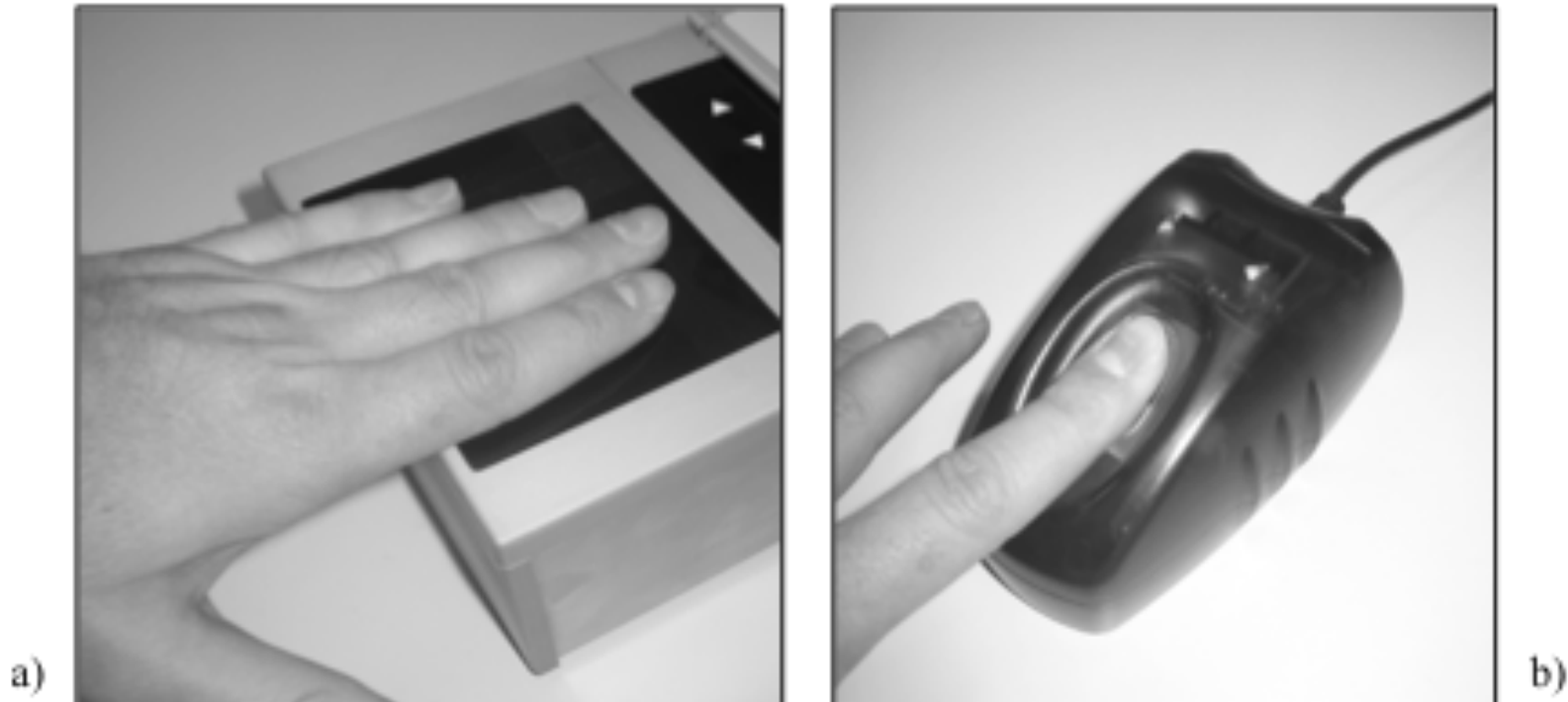


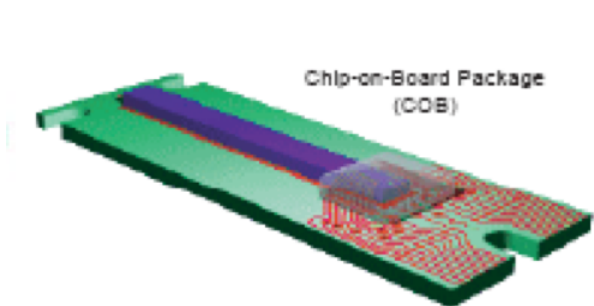
Figure 2.2. Fingerprint scanners. a) simultaneous acquisition of four fingers through a multi-finger scanner; b) acquisition with a single-finger scanner.

Rolled versus dab



Figure 2.3. The same finger acquired as a plain impression (on the left) and as a rolled impression (on the right): the portion of the rolled fingerprint corresponding to the plain fingerprint is highlighted.

Sweeping



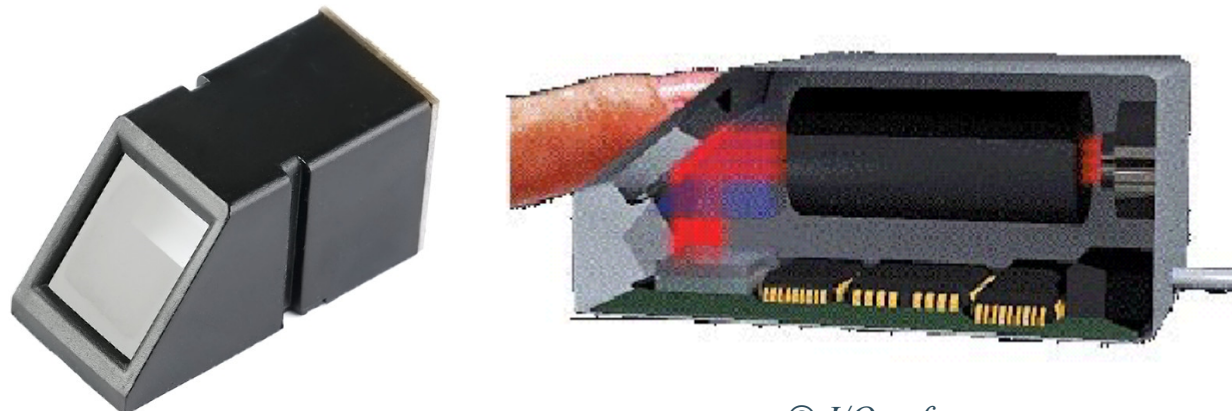
Atmel Corp.



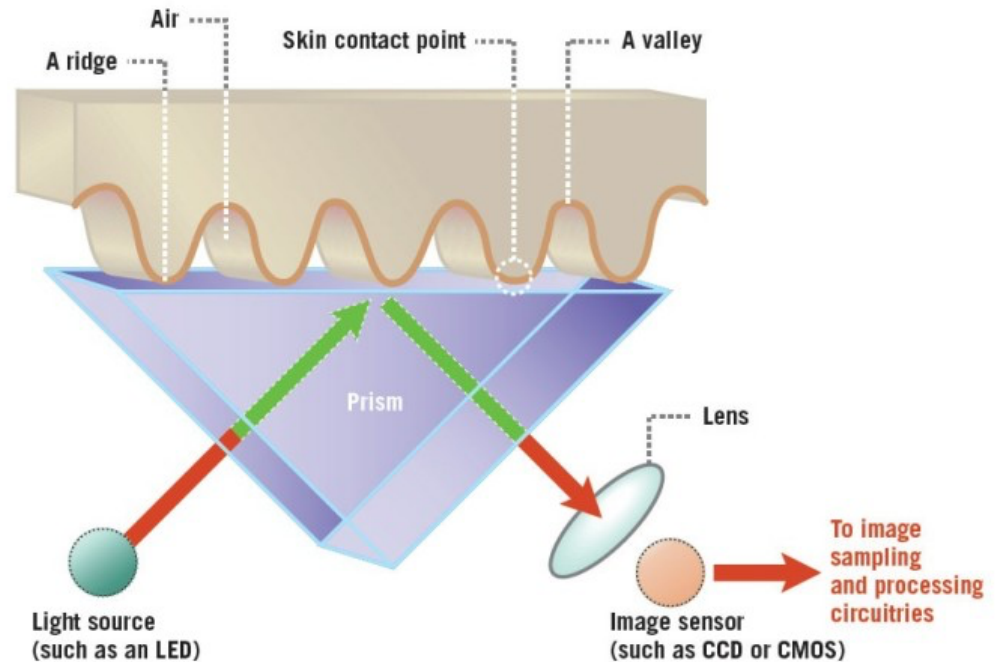
Fig. 2 Fingerprint reconstruction from a sweep sensor: some consecutive frames of a sweep fingerprint sequence and the reconstructed image.

Live-scan Devices: Optical

Optical Frustrated Total Internal Reflection (FTIR)



An optical sensor.



- the rays incident at the ridge/glass interface scatter
- the rays incident at the valley/glass interface suffers total internal reflection
- the reflected rays are collected at the imaging surface

Live-scan Devices: Optical

- + Oldest and most commonly used (law enforcement)
- + relatively low cost
- + Generally superior quality
- + Potentially larger sensing areas
- Problems with latent fingerprints
- + Cannot be fooled with 2D picture
- Bulky (optical path), can not be miniaturized



© Biometric Access Corporation

Live-scan Devices: Optical: smaller alternatives

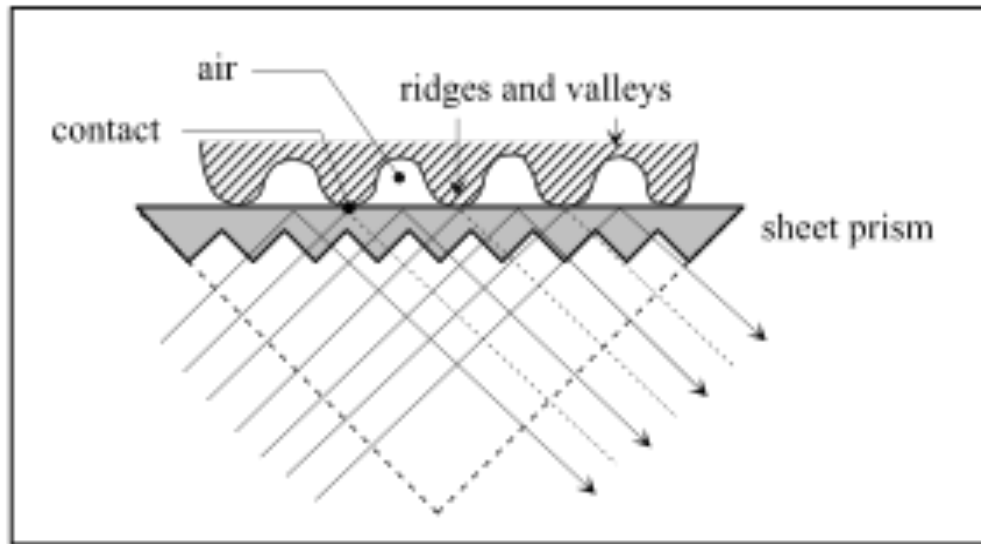


Figure 2.7. The use of a sheet prism in FTIR fingerprint acquisition.

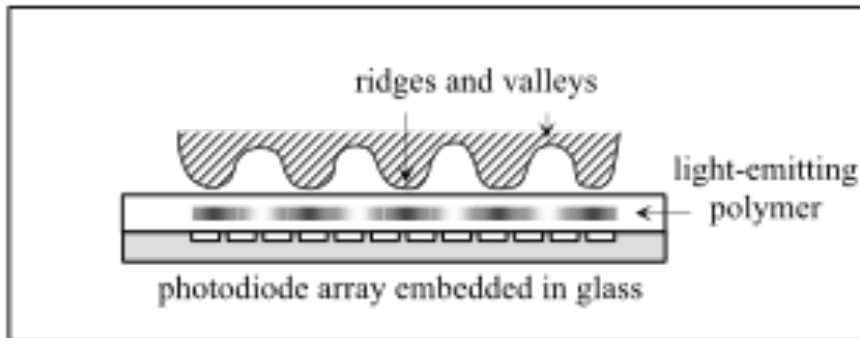


Figure 2.9. Electro-optical fingerprint sensor.

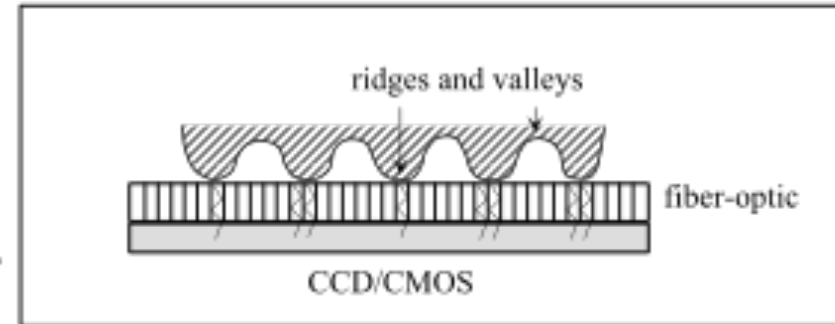


Figure 2.8. A sensor based on optical fibers. Residual light emitted by the finger is conveyed through micro-optical guides to the array of pixels that constitute the CCD/CMOS.

Condition-dependent quality



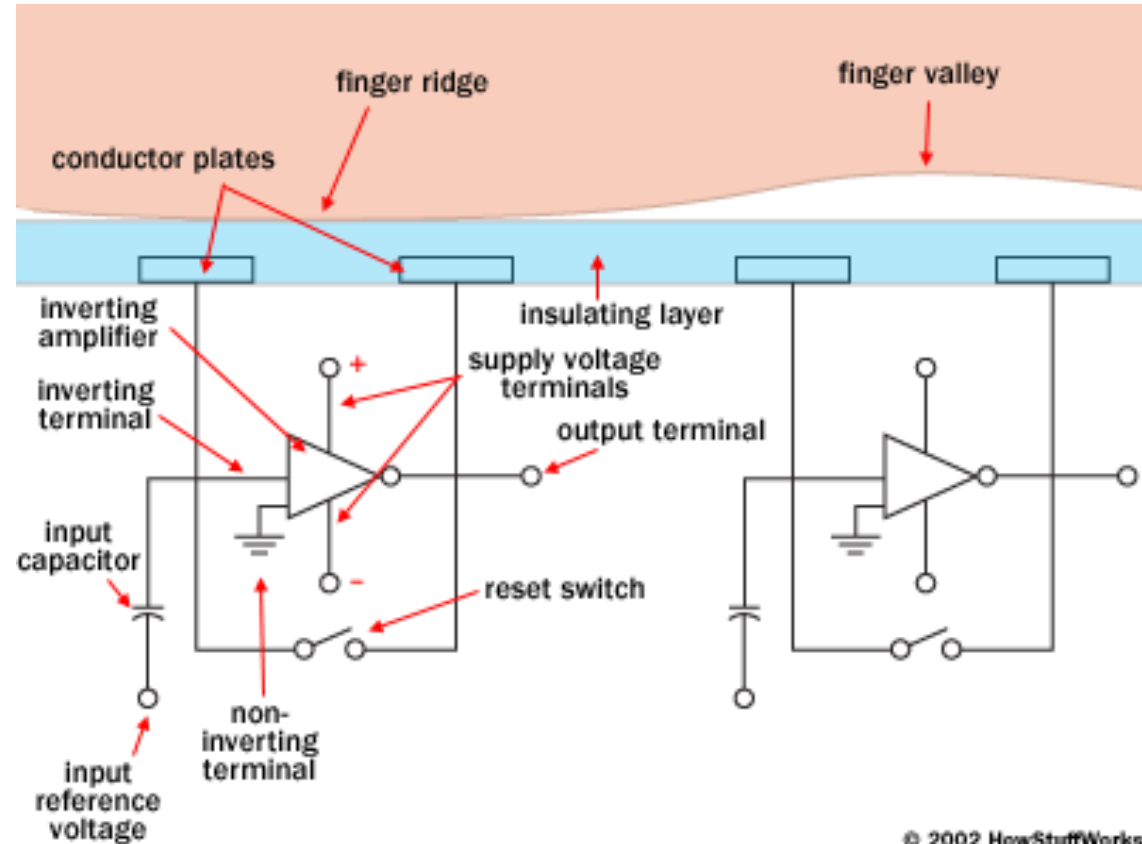
Figure 2.14. Examples of fingerprint images acquired with an optical scanner: a) a good quality fingerprint; b) a fingerprint left by a dry finger; c) a fingerprint left by a wet finger; d) an intrinsically bad fingerprint.

Live-scan FP acquisition: Differential Capacitance



Source: Veridicom [18]
Beneath the surface passivation layer is a 300×300 array of capacitor plates. The ridges and valleys of a finger are different distances from the capacitor plates. That difference corresponds to a capacitance difference which the sensor measures. The

analog-to-digital converter translates that capacitance to into an 8-bit digital value. The resolution of the image is 500 DPI.



© 2002 HowStuffWorks

Differential Capacitance

- small surface area: 15x15 mm
- + compact
- + durable and easy to integrate
- + good resolution 500 dpi
- + liveness detection
- + difficult to fool
- + minimal power consumption
- + fast
- + low cost
- sensitive to electrical discharges

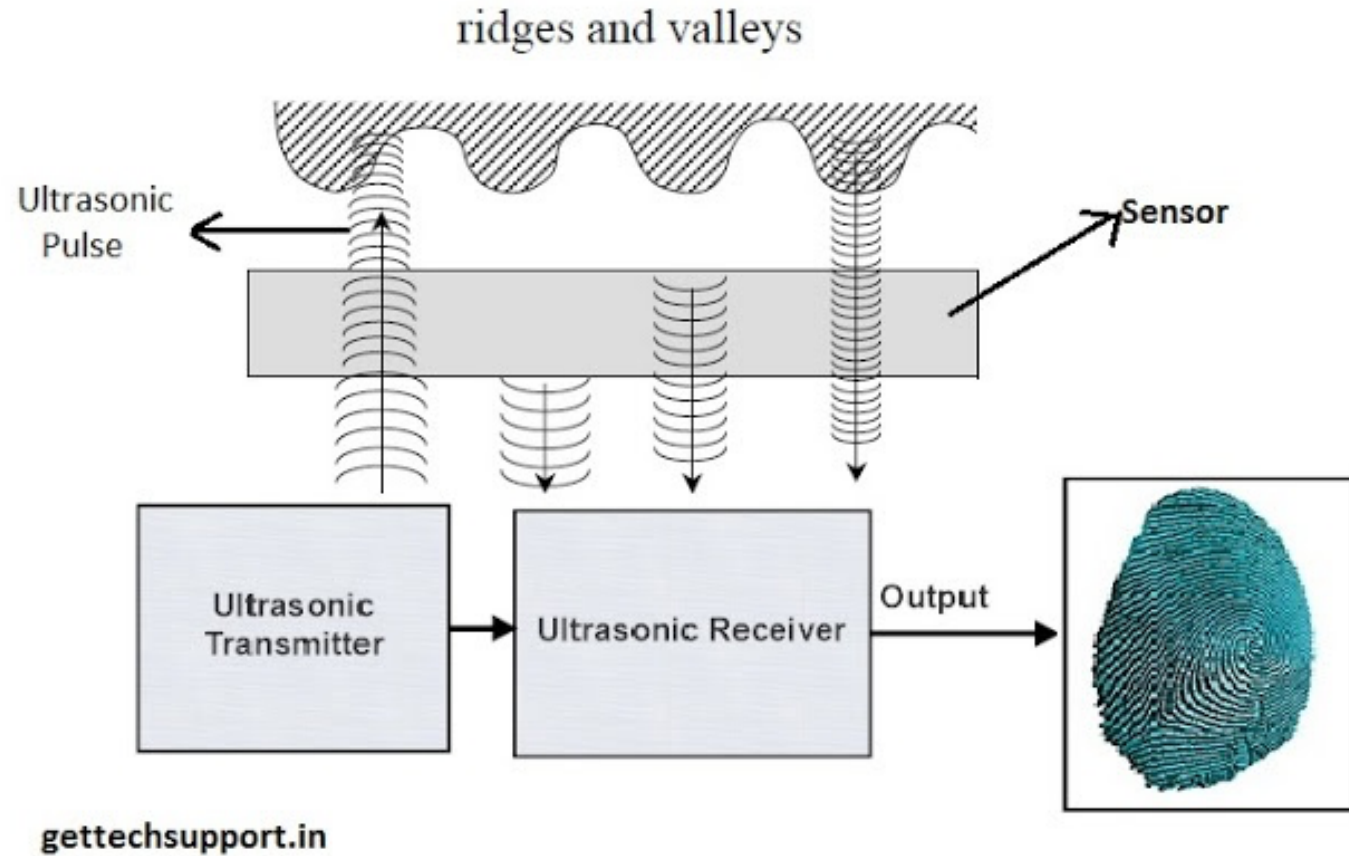


© Precise Biometrics

300x300, 8-bit

Live-scan FP acquisition: Ultrasound

- Independent of moisture
- Independent of dust (cf. infra)
- ~~Expensive (2500 Euro)~~
- ~~Bulky still (15x15x20cm)~~
- High Resolution (up to 1000dpi)
- 3D



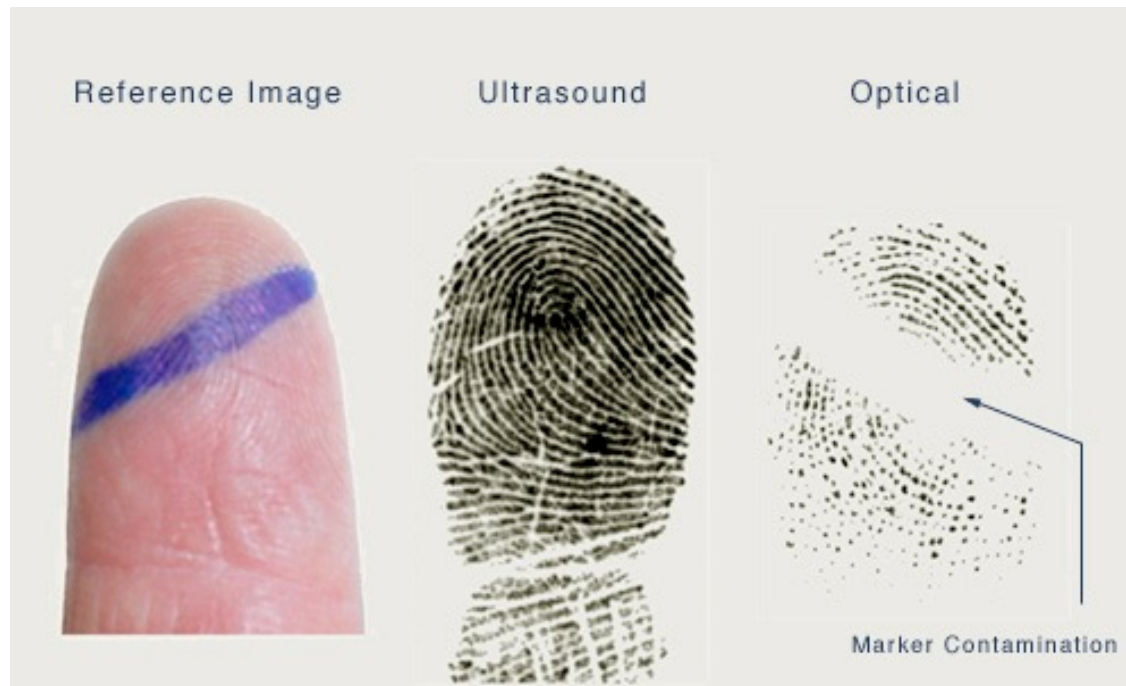
gettechsupport.in

From bulky to under-glass ...



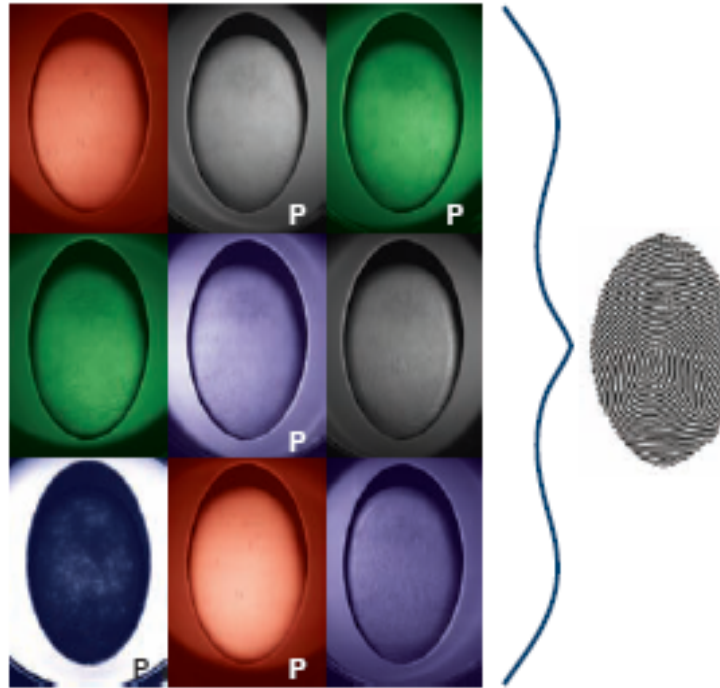
Samsung Galaxy S10
[@AndroidAuthority](#)

Ultrasound vs. Optical



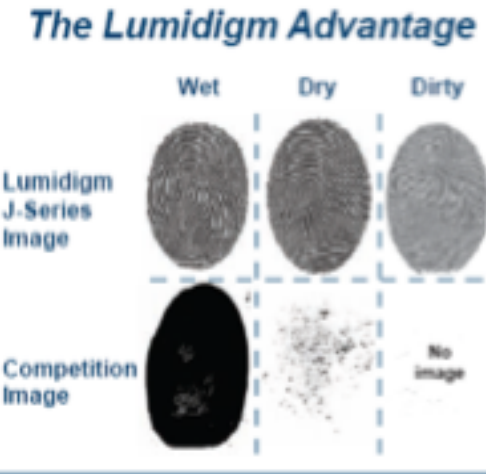
© Ultra-Scan

MultiSpectral Fingerprint Acquisition



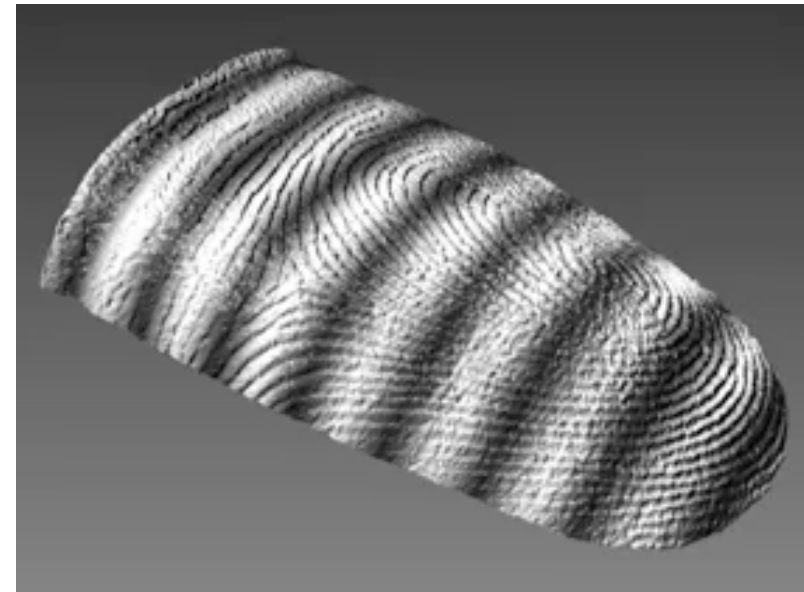
Multispectral Imaging

Lumidigm's J-Series fingerprint sensors are powered by multispectral imaging. This enables the capture of nine different fingerprint images in a fraction of a second. Each image uses a unique illumination and polarization. This allows the capture of data from both the surface and beneath the surface of the skin. The resulting images are combined using a patented process that yields fingerprints of unparalleled image quality.

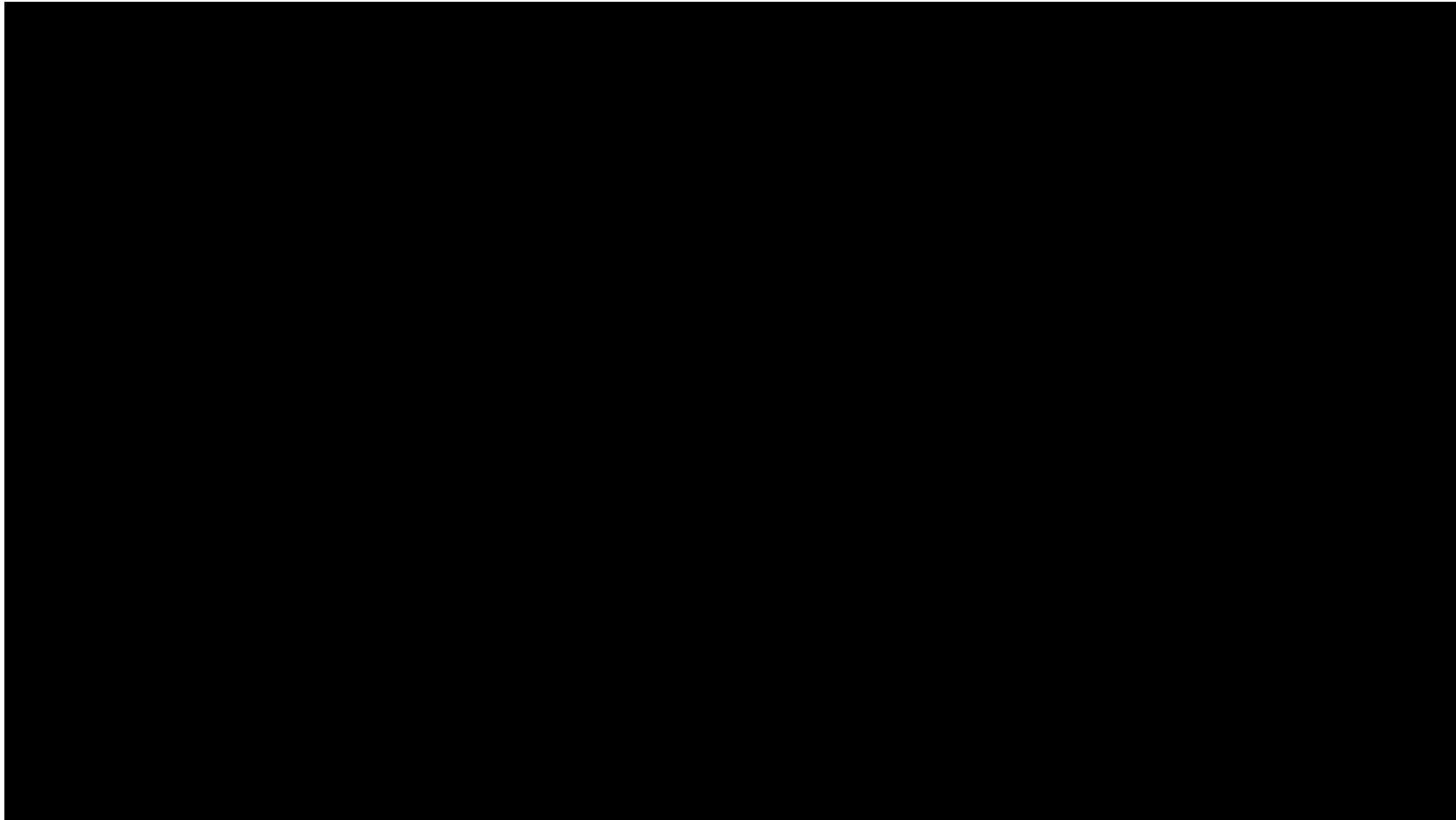


3D Touchless FP acquisition

- Improved Quality
- Additional Challenge: 3D/2D matching



MorphoWave Desktop



Touchless (3D) optical scanner

- MorphoWave Desktop by IDEMIA scans and processes simultaneously four fingerprints with a single hand movement over its large contactless scanning surface.
- This sequence lasting less than a second, MorphoWaveDesktop is then capable of enrolling all 10 fingerprints (2 slaps* and 2 thumbs) in under 5 seconds.
- In addition, the 3D technology captures more than just ridges but also surface, shape and curvature of fingers, resulting in a 20%+ higher hit rate than any competing solution (based on an independent study) and a proven compatibility with standard flat and rolled fingerprint databases and AFIS systems.
- MorphoWave Desktop copes with wet and dry fingers, mitigates hygiene concerns and is robust against external light and dust.

Touchless (3D) optical scanner

New AI engine boosts MorphoWave Compact biometric fingerprint performance

⌚ Sep 9, 2019 | [Chris Burt](#)

CATEGORIES [Biometric R&D](#) | [Biometrics News](#) | [Fingerprint Recognition](#)

[Idemia](#) has added new artificial intelligence capabilities to its MorphoWave Compact touchless 3D biometric fingerprint terminal, significantly improving the terminal's user experience and performance, according to a company announcement.

The MorphoWave Compact was launched [last year](#) to provide high-volume biometric scanning with an 86 percent smaller footprint than the MorphoWave Tower.

Idemia says the new AI-based embedded biometric engine improves matching speed by 85 percent, for a 25 percent increase in throughput speed to over 50 people per minute at each access point. The algorithms also increase matching accuracy, and enable capacity of up to 100,000 users for one-to-many identification. The company also says the new AI capabilities help the MorphoWave Compact process the most challenging fingerprints.



<https://www.idemia.com/morphowave-desktop>

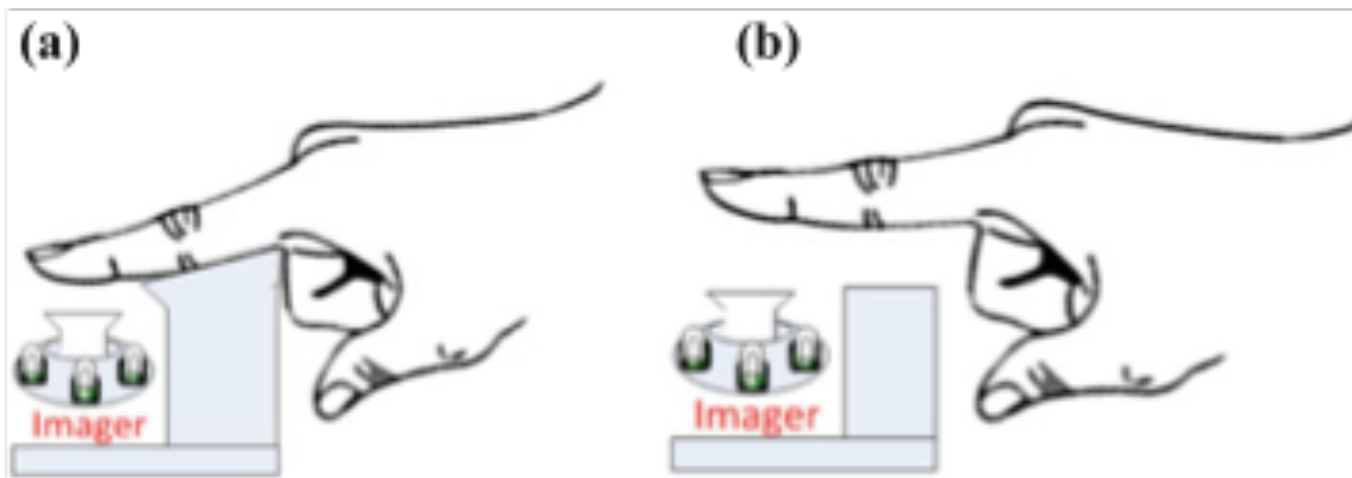


Fig. 1.2 Contactless fingerprint image acquisition setups: The setup in a uses *support* to limit the range of finger movement which can reduce the cost of sensor or camera optics. The setup in b requires larger depth of focus and view, which adds to the cost of contactless fingerprint sensing

Table 1.3 Comparison between touch-based, contactless 2D and contactless 3D fingerprint identification

	Touch-based 2D fingerprint	Contactless 2D fingerprint	Contactless 3D fingerprint
Recognition accuracy	High	High	Very High
Security hazards with sensor usage	High	Very Low	Very Low
Skin deformation	High	NIL	NIL
Sensor surface smear/noise	High	Very Low	Very Low
Identification of spoof and alterations	Low	Medium	High
Sensor cost	Low	High	Very High
Bulk/size	Compact	Medium/large	Bulky

3D fingerprint image acquisition methods, in Kumar, A., 2018. Contactless 3D Fingerprint Identification, ch. 1 Advances in Computer Vision and Pattern Recognition. Available at: <http://dx.doi.org/10.1007/978-3-319-67681-4>.

Table 2.1 Comparative summary of emerging 3D fingerprint image acquisition solutions

	Imaging principle	Source data	Acquisition mode	Relative cost ^a	Reconstruction accuracy ^a
Stereo camera	Triangulation	Range	Passive	Medium	Medium
Structured/patterned lighting	Triangulation	Range	Active	High	High
Photometric stereo	Shape from shading	Surface normal orientation	Active	Lowest	Very high
Optical coherence tomography	Interferometry	Backscattered light amplitude	Active	Very high	Very high
Ultrasonic imaging	Acoustic time of flight	Acoustic impedance	Active	Low	High-medium

^a*Estimated*

3D fingerprint image acquisition methods, in Kumar, A., 2018. Contactless 3D Fingerprint Identification, ch.2, Advances in Computer Vision and Pattern Recognition. Available at: <http://dx.doi.org/10.1007/978-3-319-67681-4>.

Live Fingerprints Acquisition Devices

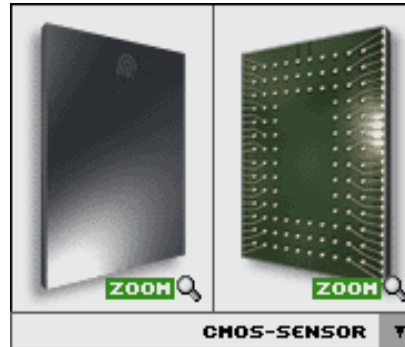
- Reference (area, resolution, contrast): inked fingerprints
- Optical FTIR (!) (bulky, best quality, large area, expensive)
- Differential capacitance (cheap, small, lower Q)
- Ultrasound TIR (bulky, quality, small area)
- Thermal sensing of temperature differential across ridges and valleys
- Non-contact 3-D scanning

See [this page](#) (and) for the latest developments and technology comparison

Fingerprint Recognition: Sensors (I)



Optical fingerprint sensor
[Fingerprint Identification Unit
FIU-001/500 by Sony]



Electro-optical sensor
[DELSY® CMOS sensor modul]



Capacitive sensor
[FingerTIP™ by Infineon]

Fingerprint Recognition: Sensors (II)



E-Field Sensor
[FingerLoc™ by Authentec]



Thermal sensor
[FingerChip™ by ATTEL
(was: Thomson CSF)]

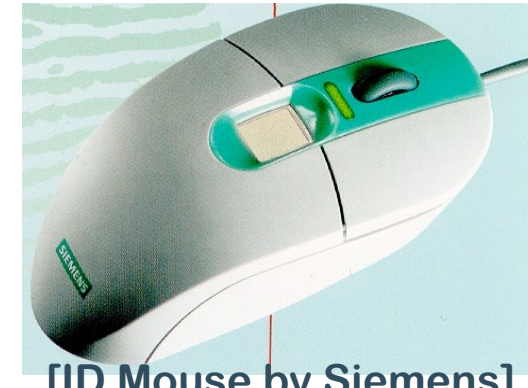
Fingerprint Recognition: Integrated Systems (I)



Physical Access Control System
[BioGate Tower by Bergdata]



[BioMouse™ Plus by American Biometric Company]



[ID Mouse by Siemens]

Fingerprint Recognition: Integrated Systems (II)



[TravelMate 740 by Compaq und Acer]



/board [G 81-12000
Cherry]

Precise 100 PC-Card by Precise Biometrics

Advanced fingerprint scanners



[Futronic FS60 EBTS/F Certified ID Flat -
USB multi finger fingerprint scanner \(1900\\$\)](#)



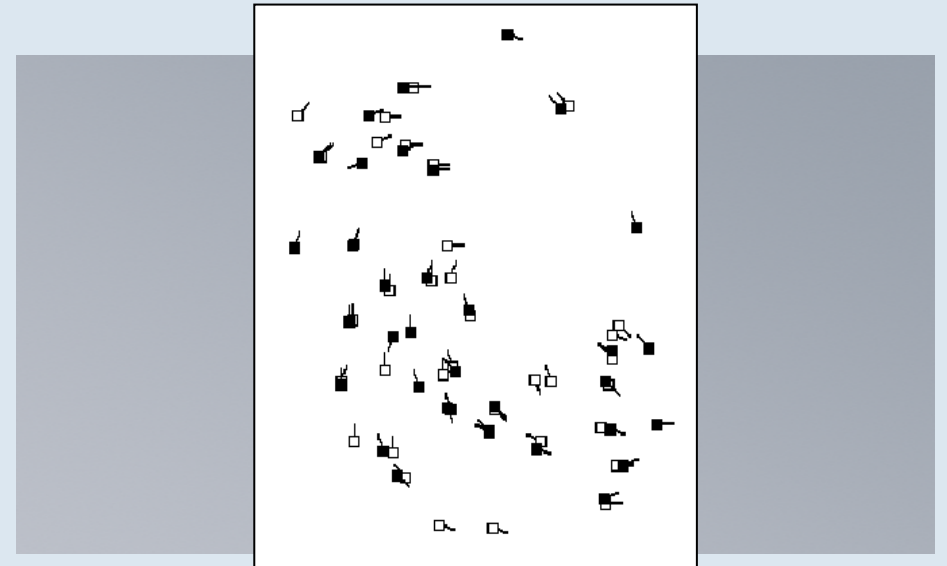
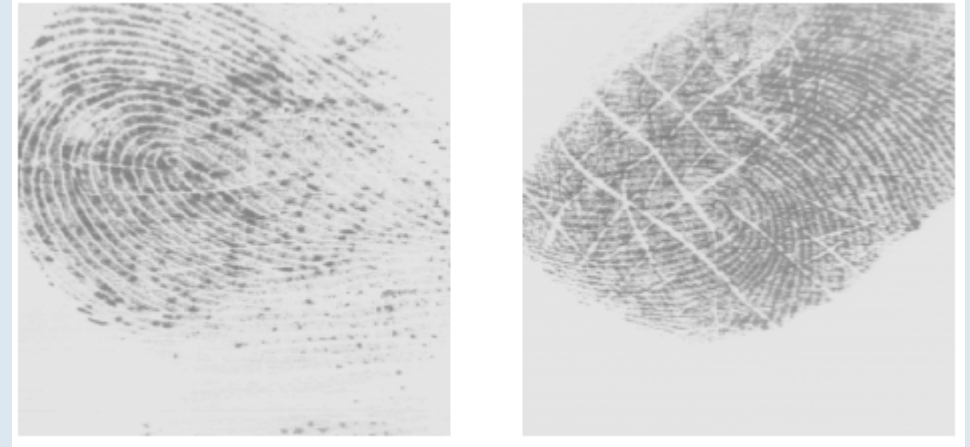
[Lumidigm Mercury Series M301 Fingerprint Reader -
USB multi-spectral fingerprint scanner \(200\\$\)](#)

Touch ID (Apple)



Capacitance Sensor, 500 DPI

Fingerprint Representation



FP Representation

Which **machine-readable** representation completely captures the

- **invariant** (low intra-class variations) and
- **discriminatory** (high-inter-class variation)

information in a fingerprint image?

Constitutes essence of fingerprint verification system design!

Properties

Saliency

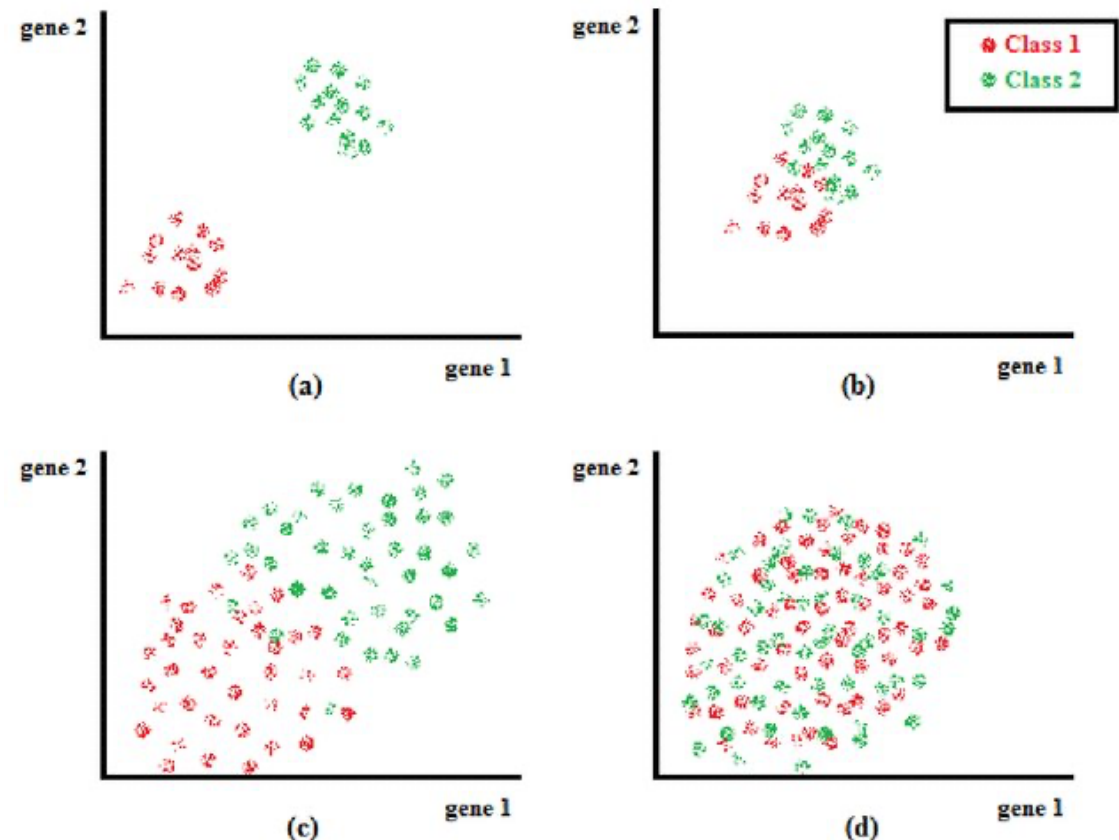
contains distinctive information

Suitability

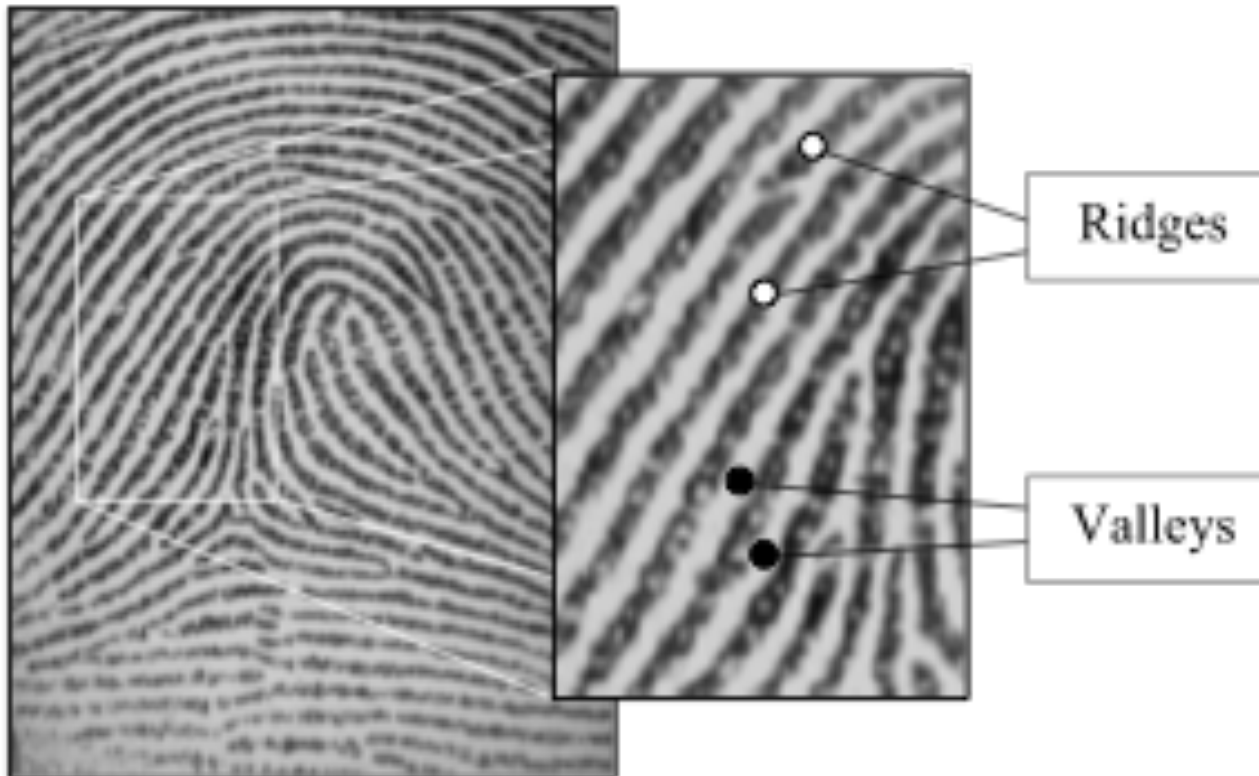
Easily extractable

Compact storage

Useful for matching



Structural characteristics: ridges and valleys



Ridge/valley width: 100-300 μ m

How much DPI required?

Figure 3.1. Ridges and valleys in a fingerprint image.

Representational levels L0-L3

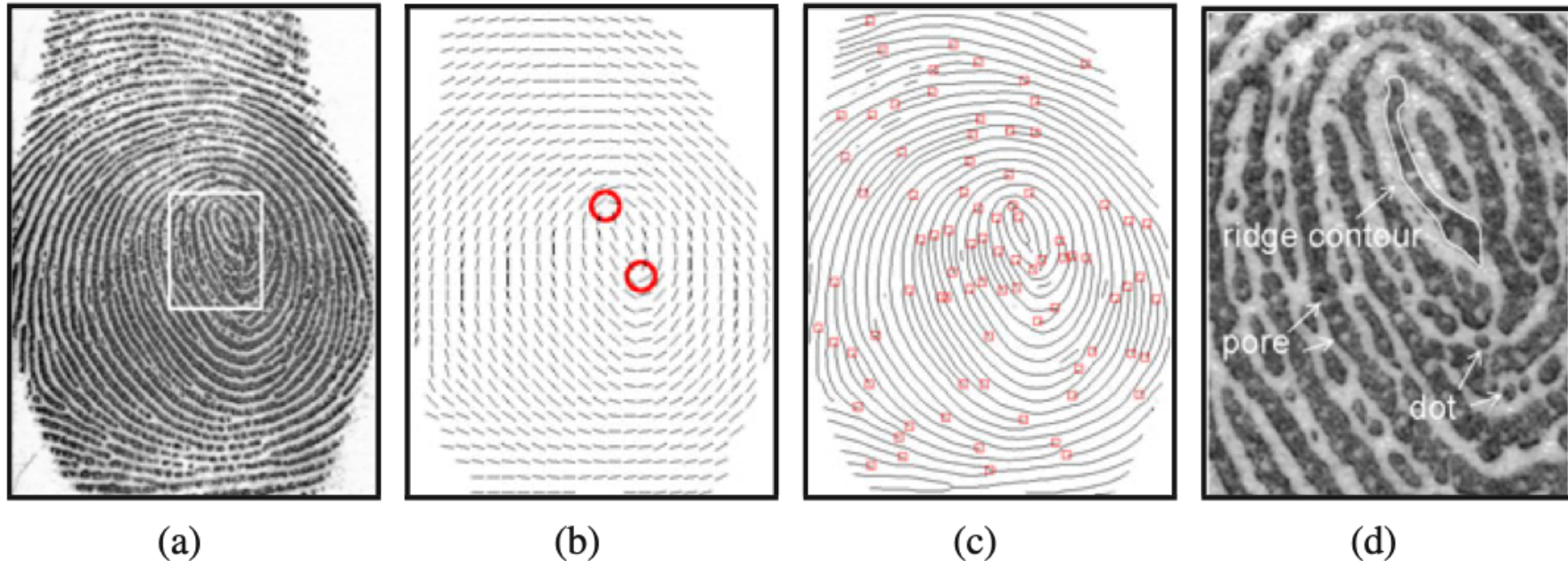


Fig. 2.5 Features at three different levels in a fingerprint. (a) Grayscale image (NIST SD30, A067_11), (b) Level 1 feature (orientation field or ridge flow and singular points), (c) Level 2 feature (ridge skeleton), and (d) Level 3 features (ridge contour, pore, and dot).

Representation L0: Entire Gray Scale Profile

Used in optical matching

Verification by template matching

Limitations due to:

- Brightness variations
- Image quality variations
- Scars
- Large global distortions

Representation size is large



Representation L1: global ridge flow pattern

- Only **ridge flow** and **ridge frequency** are coded
- Singular regions
 - Delta (Δ -shape)
 - Loop (\sim -shape)
 - Whorl (O-shape)
 - Used for classification

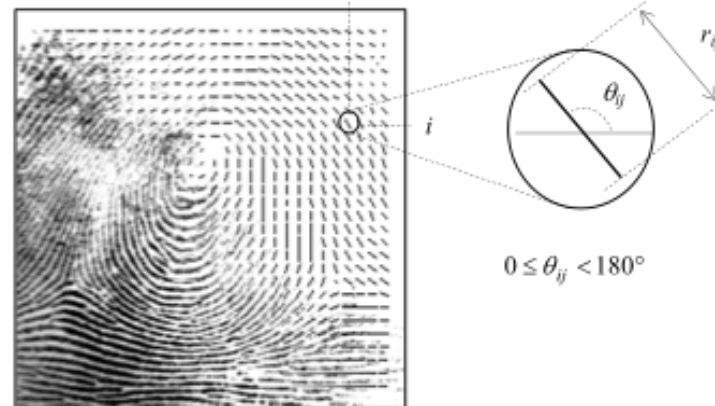


Figure 3.9. A fingerprint image faded into the corresponding orientation image computed over a square-meshed grid of size 16×16 . Each element denotes the local orientation of the fingerprint ridges; the element length is proportional to its reliability.

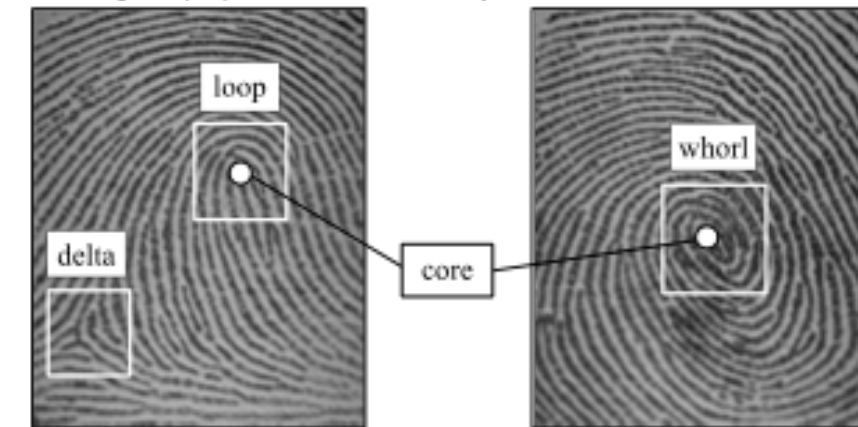


Figure 3.2. Singular regions (white boxes) and core points (small circles) in fingerprint images

Representation L2: Landmark Features - minutiae

local invariant ridge discontinuities, called **minutiae**

Defined by Sir Francis Galton (1892)!

$\exists \pm 150$ different types of local ridge structures.

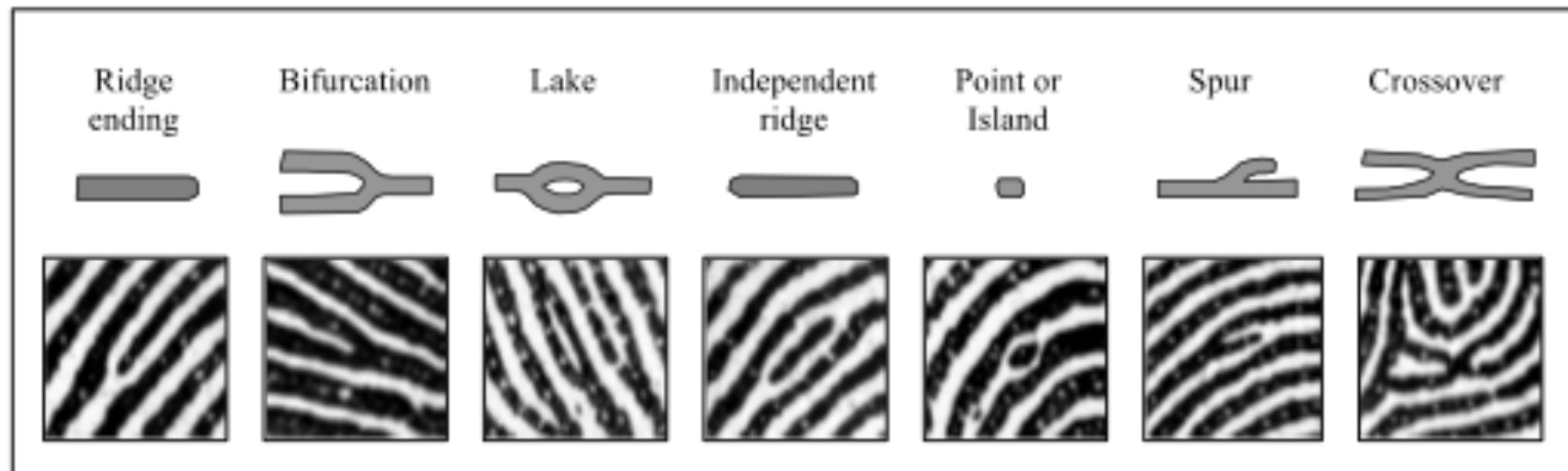
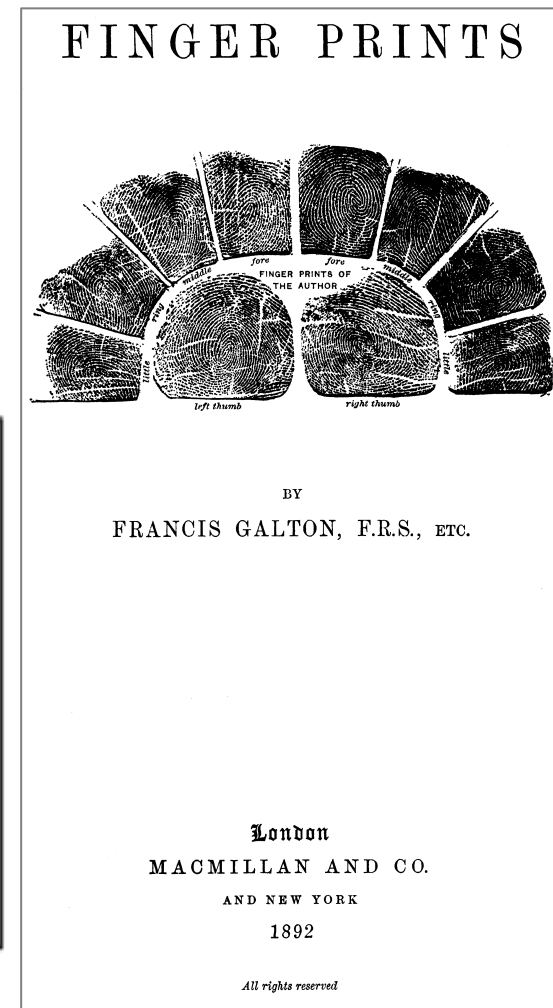
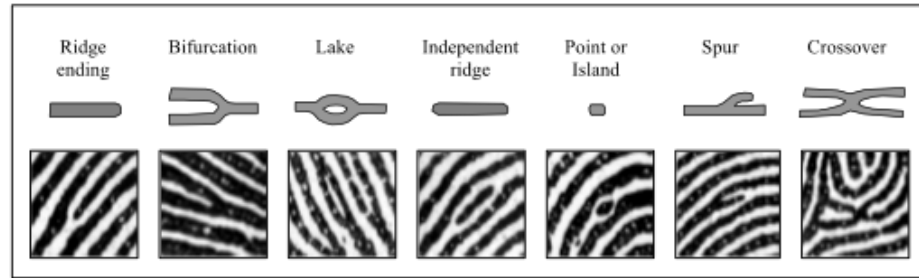


Figure 3.4. Seven most common minutiae types.



Minutiae example



Difficult to automatically, quickly and reliably extract (too similar and image quality dependent).

Density: 100/FP but only 10 to 15 needed for matching

In practice only **ridge bifurcations** and **endings** are used

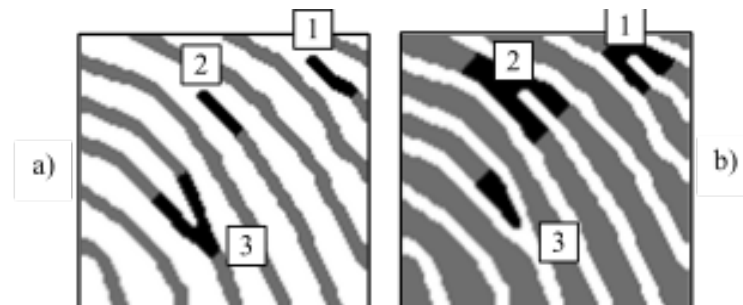
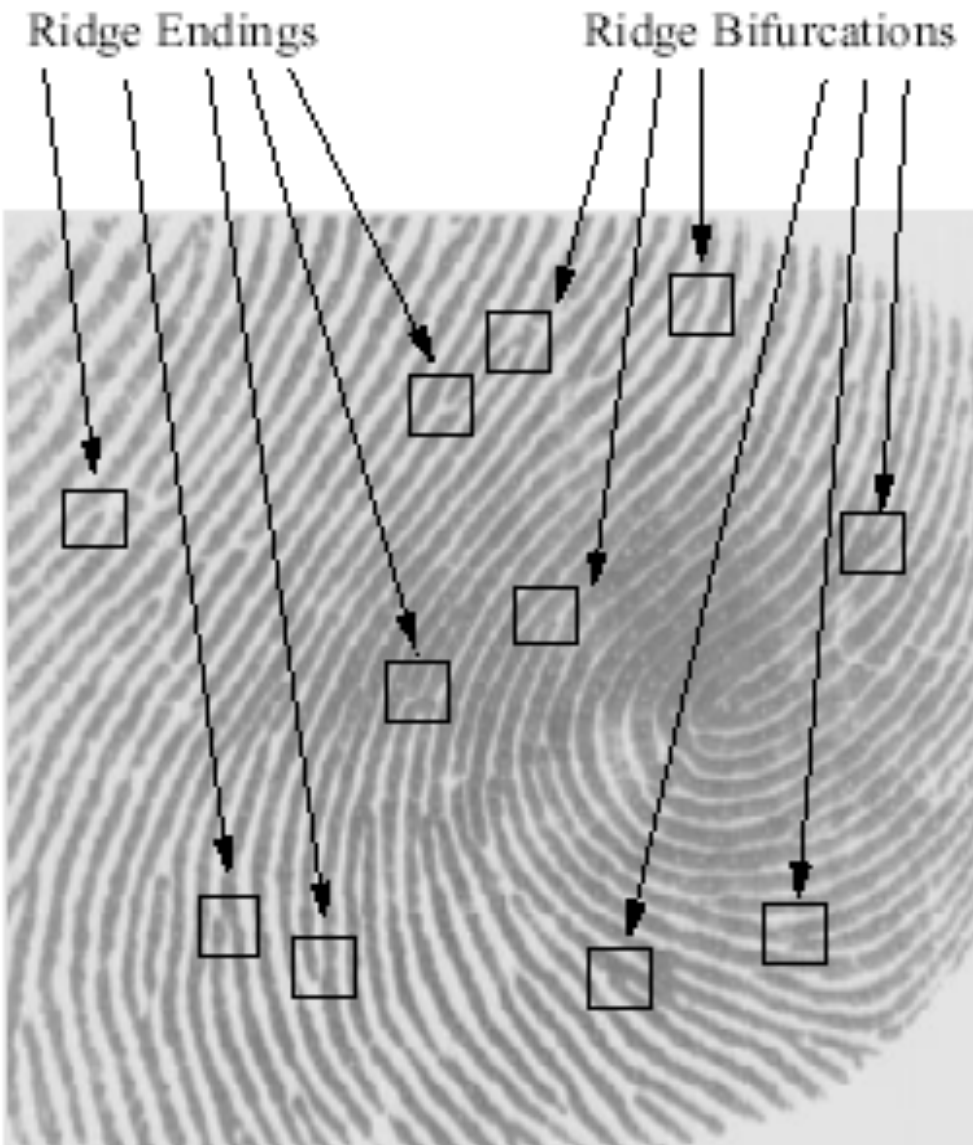


Figure 3.6. The ridge ending/bifurcation duality in a) a binary image and b) its negative image (i.e., dark and bright pixels are swapped).



L2 Minutiae Representation

- List of minutiae coordinates
- Enhanced by tagging each minutiae (or pairs, triplets) with:
 - Orientation of the ridge at that minutiae
 - Ridge density (# ridges on a line) between each pair of minutiae
- Enhanced by global attributes:
 - Global orientation of the finger
 - Locations of cores or delta's
 - Fingerprint class

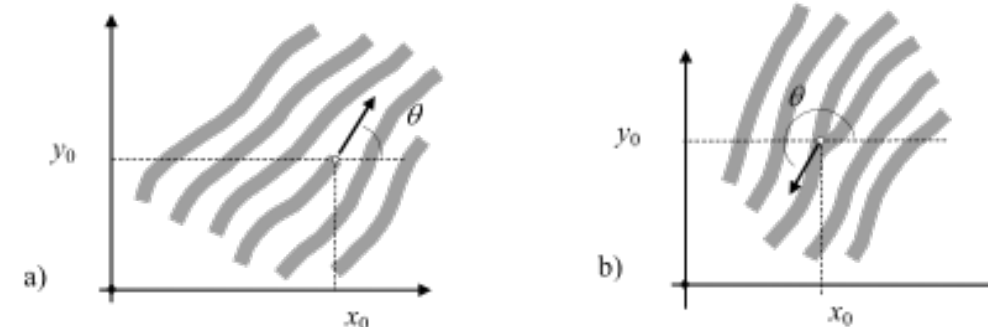
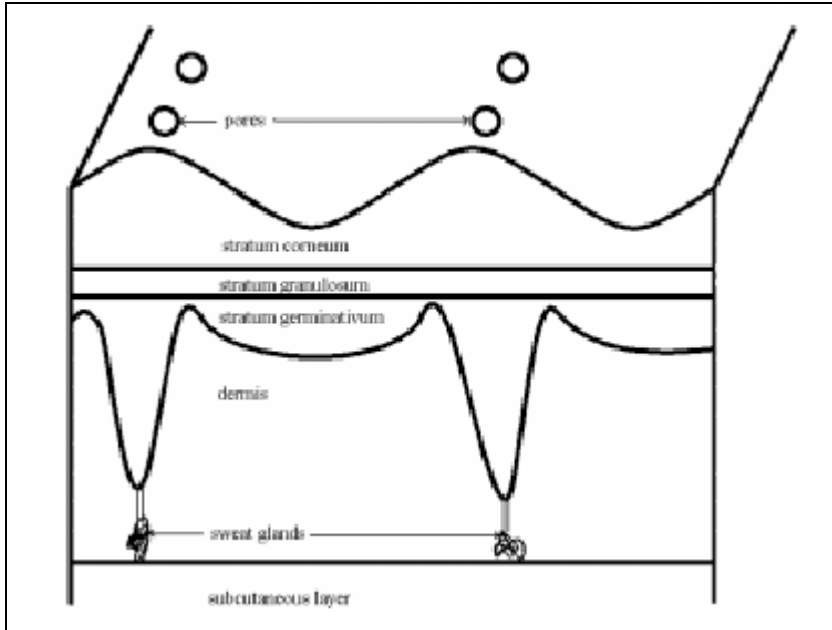


Figure 3.5. a) a ridge ending minutia: $[x_0, y_0]$ are the minutia coordinates; θ is the angle that the minutia tangent forms with the horizontal axis; b) a bifurcation minutia: θ is now defined by means of the ridge ending minutia corresponding to the original bifurcation that exists in the negative image.

Representation L3 Representations: Pores



Pores are formed where sweat glands in the subcutaneous layer of the skin generate sweat ducts; these sweat ducts grow through the subcutaneous layer and dermis to the epidermis, where the open duct on the skin's surface presents itself as a pore

Pores

- The regularity of their appearance plays a significant part in the uniqueness of pore configurations.
- Once these pores form on the ridge, they are fixed at that location.
- Pores do not disappear, move or spontaneously generate over time.
- Pore sizes: 60-250 μm (Ridges: 100-300 μm).
- Pore density: ± 6 pores/mm².
- High resolution sensors needed: **1000dpi** (compared to standard 500dpi of FBI's AFIS specifications).

1000 dpi



500 dpi



Fingerprint Enhancement



FP image degradation



Figure 2.22. Three fingerprint images of the same finger with different skin conditions acquired with an optical FTIR scanner: a) normal, b) dry, c) wet.

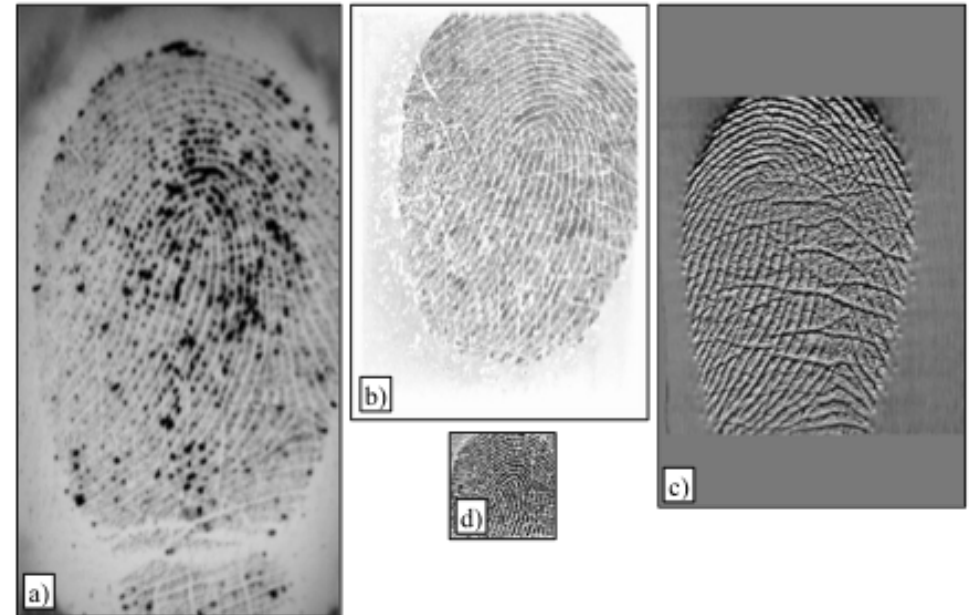


Figure 2.23. Fingerprint images of the same poor quality finger acquired with scanners based on four different sensing technologies: a) Optical FTIR, b) Solid state Capacitive, c) Solid state Thermal, and d) Solid state Electric field.

FP image degradation

Types of degradation associated with FP images:

1. **The ridges are not strictly continuous**; that is, the ridges have small breaks (gaps).
2. **Parallel ridges are not well separated**. This is due to the presence of noise which links parallel ridges, resulting in their poor separation.
3. **Cuts, creases, and bruises** on the finger.

This leads to the following problems in minutiae extraction:

- (i) a significant number of spurious minutiae are extracted
- (ii) a large number of genuine minutiae are missed
- (iii) large errors in the location (position and orientation) of minutiae are introduced.

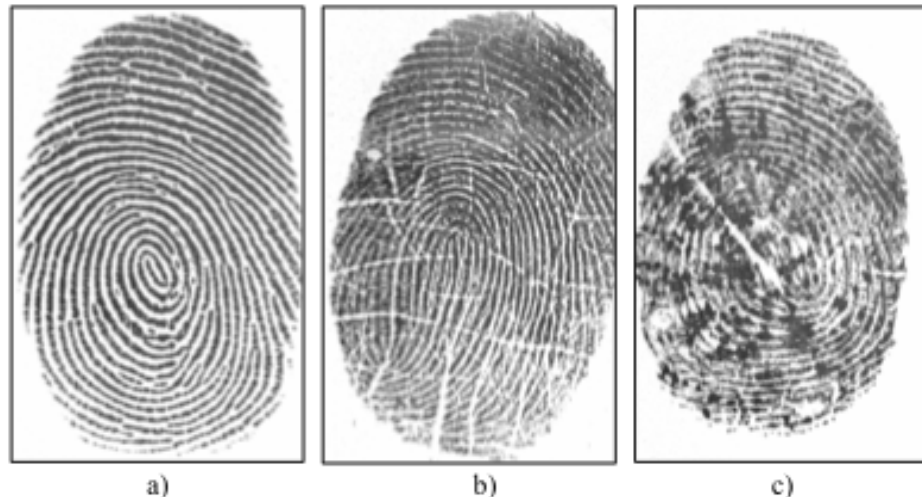


Figure 3.29. a) A good quality fingerprint; b) a medium quality fingerprint characterized by scratches and ridge breaks; c) a poor quality fingerprint containing a lot of noise.

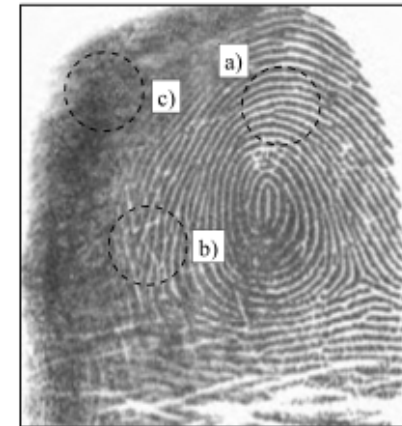
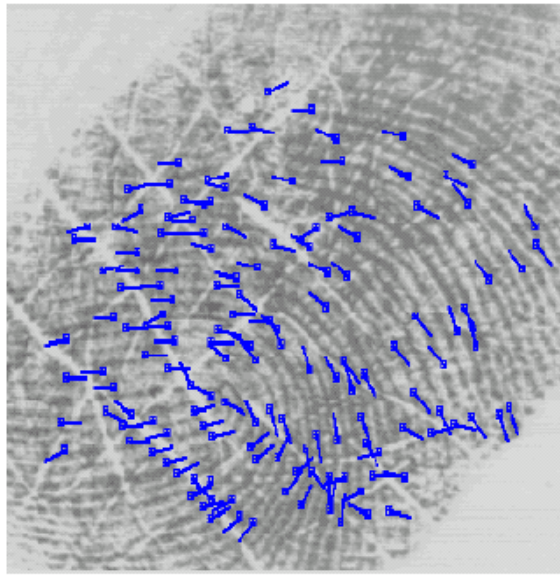


Figure 3.30. A fingerprint image containing regions of different quality: a) a well-defined region; b) a recoverable region; c) an unrecoverable region.

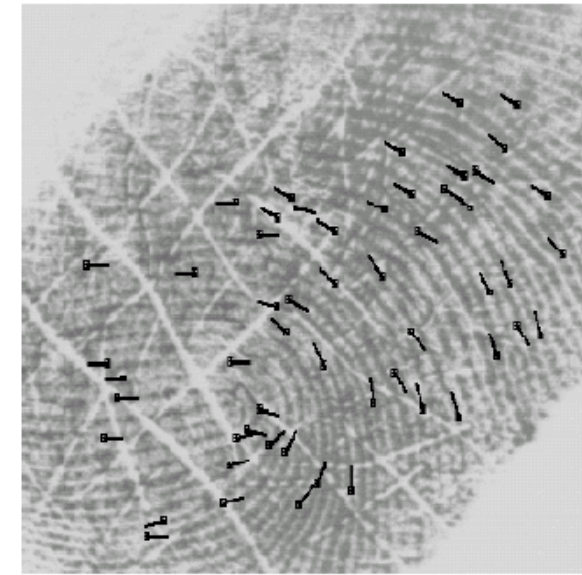
FP image enhancement



(a)



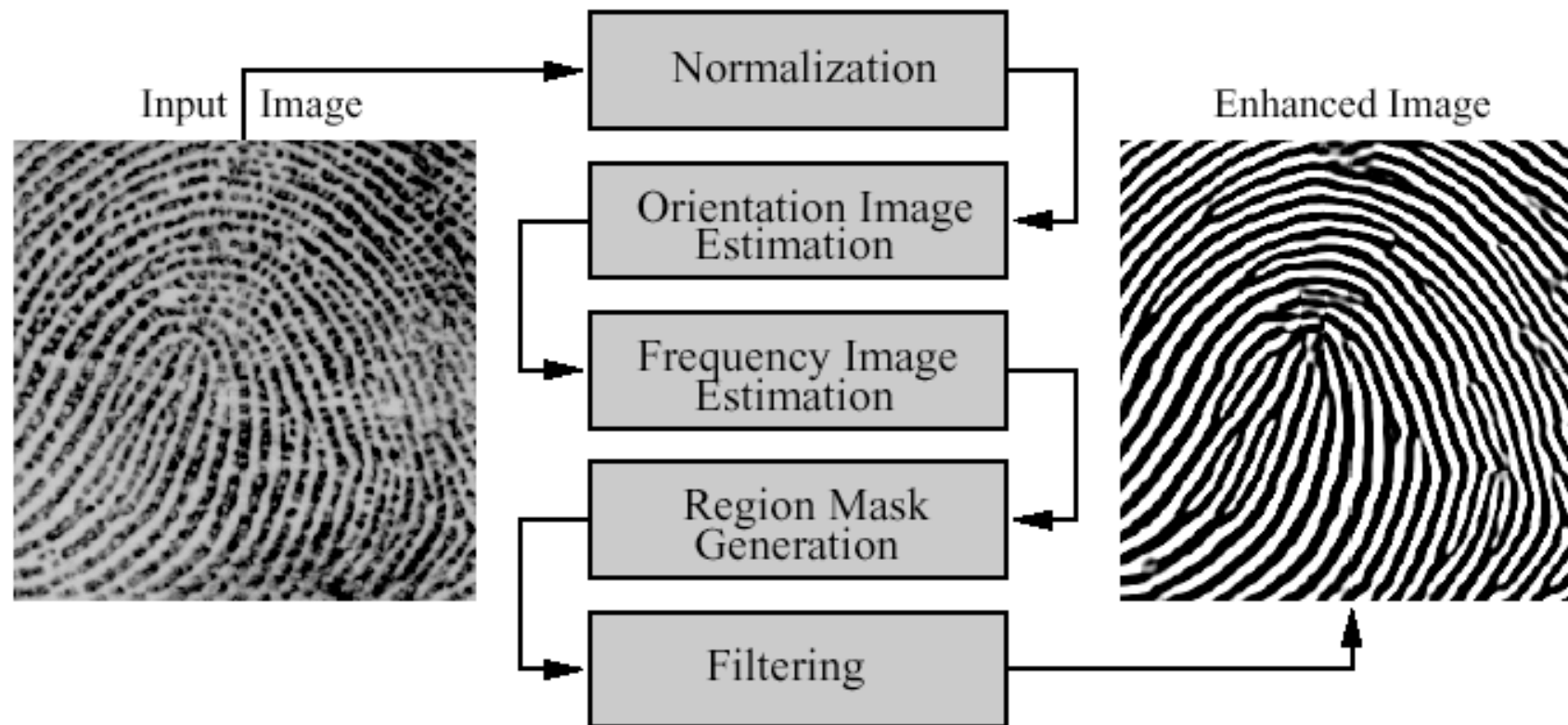
(b)



(c)

Figure 20: Fingerprint Enhancement Results: (a) a poor quality fingerprint; (b) minutia extracted without image enhancement; and (c) minutiae extracted after image enhancement [10].

Fingerprint Enhancement



Enhancement: global enhancement

- Contrast stretching, Histogram normalization (e.g. standard μ, σ)



Enhancement: local adaptive/matched filtering

- In **contextual filtering**, the filter characteristics change according to the local context.
- In FP enhancement, the context is defined by the **local ridge orientation and local ridge frequency**.
- An appropriate **matched filter** that is tuned to the local ridge frequency and orientation can efficiently remove the undesired noise and preserve the true ridge and valley structure.
- The intended behaviour :
 - 1) provide a **low-pass (averaging) effect along the ridge direction** with the aim of linking small gaps and filling impurities due to pores or noise;
 - 2) perform a **bandpass (differentiating) effect in the direction orthogonal to the ridges** to increase the discrimination between ridges and valleys and to separate parallel linked ridges.
- Using a bank of frequency and orientation selective **Gabor filters**

$$g(x, y; \theta, f) = \exp\left\{-\frac{1}{2}\left[\frac{x_\theta^2}{\sigma_x^2} + \frac{y_\theta^2}{\sigma_y^2}\right]\right\} \cdot \cos(2\pi f \cdot x_\theta)$$

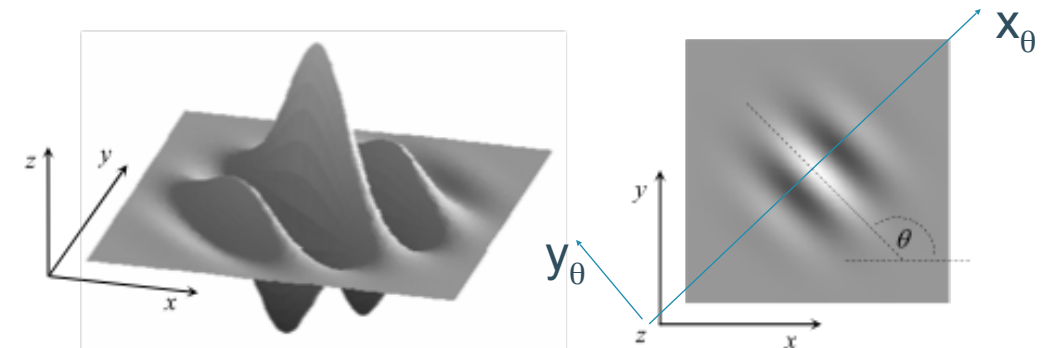
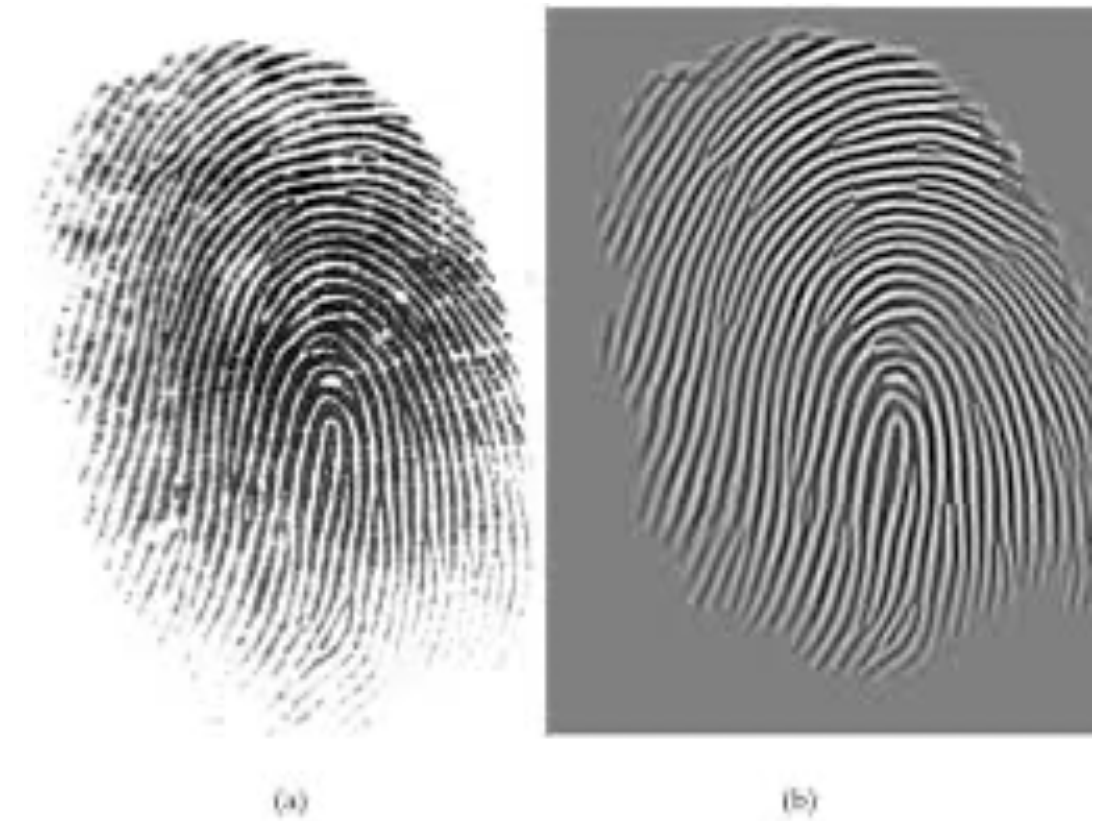
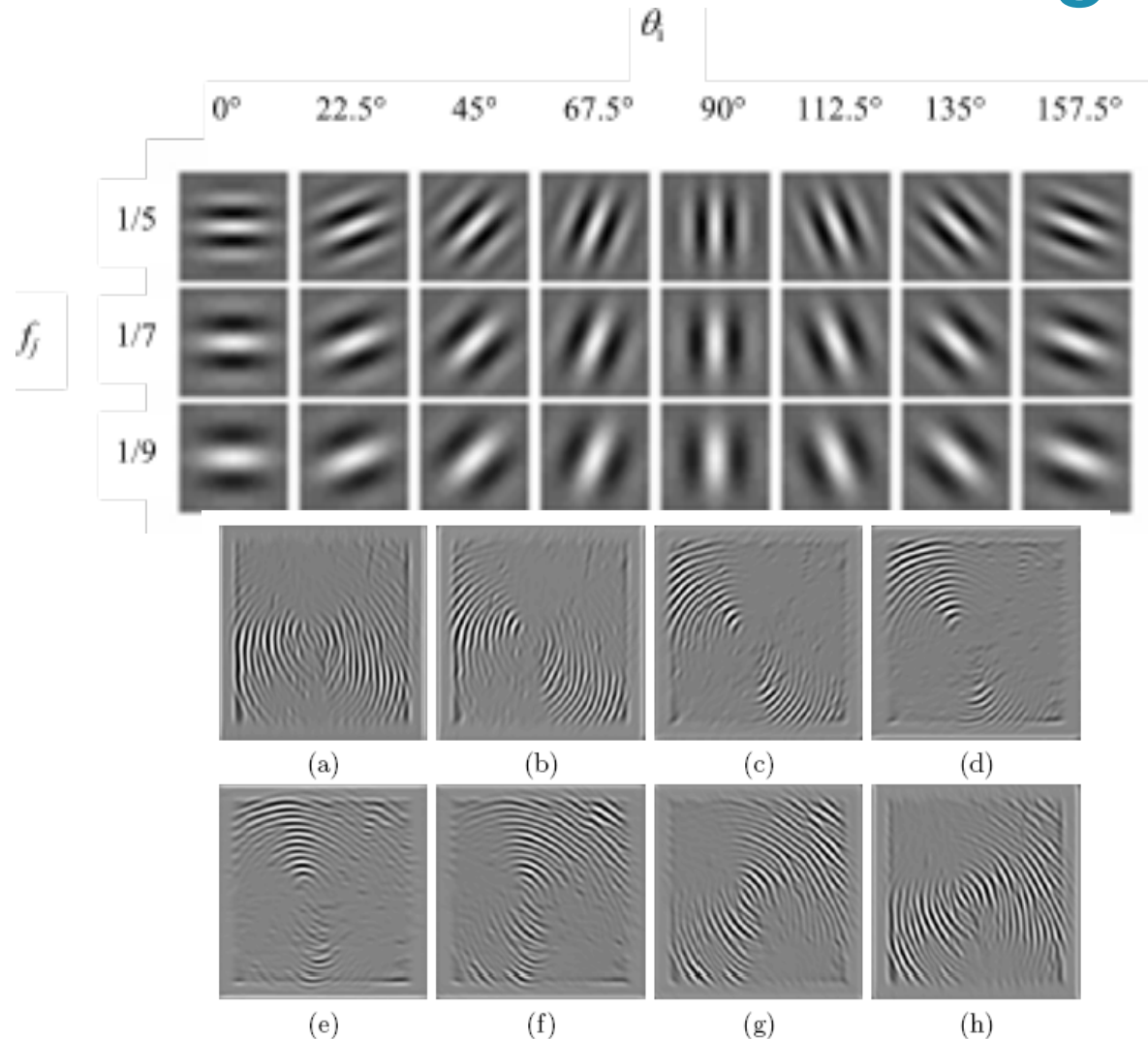


Figure 3.34. Graphical representation (lateral view and top view) of the Gabor filter defined by the parameters $\theta = 135^\circ$, $f = 1/5$, and $\sigma_x = \sigma_y = 3$.

FP enhancement using bank of Gabor Filters



FP Segmentation



FP segmentation

- Discriminating
 - Foreground (striped, oriented pattern)
 - Background (flat, isotropic)
- Methods
 - Local Histogram of Ridge Orientations
 - Local gray scale variance
 - Variance high perpendicular to ridge and low parallel with
 - Average of local gradient magnitude

See assignment 2: minutiae-based fingerprint recognition

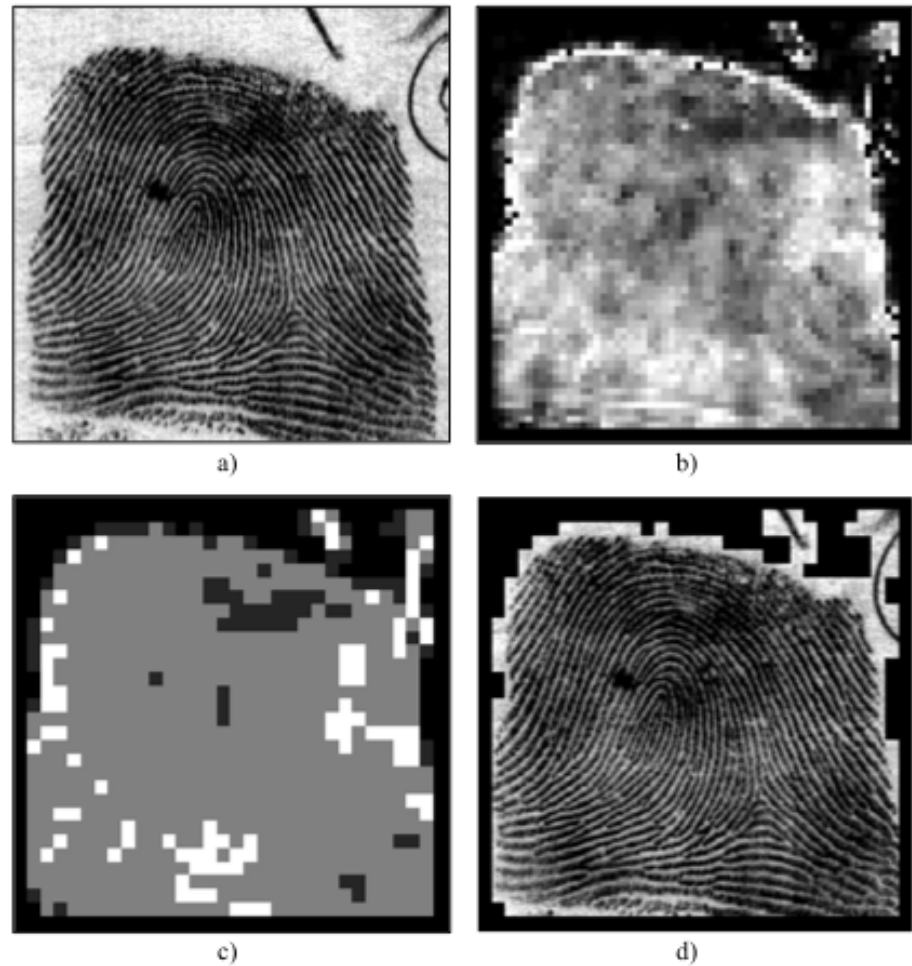


Figure 3.16. Segmentation of a fingerprint image as proposed by Ratha, Chen, and Jain (1995): a) original image; b) variance field; c) quality image derived from the variance field: a quality value "good," "medium," "poor" or "background" is assigned to each block according to its variance; d) segmented image. © Elsevier.

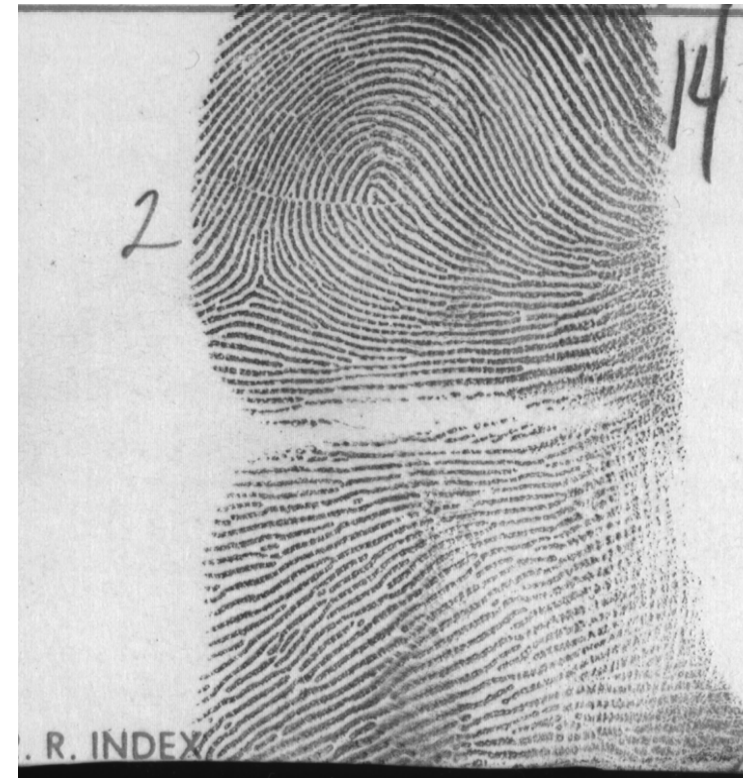
Fingerprint Compression

Fingerprint Image Compression

- IAFIS (FBI,1995): 200 million FP cards (10 fingers)
- Each FP cars scanned at 500dpi: 10MByte
- Making 2000 Terabyte in total (1995)
- Adding 30.000-50.000 cards A DAY!

Need for compression!

Wavelet Scalar Quantization (WSQ) LOSSY
compression (FBI standard for the compression of
500 dpi fingerprint images)



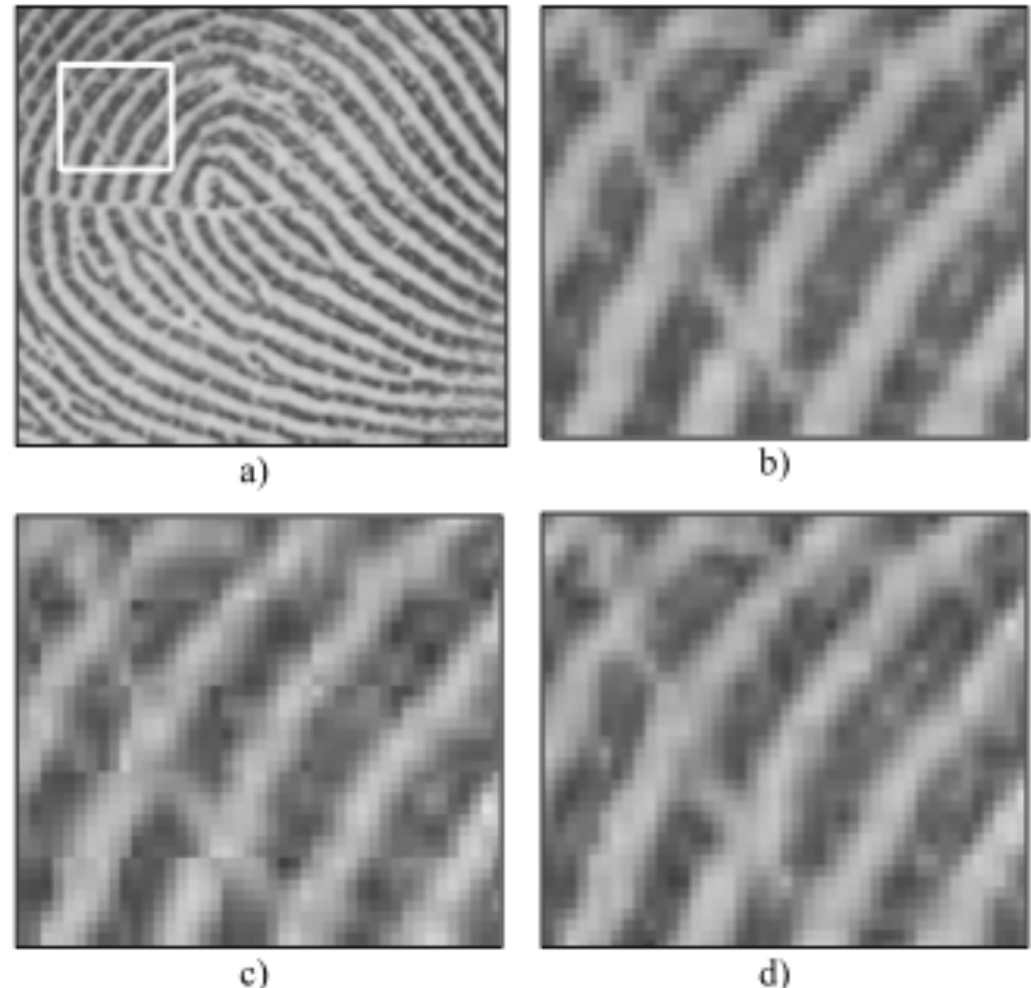
Fingerprint Image Compression

- a. the central section of a fingerprint image scanned at 500 dpi resolution
- b. the marked portion of the image in a)
- c. the marked portion of the image in a) after the image was compressed using JPEG
- d. the marked portion of the image in a) is shown after the image was compressed using the WSQ compression algorithm.

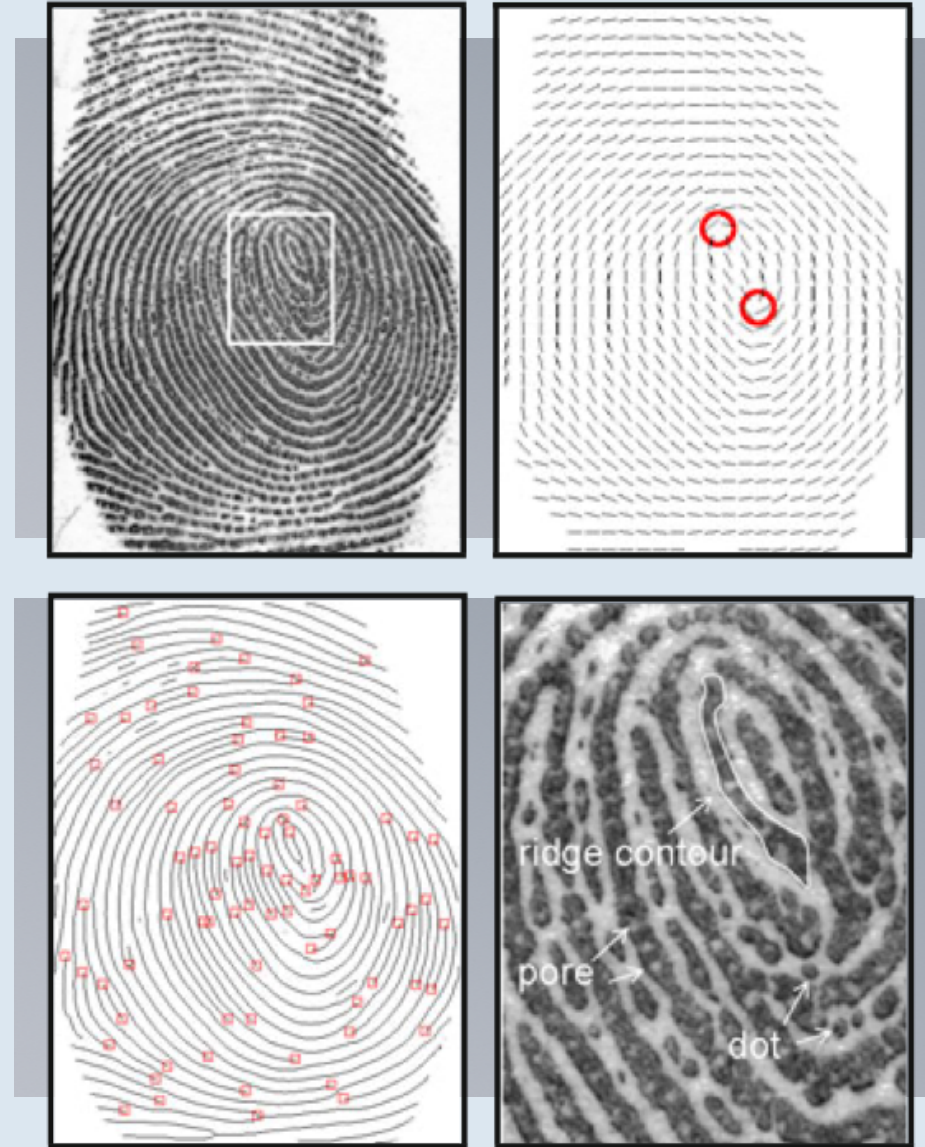
Both JPEG and WSQ examples used a compression ratio of 1:12.9;

JPEG typically introduces blocky artifacts and obliterates detailed information.

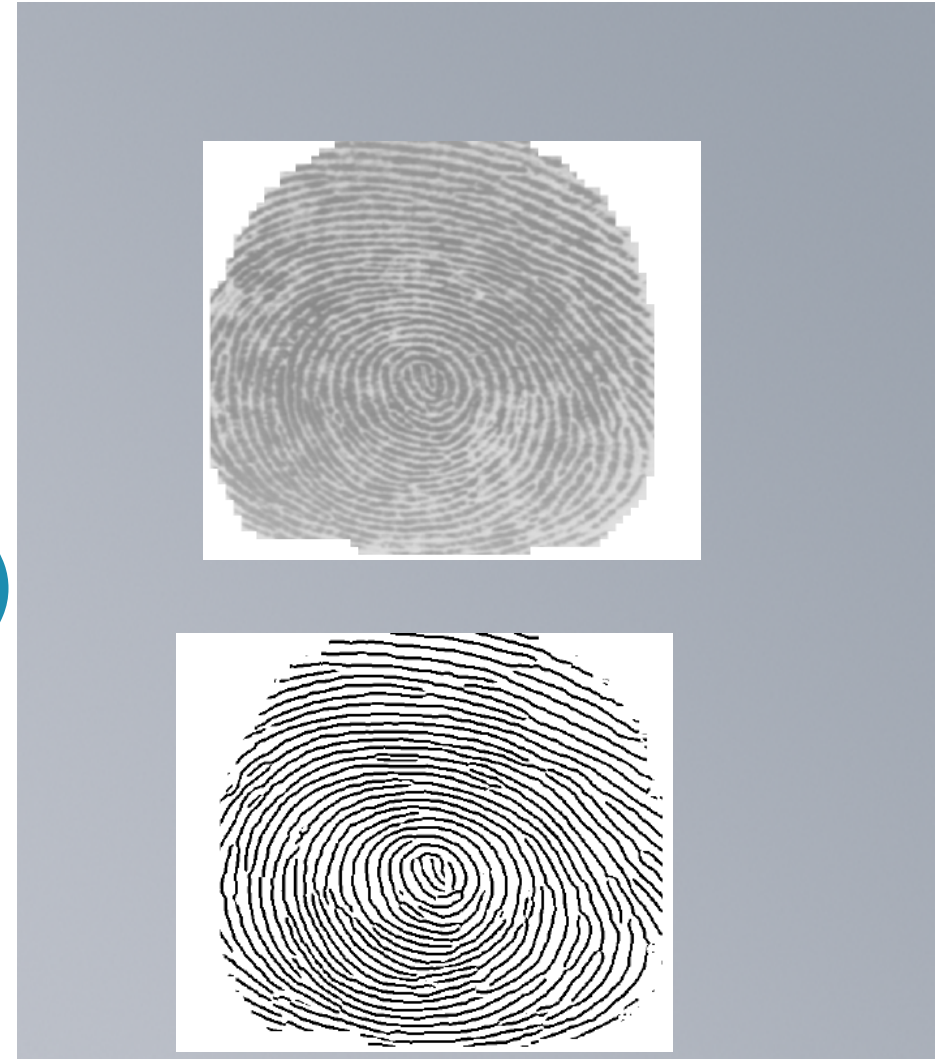
Images courtesy of Chris Brislawn, Los Alamos National Laboratory.



FP feature extraction



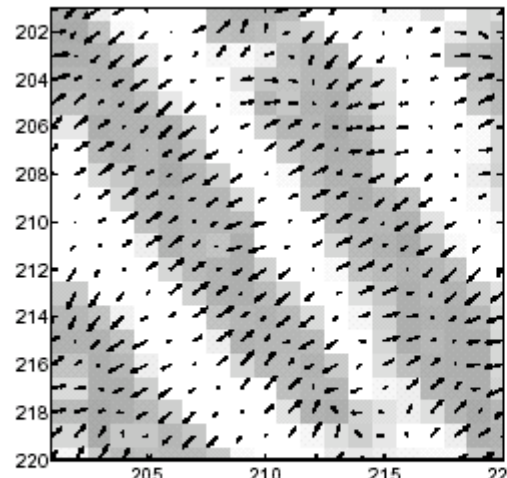
Representation L1 Ridge (frequency, orientation) extraction



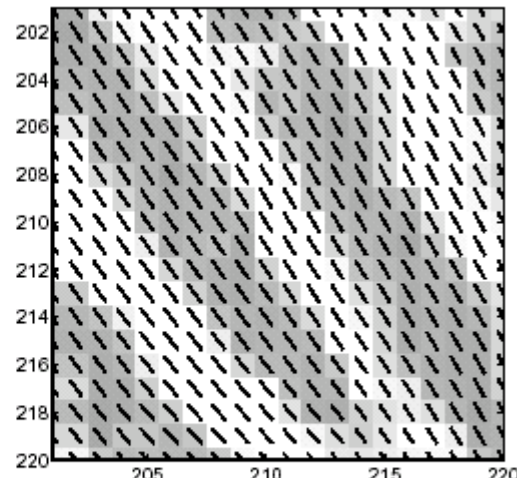
Orientation Field Estimation

- Divide the input fingerprint image into non-overlapping blocks of size $W \times W$ (e.g. 16×16)
- Compute the gradients G_x and G_y at each pixel in each block
- Estimate the (optimal in the least squares sense) local orientation at each pixel $[i,j]$ using the following equations:

$$V_x(i,j) = \sum_{u=i-\frac{W}{2}}^{i+\frac{W}{2}} \sum_{v=j-\frac{W}{2}}^{j+\frac{W}{2}} 2G_x(u,v)G_y(u,v),$$
$$V_y(i,j) = \sum_{u=i-\frac{W}{2}}^{i+\frac{W}{2}} \sum_{v=j-\frac{W}{2}}^{j+\frac{W}{2}} (G_x^2(u,v) - G_y^2(u,v)),$$
$$\theta(i,j) = \frac{1}{2} \tan^{-1} \left(\frac{V_x(i,j)}{V_y(i,j)} \right),$$



(a) Gradients



(b) Directional field

Orientation Field Estimation (2)

Hierarchical re-estimation based on consistency level of the orientation field in the local neighborhood of a block with the following formula:

$$C(i,j) = \frac{1}{N} \sqrt{\sum_{(i',j') \in D} |\theta(i',j') - \theta(i,j)|^2},$$
$$|\theta' - \theta| = \begin{cases} d & \text{if } (d = (\theta' - \theta + 360) \bmod 360) < 180, \\ d - 180 & \text{otherwise,} \end{cases}$$

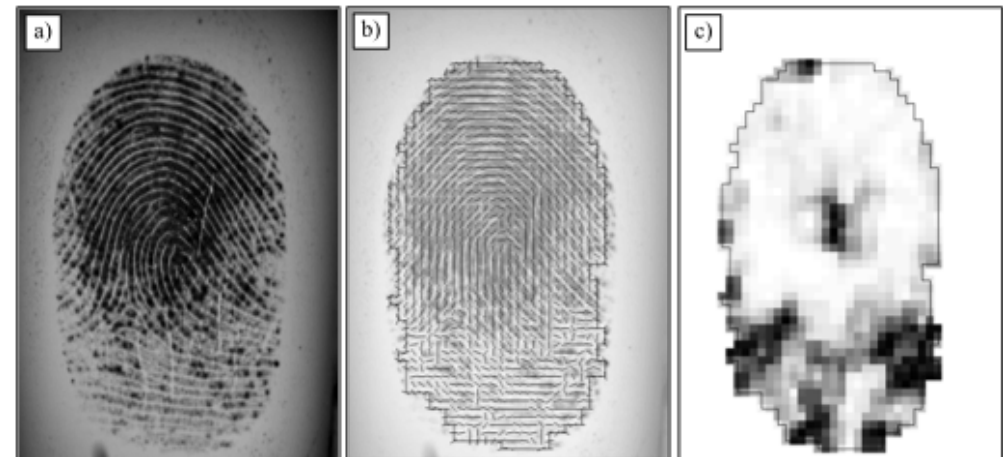


Figure 3.10. A fingerprint image (a), its local orientation (b) computed with Equation (3) and its local coherence (c) computed with Equation (4) over 3x3 blocks.

D represents the local neighborhood (e.g. 5x5) around the block (i, j) ; N is the number of blocks within D ; $\theta(i',j')$ and $\theta(i,j)$ are local ridge orientations at blocks (i',j') and (i,j) , respectively.

Orientation Field Estimation



(a) Method proposed in [56]



(b) Hierarchical method

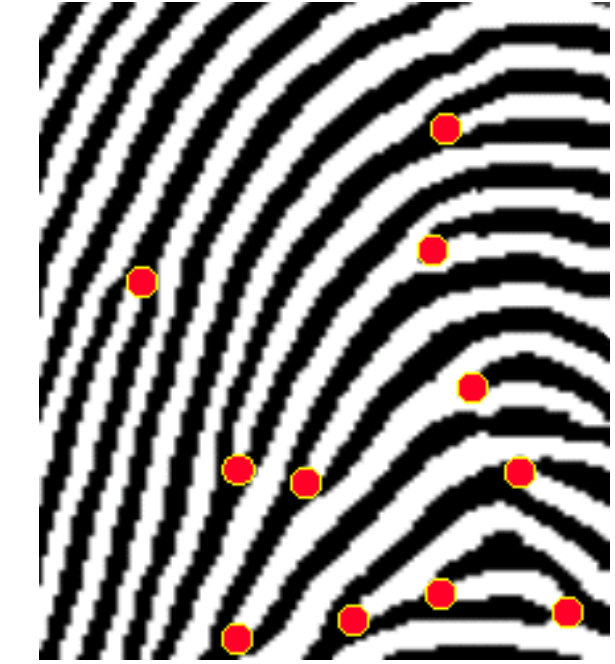
Figure 9. Comparison of orientation fields by the method proposed in [56] and the hierarchical method; the block size ($W \times W$) is 16×16 and the size of D is 5×5 .

Representation L2 Minutiae extraction



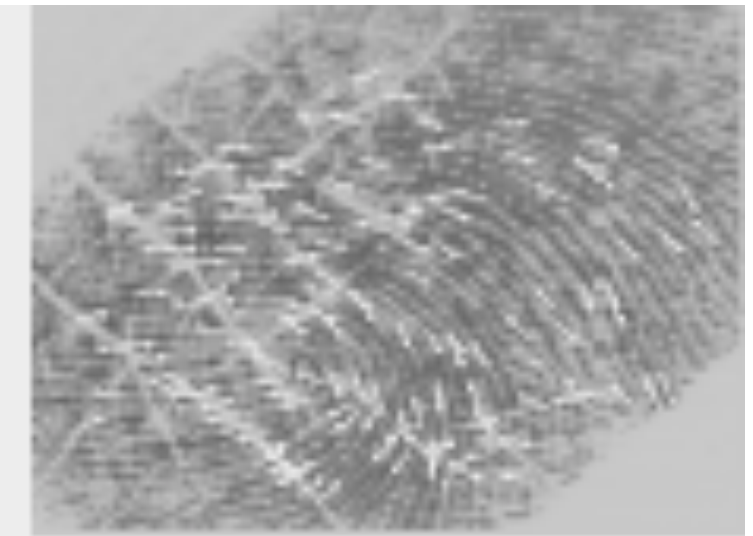
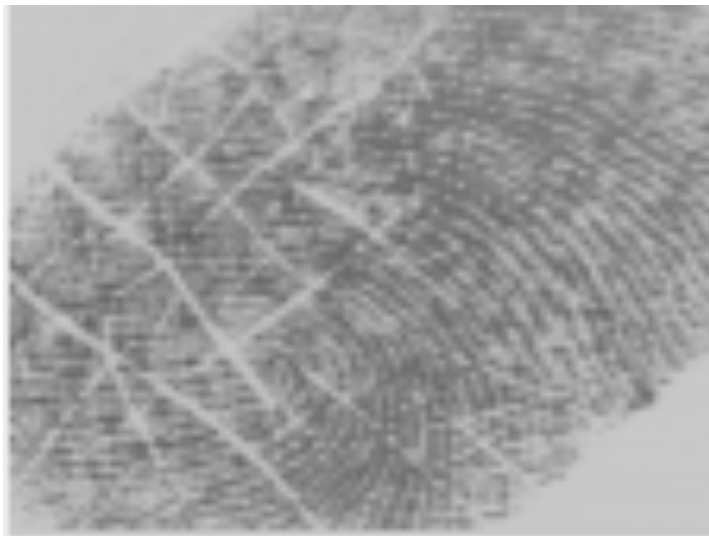
Minutiae Detection (1)

- Minutiae extracted from ridge image
- Trivial if ridge image perfect



Minutiae Detection (1)

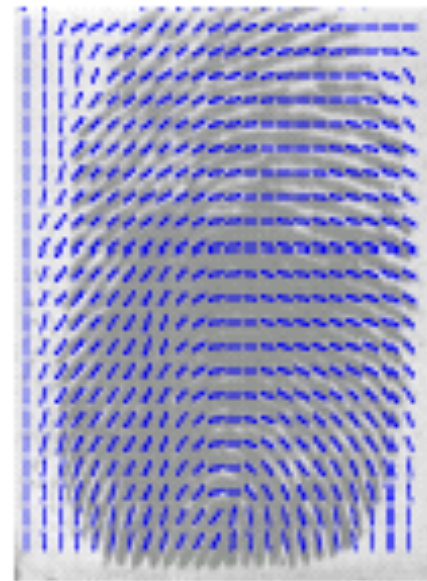
- Ridge image not perfect!
- Extraction should degrade gracefully with quality



Minutiae Detection (1): Algorithm



original



directional field



ridges



thinned



minutiae

Ridge detection: Gray Scale to Binary Conversion



(a) G_S



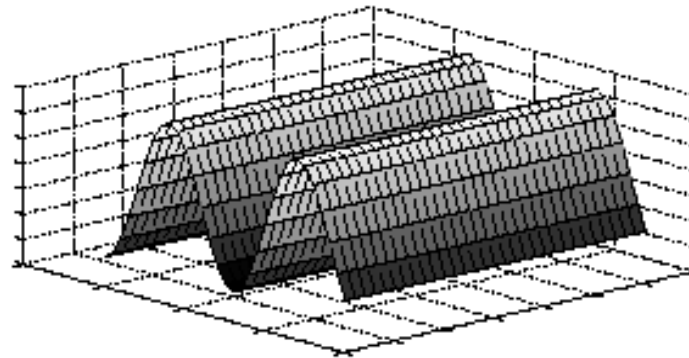
(b) B



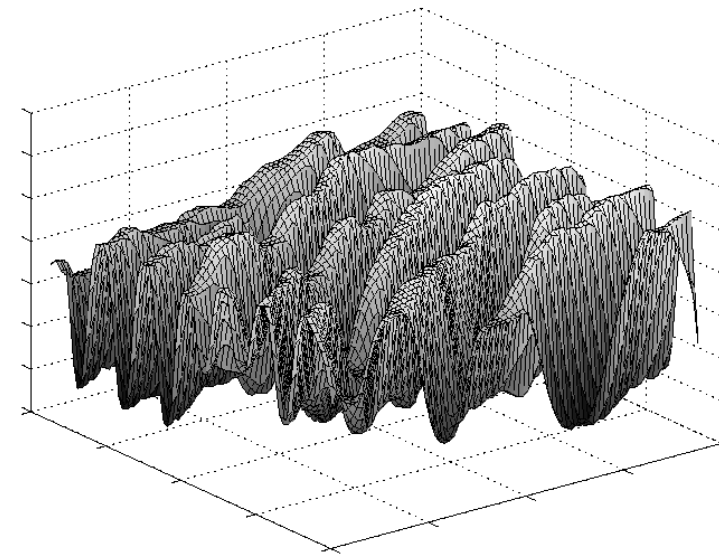
Ridge Detection: template matching

Gray level values in ridges attain local maxima along direction normal to the local ridge orientation
or

Maximum along one of the principal curvatures and zero other principal curvature



ideal

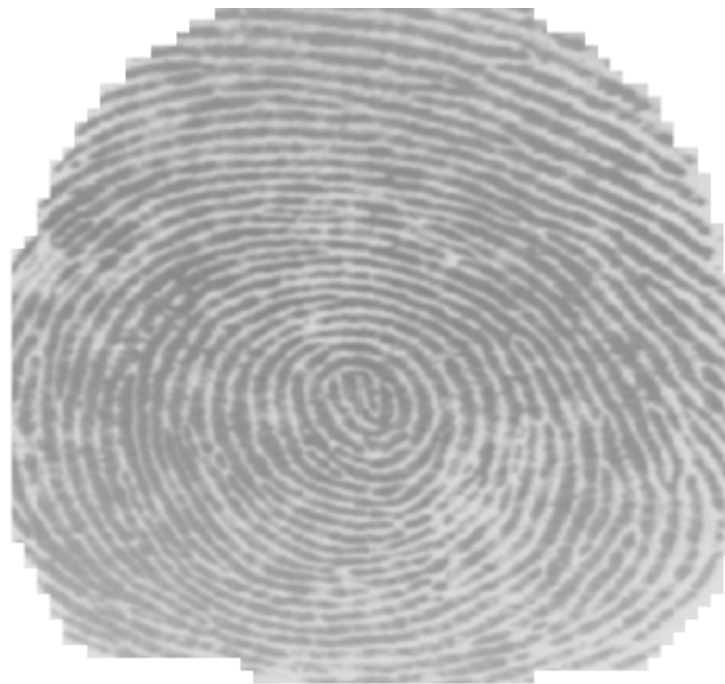


Real fingerprint detail

Ridge Detection: Binary to Skeleton Conversion



Ridge Detection



original



Ridge
Thinned
Cleaned:

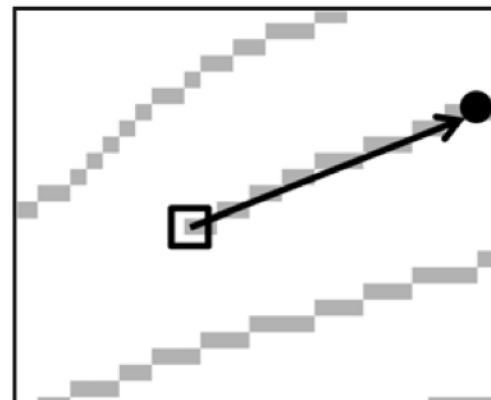
- remove spikes
- join broken ridges

Minutiae Detection (1)

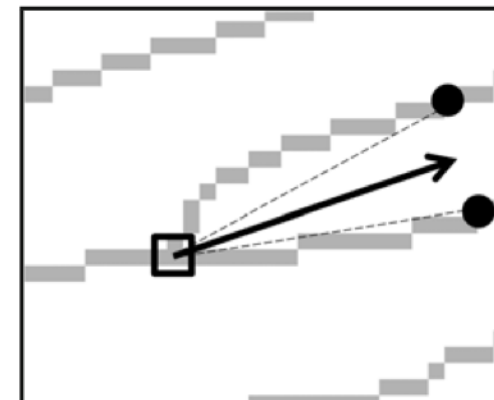
Let (x,y) denote a pixel on a thinned ridge
and N_0, \dots, N_7 its 8 neighbors

$$\sum_{i=0}^7 N_i = 1$$

$$\sum_{i=0}^7 N_i > 2$$



(a)



(b)

Fig. 2.25 Direction of a minutia. (a) Ridge ending and (b) ridge bifurcation.

Minutiae filtering

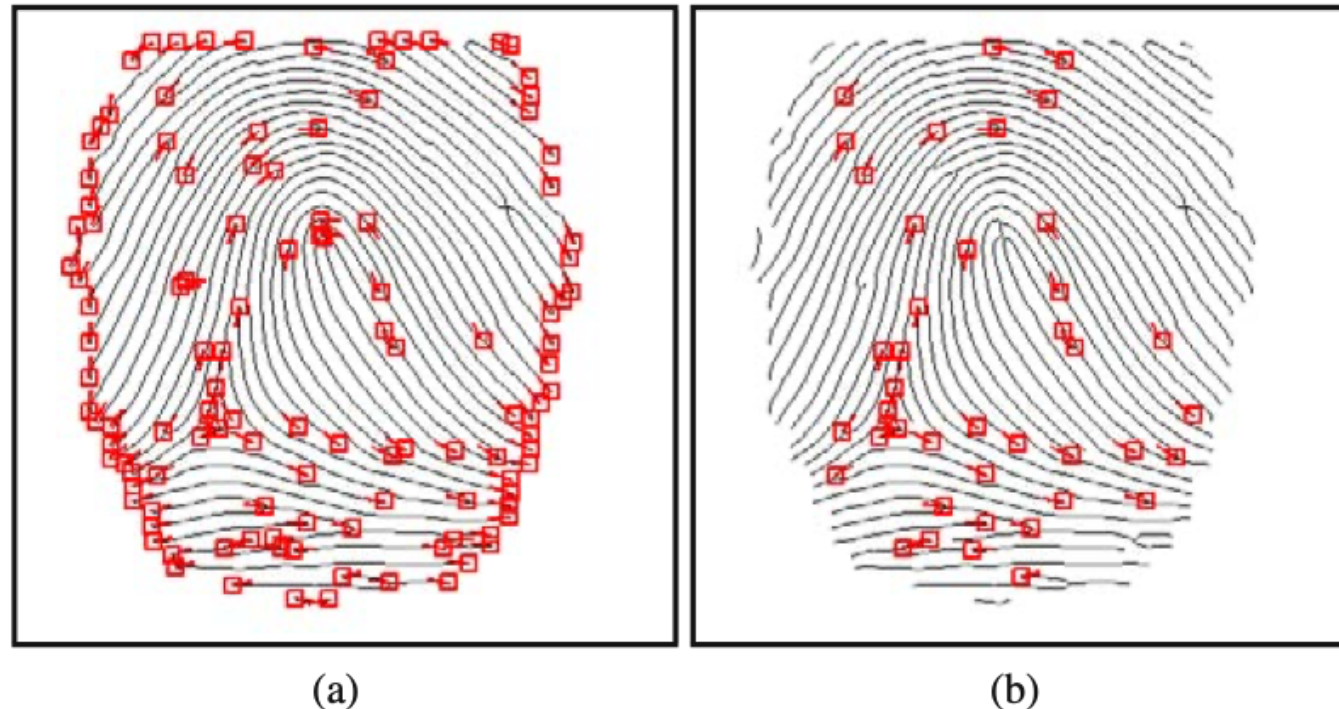


Fig. 2.26 Removing spurious minutiae. (a) Before minutiae filtering and (b) after minutiae filtering.

Minutiae Detection: number of minutiae

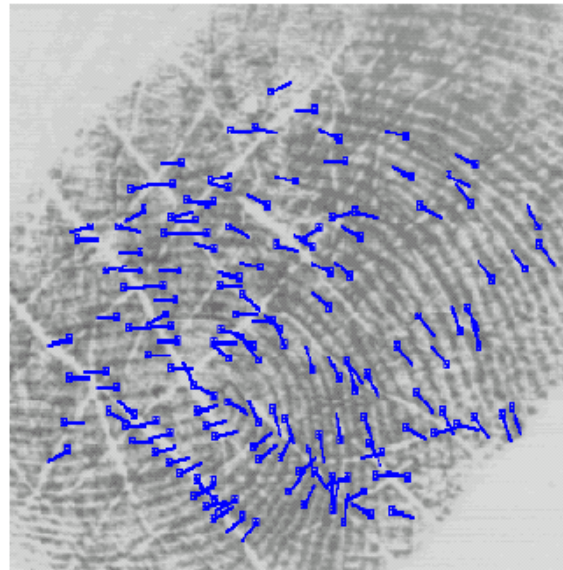
Impression type	Average number of minutiae	Sensor area
Rolled fingerprints	~80	~422 mm ²
Flat fingerprints	~20–30	211 mm ²
Latent fingerprints	~13–22	—
Smartphone fingerprints	~5–8	50–100 mm ²

Table 1.1 Average number of minutiae recovered from typical fingerprint impressions

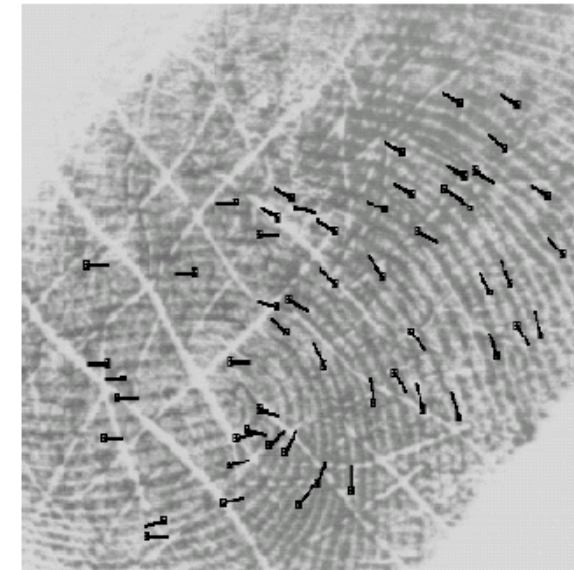
Minutiae Quality =f(preprocessing)



(a)



(b)



(c)

Figure 20: Fingerprint Enhancement Results: (a) a poor quality fingerprint; (b) minutia extracted without image enhancement; and (c) minutiae extracted after image enhancement [10].

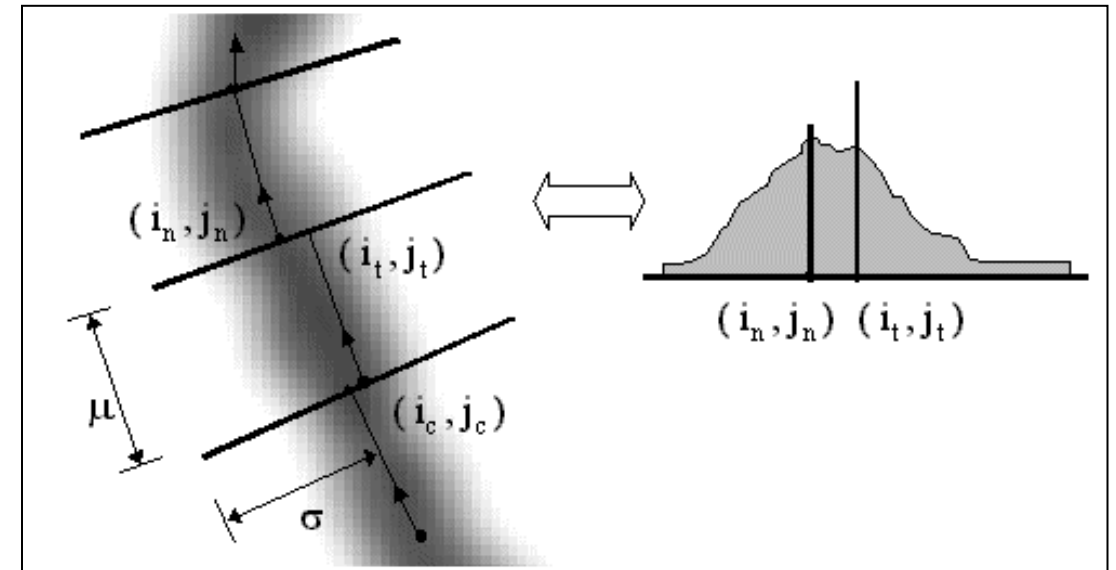
Minutiae Detection (2): directly from gray scale images

Some authors have proposed minutiae extraction approaches that work **directly on the gray-scale images without binarization and thinning**. This choice is motivated by the following considerations:

- A significant amount of information may be lost during the binarization process.
- Binarization and thinning are time consuming; thinning may introduce a large number of spurious minutiae.
- In the absence of an a priori enhancement step, most of the binarization techniques do not provide satisfactory results when applied to low-quality images.

Minutiae Detection (2): directly from gray scale images

- Minutiae detected directly from gray scale images
- The basic idea of this method is to follow the ridge lines on the gray-scale image, by "sailing" according to the fingerprint directional image. The algorithm keeps following the ridge lines until they terminate or intersect other ridge lines (minutiae detection).



NN-based detection

- Minutiae detection by NN or filter-based classification

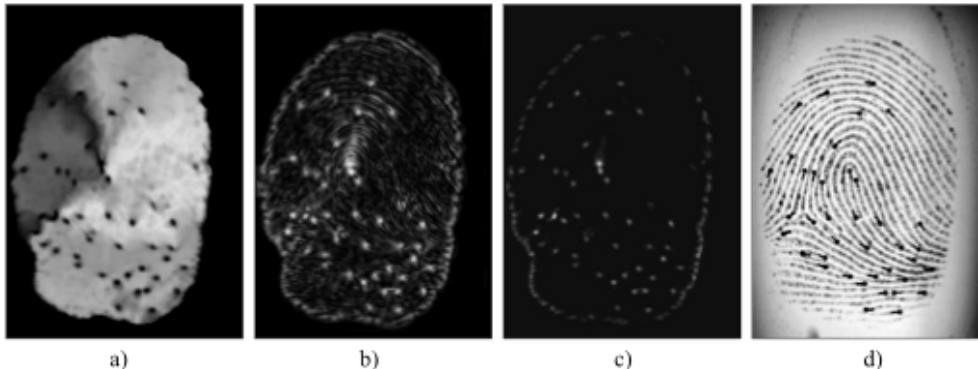


Figure 3.48. Application of the minutiae detection method proposed by Fronthaler, Kollreider, and Bigun (2008) to the fingerprint image d). a) Linear Symmetry (LS), b) Parabolic Symmetry (PS), c) $PS \cdot (1 - |LS|)$, d) minutiae detected as local maxima of c) superimposed to the original fingerprint image. Images courtesy of J. Bigun.

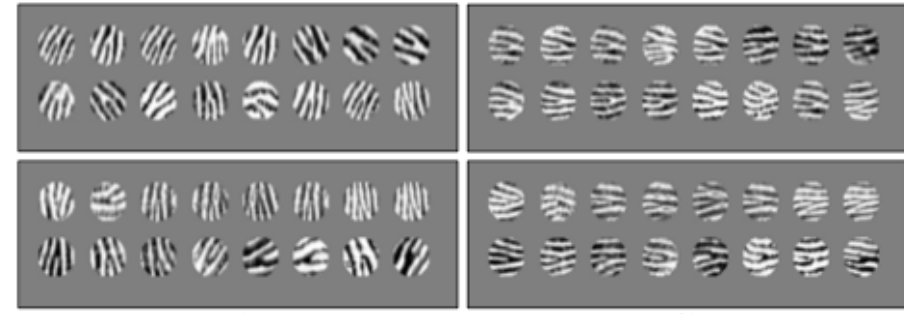


Figure 3.52. a) Minutiae neighborhoods (ridge ending minutiae at the top, bifurcation minutiae at the bottom) as they appear in the original gray-scale images; b) the same neighborhoods have been normalized with respect to minutiae angle and local ridge frequency (Maio and Maltoni, 1998b). © IEEE.

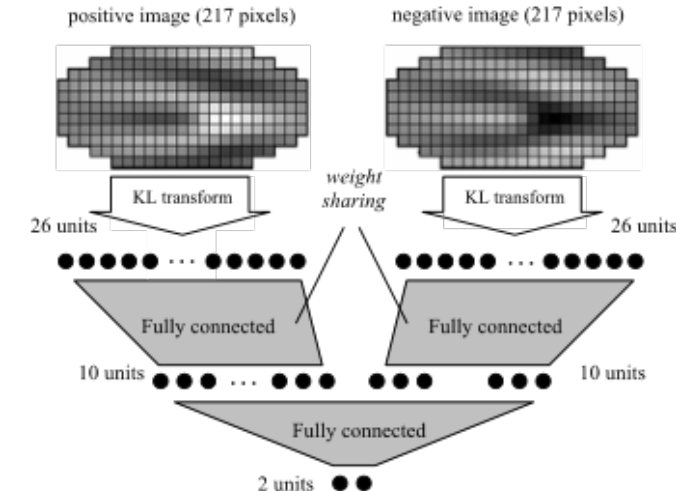


Figure 3.53. The neural network architecture to classify gray-scale minutiae neighborhoods into ridge ending, bifurcation, and non-minutiae (Maio and Maltoni, 1998b). © IEEE.

3D FP minutiae extraction

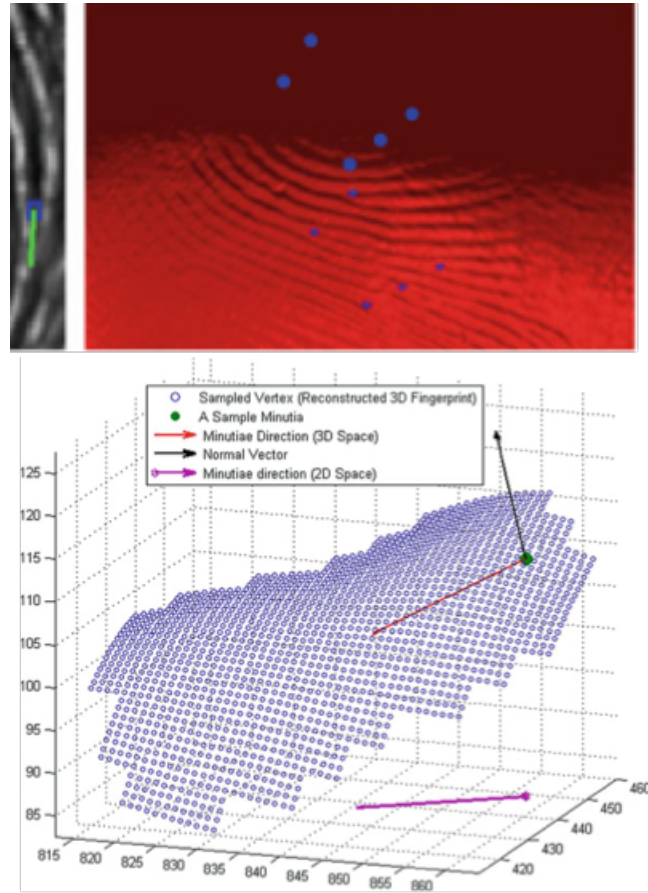


Fig. 6.3 Representation of minutiae feature in 3D space on a reconstructed 3D fingerprint surface. The purple arrow on 2D or $x-y$ plane illustrates the orientation of original 3D minutia in a conventional 2D fingerprint template. This 2D minutia orientation (purple arrow) is defined on a local ridge surface (blue dot) and can be used to estimate the 3D minutia orientation (red arrow)

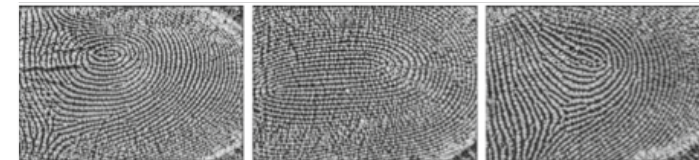


Fig. 6.4 Sample images representation of local 3D surface curvature using shape index images

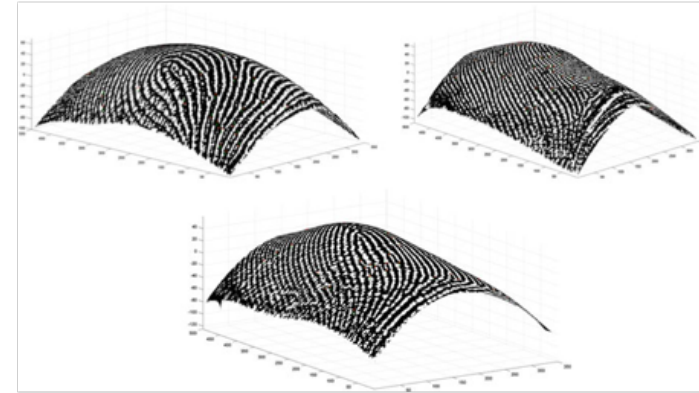


Fig. 6.5 Sample 3D fingerprint images illustrating ridge–valley structure identified from the local surface curvature values

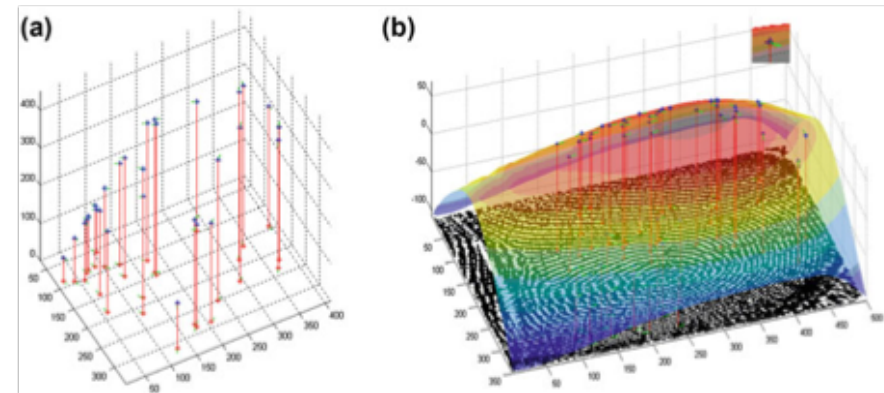
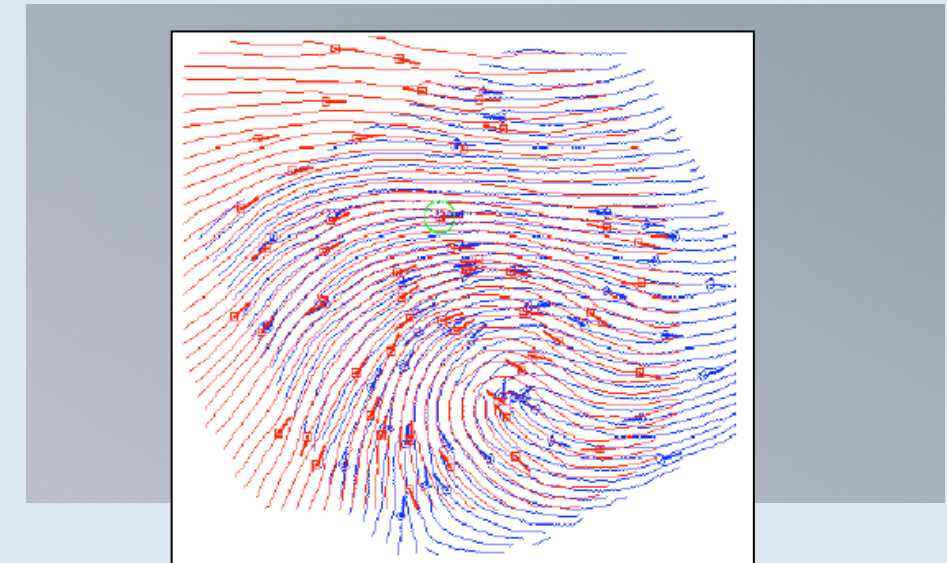


Fig. 6.6 Localization of minutiae in 3D space by incorporating minutiae height in (a) and illustration of 3D fingerprint with recovered minutiae locations in 3D space (b)

Fingerprint Matching



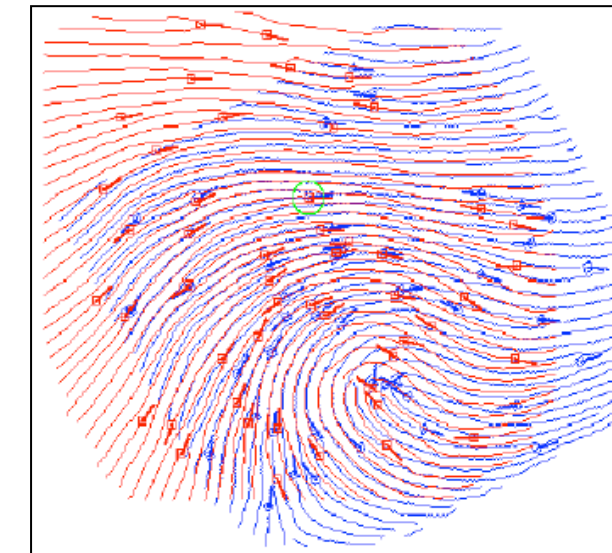
Fingerprint Matching

Compare probe and template representation

- define/calculate **correspondence between features**
- define/calculate **transformation** (rigid/non-rigid)
- define/calculate matching **metric**
- define a threshold on acceptable matching



Figure 4. Two different fingerprint impressions of the same finger. In order to know the correspondence between the minutiae of these two fingerprint images, all the minutiae must be precisely localized and the deformations must be recovered.



Fingerprint Matching difficulties: large intra-class variations

Variable positioning

- global **translation**
2mm at 500 dpi is 40 pixels
- **Rotation**
up to 20deg
- **Partial overlap**
especially with small sensors



Fingerprint Matching difficulties: large intra-class variations

Inconsistent mapping of 3-D shape of finger
onto 2-D surface of glass platen

- scaling
pressure
- shear
- local deformations
small up to only connectivity preserving)



Fingerprint Matching difficulties: large intra-class variations

Pressure and skin condition

- Non-uniform contact
 - skin dryness, sweat, dirt, humidity
- ridges not in contact, valleys in contact
 - leading to spurious or missing minutiae



Irreproducible contact

injuries changing the ridge structure

Feature extraction errors

Additional acquisition errors

parallax distortion

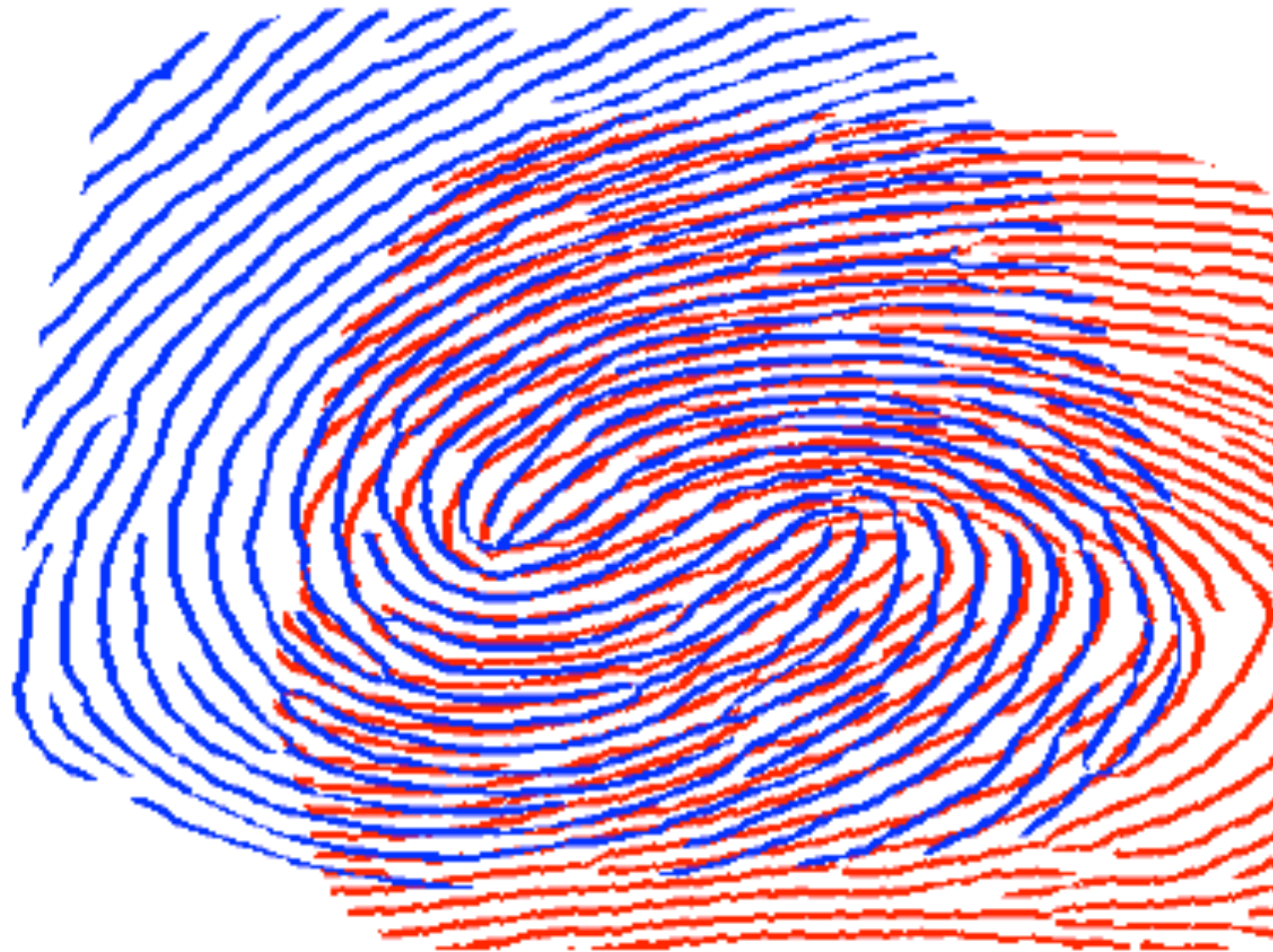
previous fingerprint residues

Matching Transformations

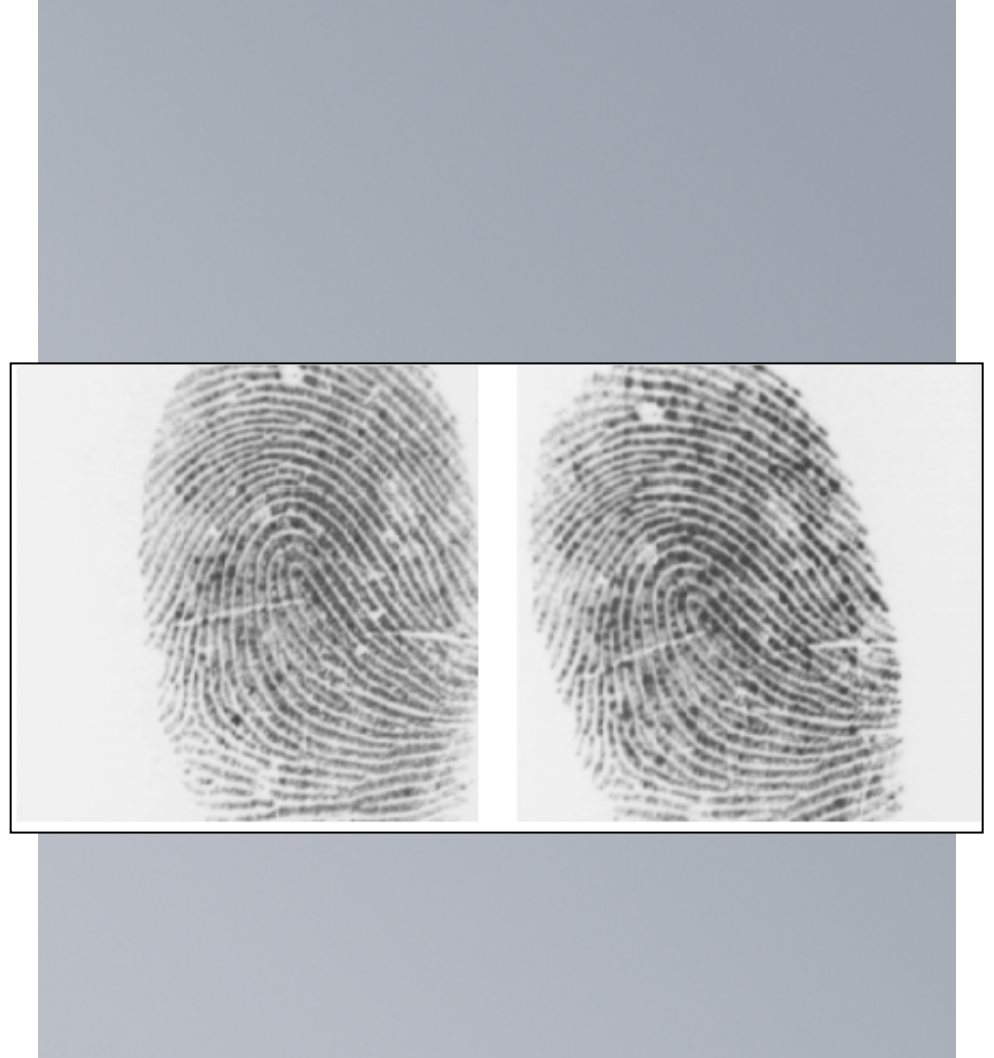
- Euclidean (translation and rotation)
- Similarity (Euclidean + scaling)
- Affine (Similarity + shear)
- Elastic (Affine + local, small, continuous perturbations)
- Topological (connectivity preserving)?



Example



L1 feature (image/ridge) matching



Correlation based matching

Enhancement



(a)



(b)



(c)

Correlation based matching

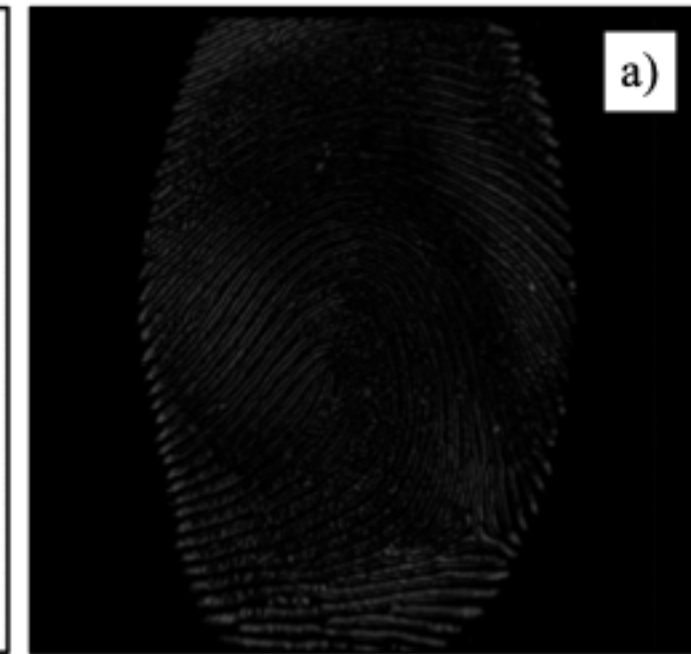
$$SSD(\mathbf{T}, \mathbf{I}) = \|\mathbf{T} - \mathbf{I}\|^2 = (\mathbf{T} - \mathbf{I})^T (\mathbf{T} - \mathbf{I}) = \|\mathbf{T}\|^2 + \|\mathbf{I}\|^2 - 2\mathbf{T}^T \mathbf{I}$$

$$CC(\mathbf{T}, \mathbf{I}) = \mathbf{T}^T \mathbf{I}$$

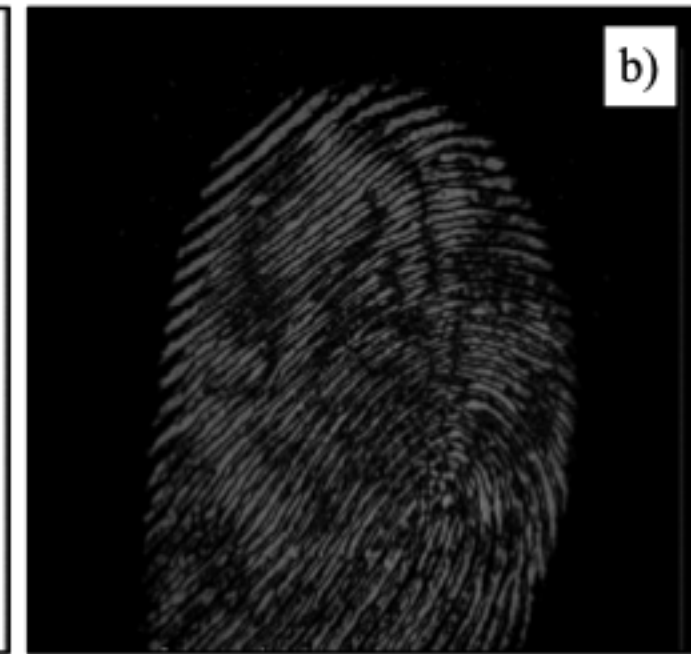
$$S(\mathbf{T}, \mathbf{I}) = \max_{\Delta x, \Delta y, \theta} CC(\mathbf{T}, \mathbf{I}^{(\Delta x, \Delta y, \theta)})$$



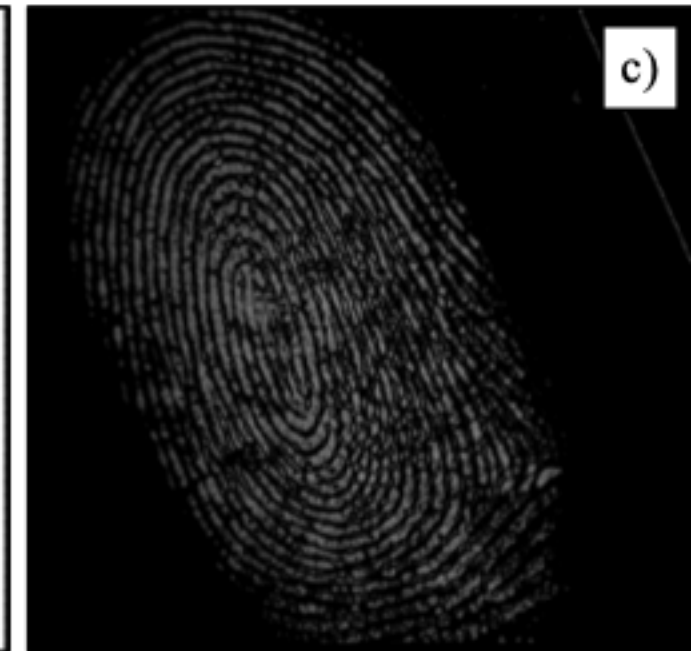
Correlation based matching



Correlation based matching

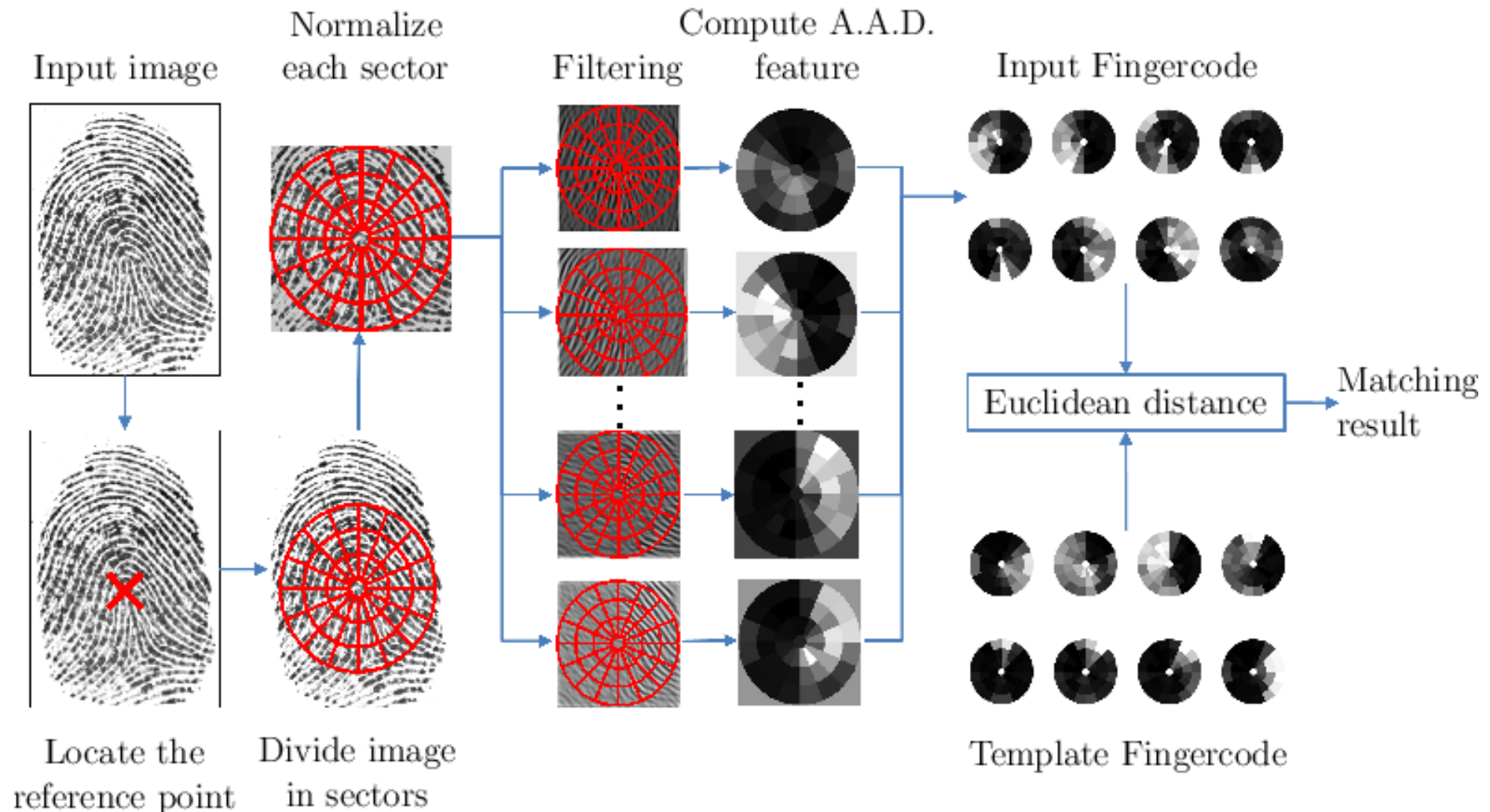


Correlation based matching

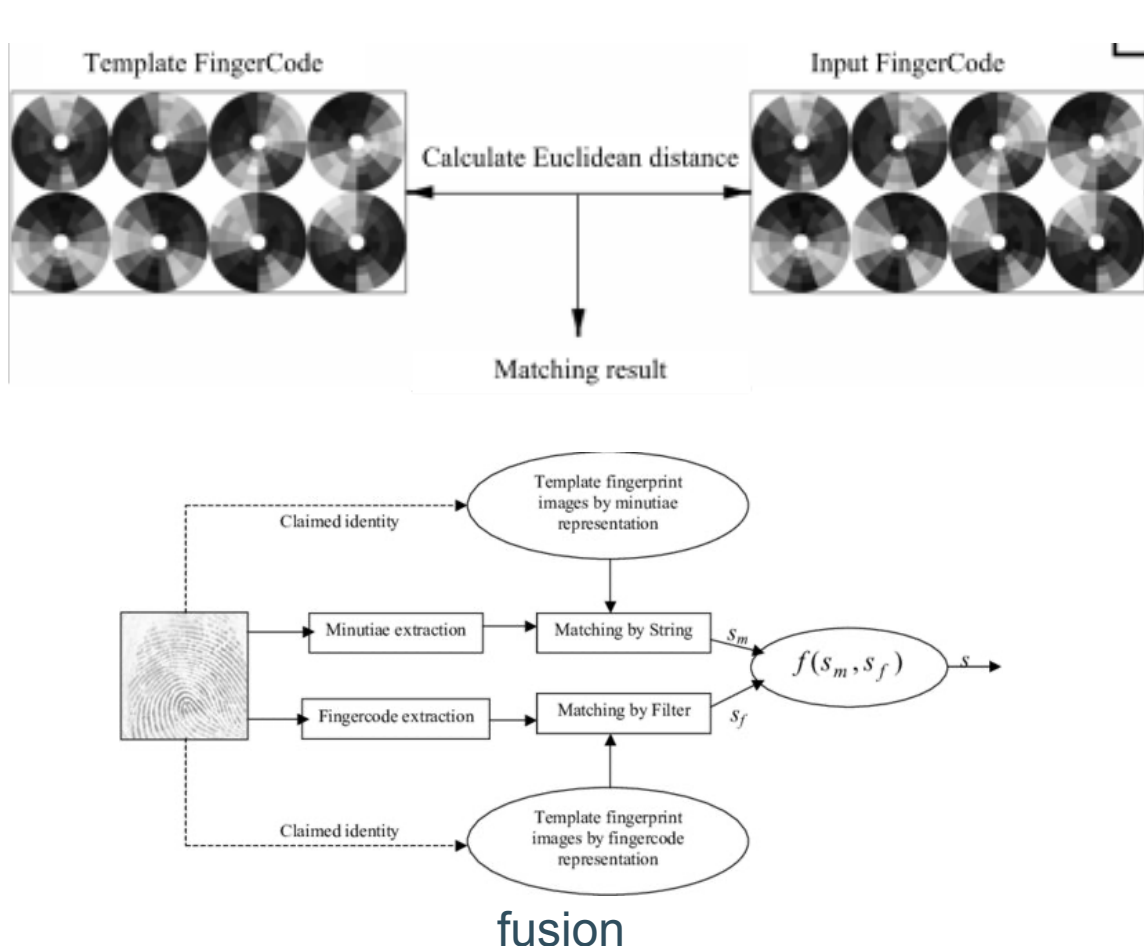


Correlation based matching

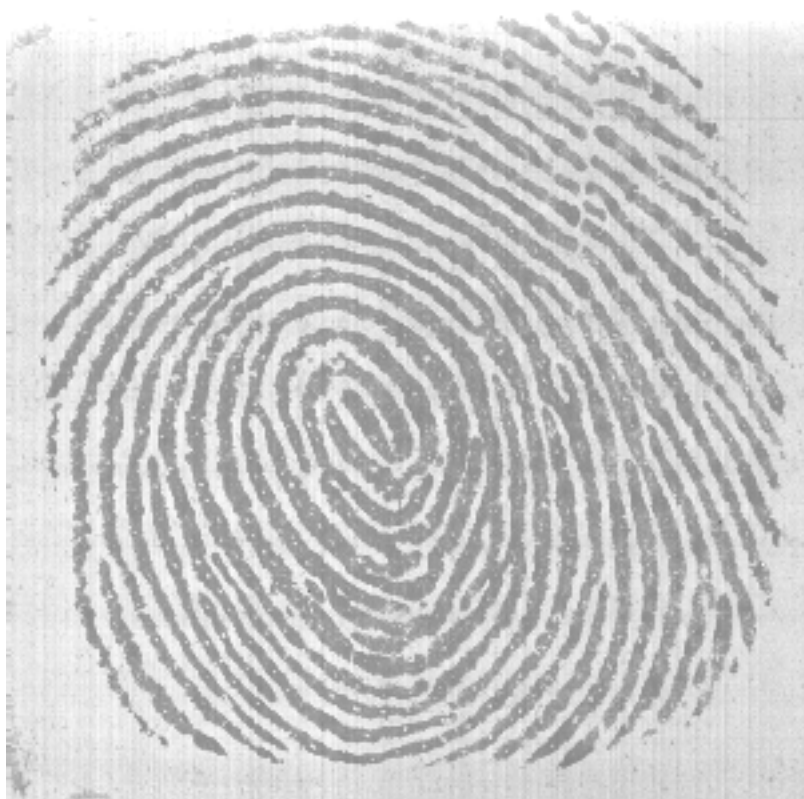
- FingerCode



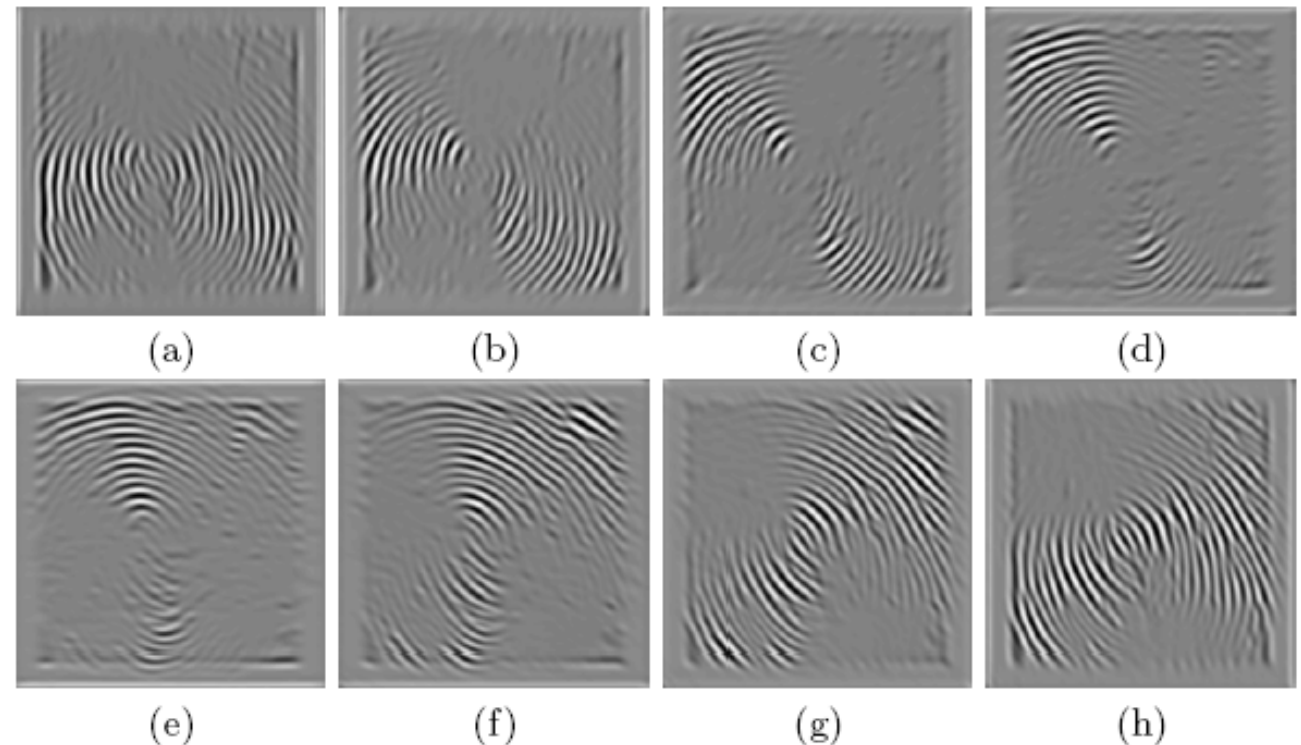
Correlation based matching



Correlation based matching

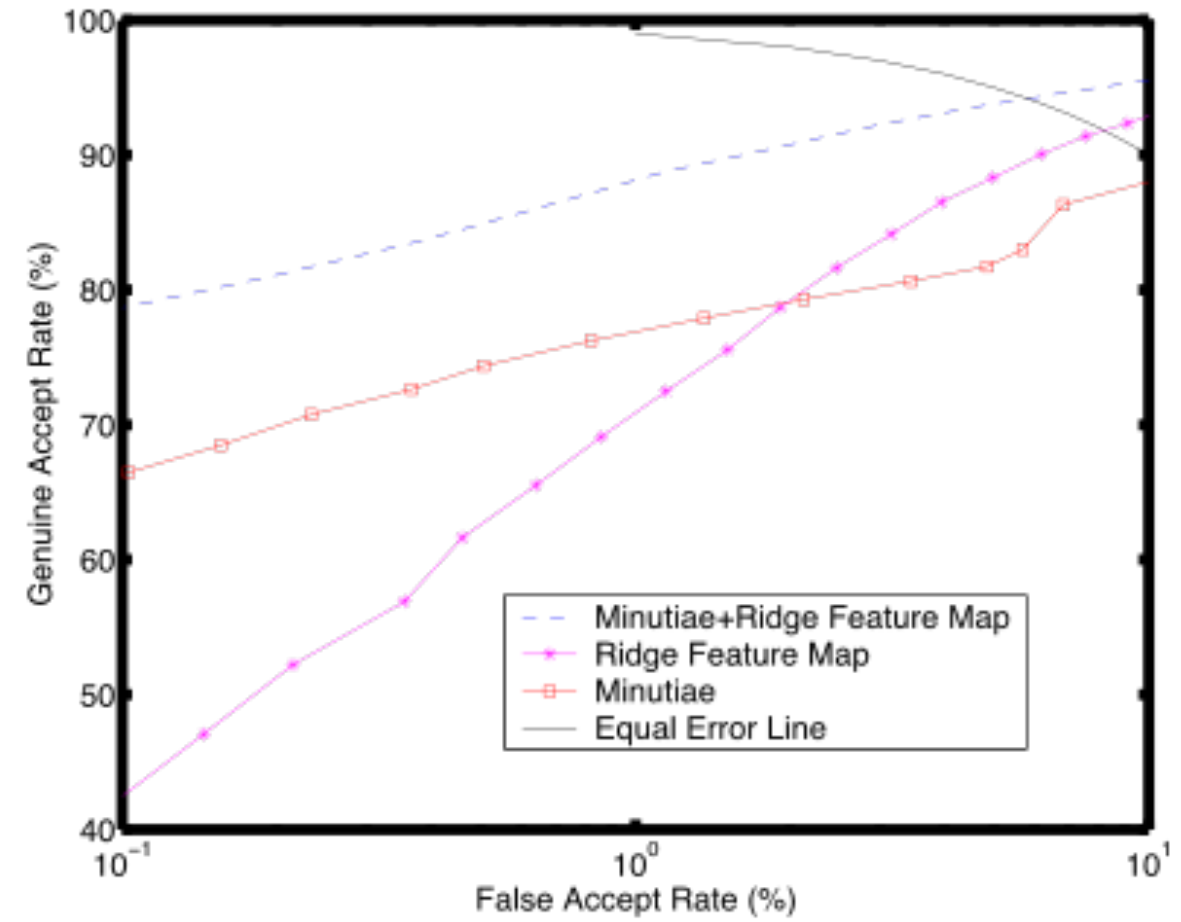
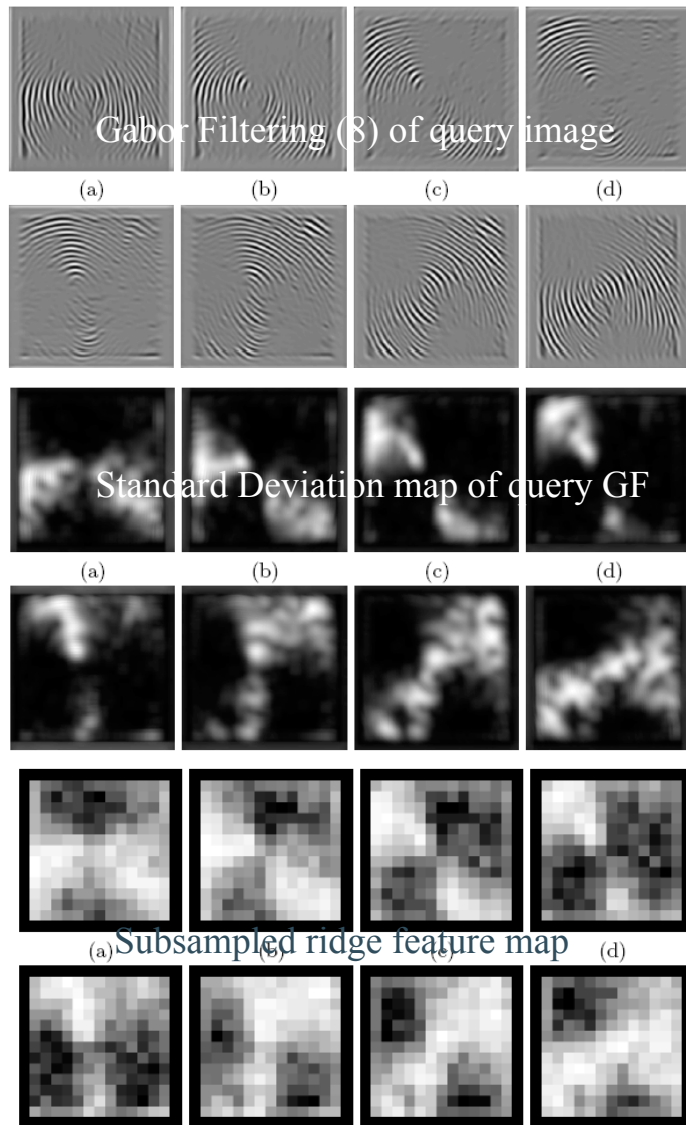


Query image

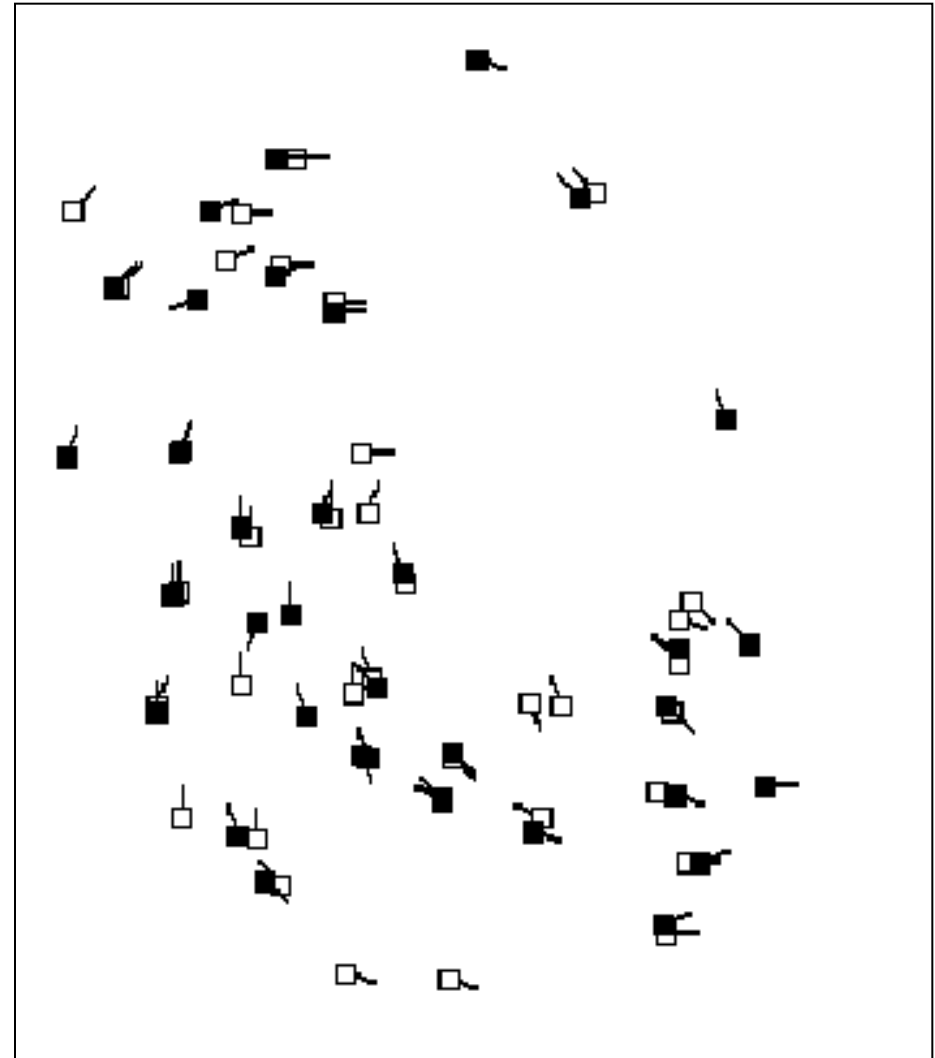


Gabor Filtering (8) of query image

Correlation based matching



L2 (minutiae) matching



Minutiae Matching

Reduces to point pattern matching

- define/calculate correspondence
- define/calculate transformation (rigid/non-rigid)
- define/calculate matching metric

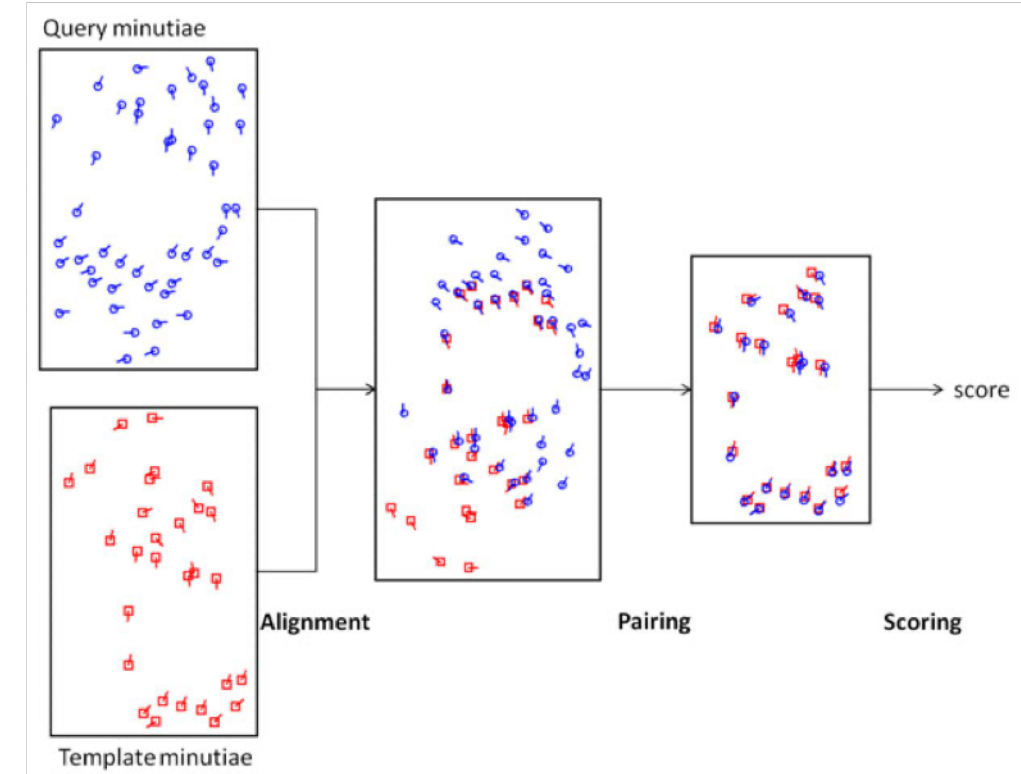
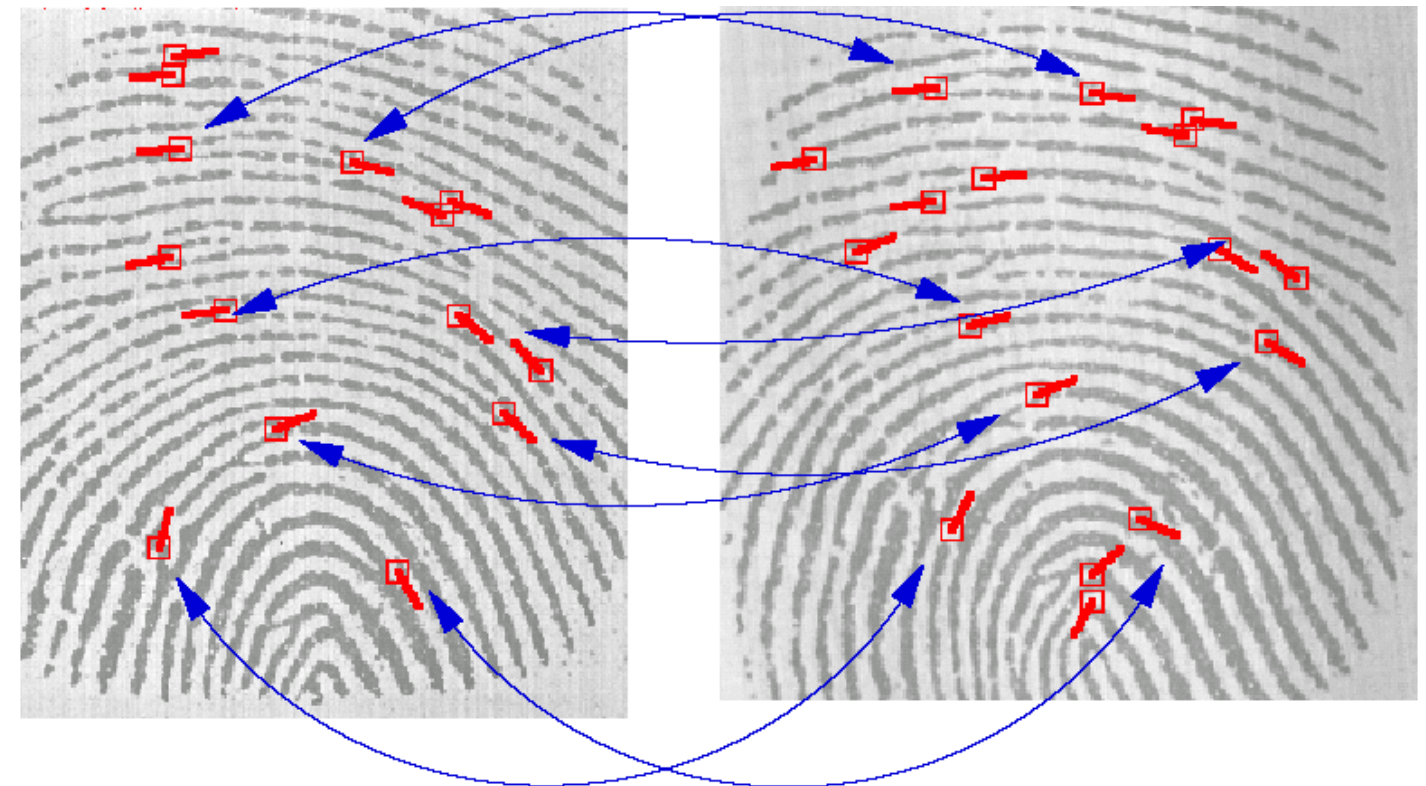


Fig. 2.27 Flowchart of a minutiae matching algorithm.

Minutiae Matching

- Strategies
 - Point Set (with attached attributes) Matching
 - Graph-matching
 - sub-graph isomorphism
- Optimisation
 - relaxation
 - simulated annealing
 - genetic algorithms
- Coping with
 - poor quality data
 - large databases
 - geometrical and structural distortion

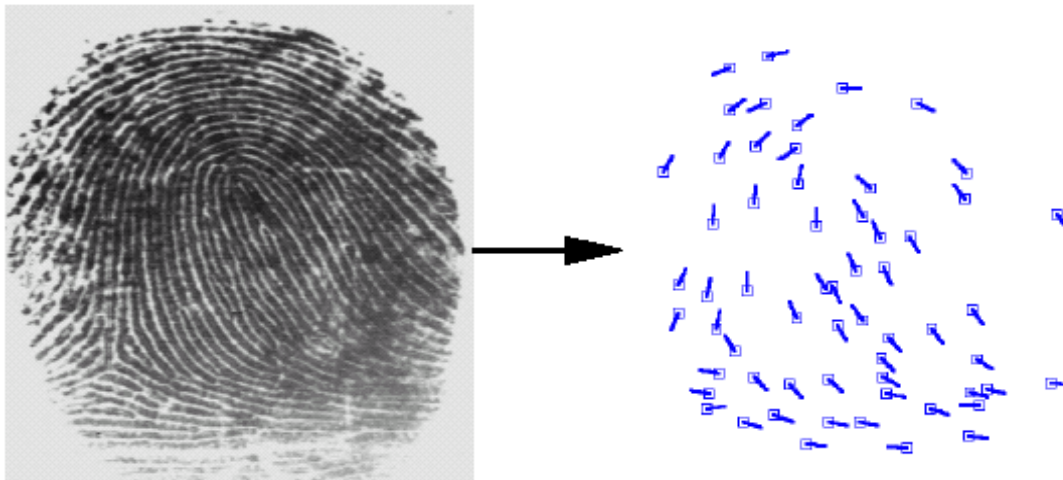


Minutiae Matching

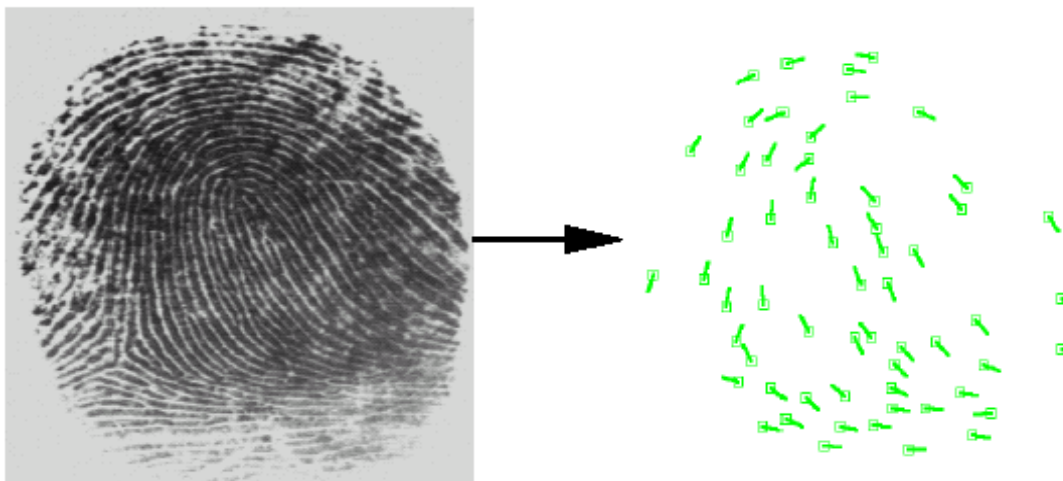
- Alignment/Registration
- Minutiae Pairing/Correspondence
- Matching score computation



Minutiae Matching: representation

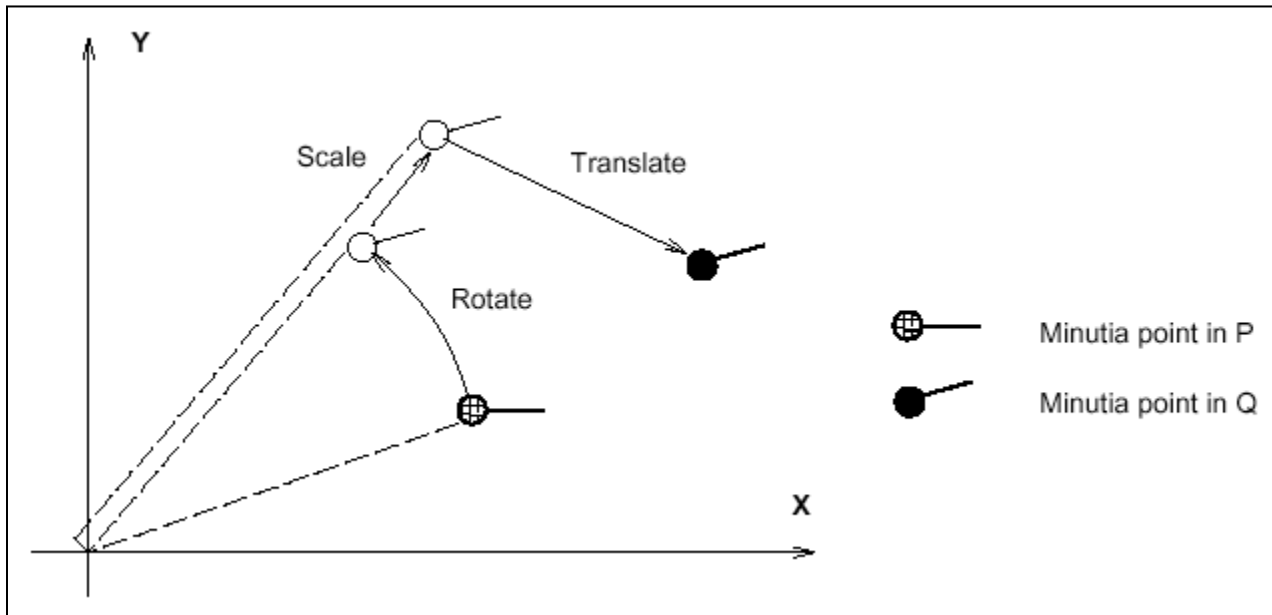


$$\mathbf{T} = \{\mathbf{m}_1, \mathbf{m}_2, \dots, \mathbf{m}_m\}, \quad \mathbf{m}_i = \{x_i, y_i, \theta_i\}, \quad i = 1 \dots m$$



$$\mathbf{I} = \{\mathbf{m}'_1, \mathbf{m}'_2, \dots, \mathbf{m}'_n\}, \quad \mathbf{m}'_j = \{x'_j, y'_j, \theta'_j\}, \quad j = 1 \dots n,$$

Minutiae Matching: rigid mapping



$map_{\Delta x, \Delta y, \theta}(\mathbf{m}'_j = \{x'_j, y'_j, \theta'_j\}) = \mathbf{m}''_j = \{x''_j, y''_j, \theta'_j + \theta\}$, where

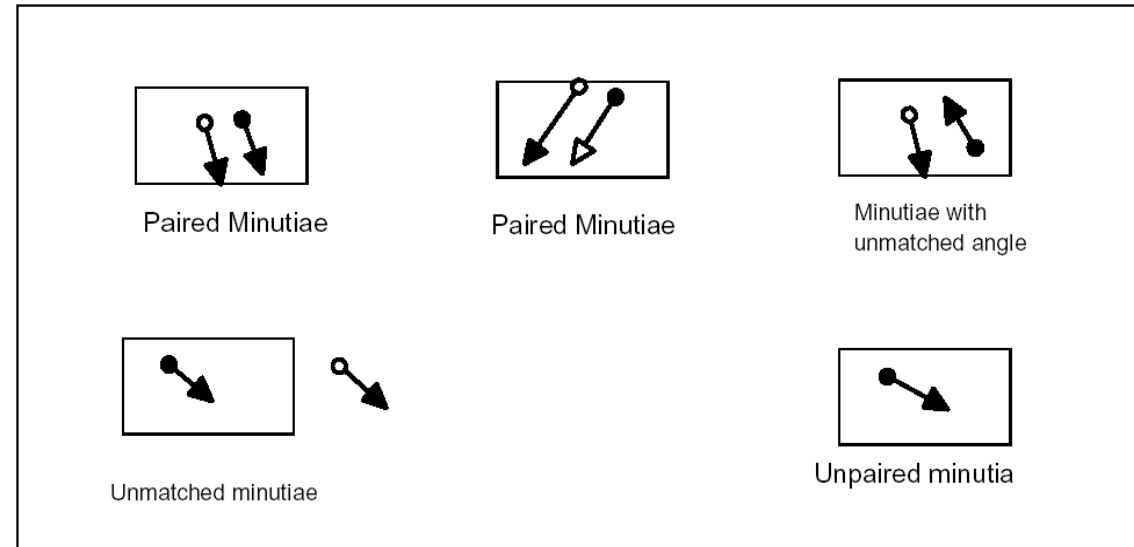
$$\begin{bmatrix} x''_j \\ y''_j \end{bmatrix} = \begin{bmatrix} \cos \theta & -\sin \theta \\ \sin \theta & \cos \theta \end{bmatrix} \begin{bmatrix} x'_j \\ y'_j \end{bmatrix} + \begin{bmatrix} \Delta x \\ \Delta y \end{bmatrix}.$$

Minutiae Matching: pairing

A minutia \mathbf{m}'_j in \mathbf{I} and a minutia \mathbf{m}_i in \mathbf{T} are considered “matching,” if the *spatial distance* (sd) between them is smaller than a given tolerance r_0 and the *direction difference* (dd) between them is smaller than an angular tolerance θ_0 :

$$sd(\mathbf{m}'_j, \mathbf{m}_i) = \sqrt{(x'_j - x_i)^2 + (y'_j - y_i)^2} \leq r_0, \text{ and} \quad (6)$$

$$dd(\mathbf{m}'_j, \mathbf{m}_i) = \min(|\theta'_j - \theta_i|, 360^\circ - |\theta'_j - \theta_i|) \leq \theta_0. \quad (7)$$



Minutiae Matching: matching

Find “best” Rigid Transform $(\theta, \Delta x, \Delta y)$ between minutiae points P and Q

Let $mm()$ be an indicator function that returns 1 in the case where the minutiae \mathbf{m}_j'' match according to Equations (6) and (7):

$$mm(\mathbf{m}_j'', \mathbf{m}_i) = \begin{cases} 1 & sd(\mathbf{m}_j'', \mathbf{m}_i) \leq r_0 \text{ and } dd(\mathbf{m}_j'', \mathbf{m}_i) \leq \theta_0 \\ 0 & \text{otherwise.} \end{cases}$$

Then, the matching problem can be formulated as

$$\underset{\Delta x, \Delta y, \theta, P}{\text{maximize}} \sum_{i=1}^m mm\left(map_{\Delta x, \Delta y, \theta}(\mathbf{m}'_{P(i)}), \mathbf{m}_i\right),$$

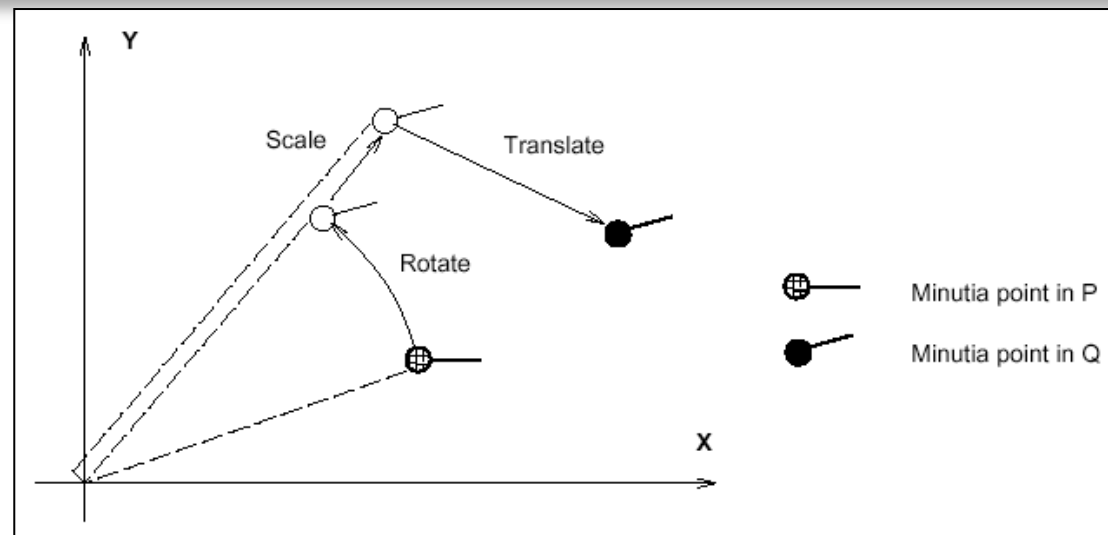
where $P(i)$ is an unknown function that determines the *pairing* between I and T minutiae

= Point Pattern Matching!

Minutiae Matching: matching using Hough Transform

Find “best” Similarity Transform ($s, \theta, \Delta x, \Delta y$) between minutiae points P and Q

$$F_{s,\theta,\Delta x,\Delta y} \begin{pmatrix} x \\ y \end{pmatrix} = s \begin{pmatrix} \cos \theta & \sin \theta \\ -\sin \theta & \cos \theta \end{pmatrix} \begin{pmatrix} x \\ y \end{pmatrix} + \begin{pmatrix} \Delta x \\ \Delta y \end{pmatrix}$$



Minutiae Matching: matching using Hough Transform

- “**Best**” = # {overlapping and matching (same orientation) minutiae points} is maximal
- Found using **generalized Hough Transform**
- Uses Accumulator Array A with $A(k,l,m,n)$ counting the evidence for $F_{s,\theta,\Delta x,\Delta y}$
- For each pair $(p,q) \in P \times Q$ find all possible transformations $F_{s,\theta,\Delta x,\Delta y}$ that map p to q:
 - $\forall (s_k, \theta_l): \exists! (\Delta x, \Delta y): F_{s,\theta,\Delta x,\Delta y}(p) = q$

$$\begin{pmatrix} \Delta x \\ \Delta y \end{pmatrix} = q - s_k \begin{pmatrix} \cos \theta_l & \sin \theta_l \\ -\sin \theta_l & \cos \theta_l \end{pmatrix} p.$$

$\Delta x, \Delta y$ quantized in bins

Minutiae Matching: matching using Hough Transform

for each \mathbf{m}_i , $i = 1 \dots m$

for each \mathbf{m}'_j , $j = 1 \dots n$

for each $\theta^+ \in \{\theta_1^+, \theta_2^+, \dots, \theta_c^+\}$

(if $dd(\theta'_j + \theta^+, \theta_i) < \theta_0$ // the minutiae directions after the rotation are sufficiently close as per Equation (7))

for each $s^+ \in \{s_1^+, s_2^+, \dots, s_d^+\}$

$$\begin{bmatrix} \Delta x \\ \Delta y \end{bmatrix} = \begin{bmatrix} x_i \\ y_i \end{bmatrix} - s^+ \cdot \begin{bmatrix} \cos \theta^+ & -\sin \theta^+ \\ \sin \theta^+ & \cos \theta^+ \end{bmatrix} \begin{bmatrix} x'_j \\ y'_j \end{bmatrix} \quad // \text{the map function including scale}$$

$\Delta x^+, \Delta y^+$ = quantization of $\Delta x, \Delta y$ to the nearest bin

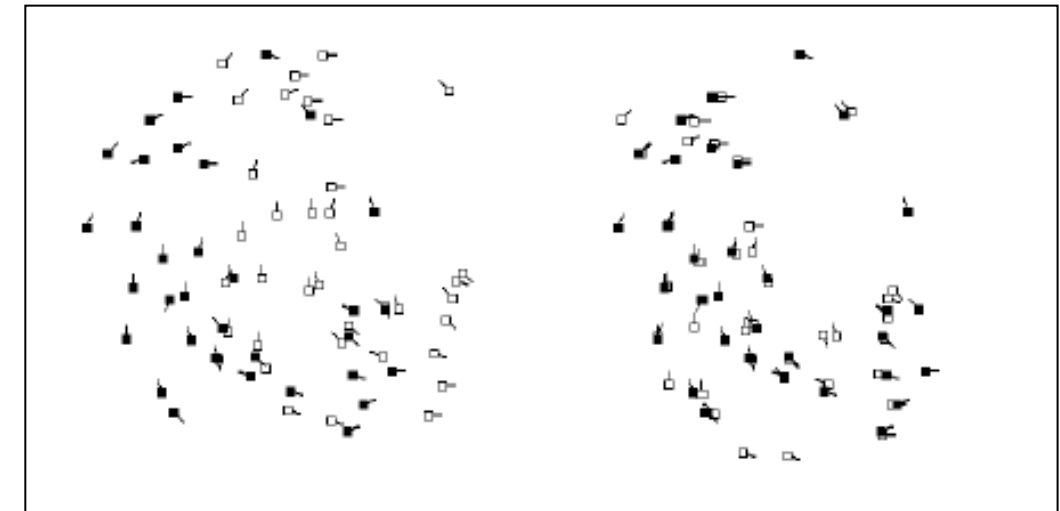
$$\mathbf{A}[\Delta x^+, \Delta y^+, \theta^+, s^+] = \mathbf{A}[\Delta x^+, \Delta y^+, \theta^+, s^+] + 1$$

At the end of the accumulation process, the best alignment transformation $(\Delta x^*, \Delta y^*, \theta^*, s^*)$ is obtained as

$$(\Delta x^*, \Delta y^*, \theta^*, s^*) = \arg \max_{\Delta x^+, \Delta y^+, \theta^+, s^+} \mathbf{A}[\Delta x^+, \Delta y^+, \theta^+, s^+]$$

Alignment improvements

- Increment neighboring bins as well
- Take directions of minutiae into account: increment only if minutiae direction at p when rotated by θ_l is the same (or about) as the direction in q
- Result:



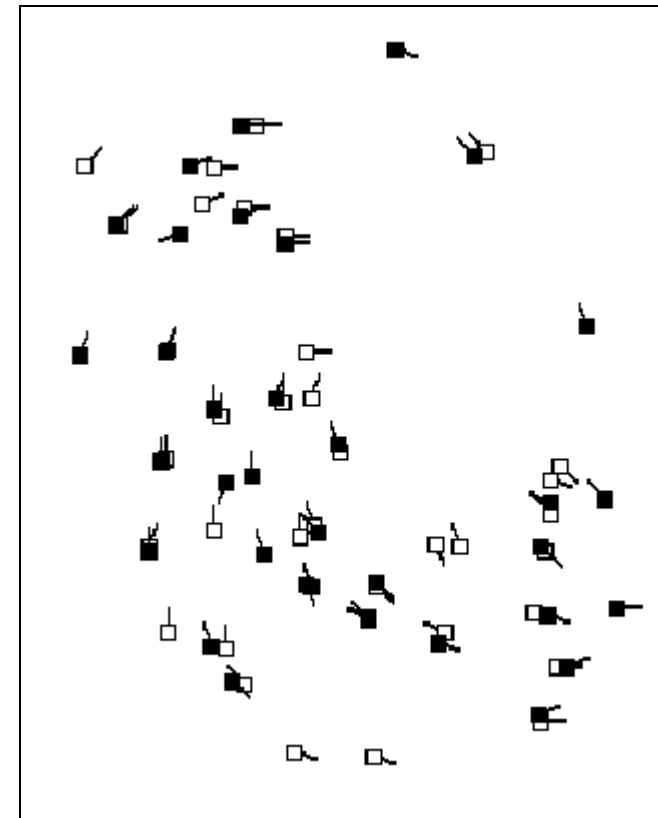
Minutiae matching scoring

- Alignment/Registration
- Minutiae Pairing/Correspondence
- Matching score computation

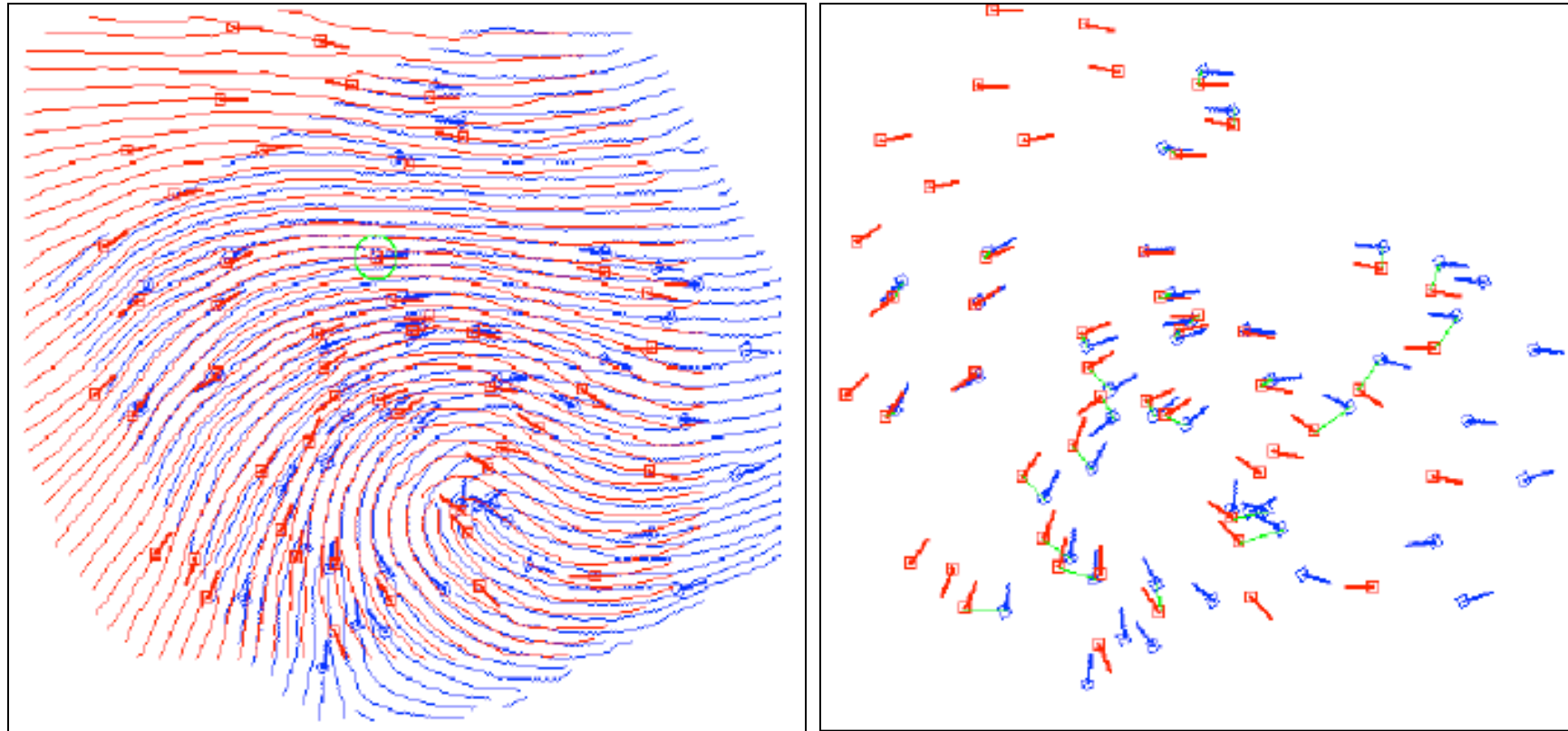
$$S = \frac{100 M_{PQ} M_{PQ}}{M_P M_Q},$$

Errors in localizing minutiae
nonlinear deformations

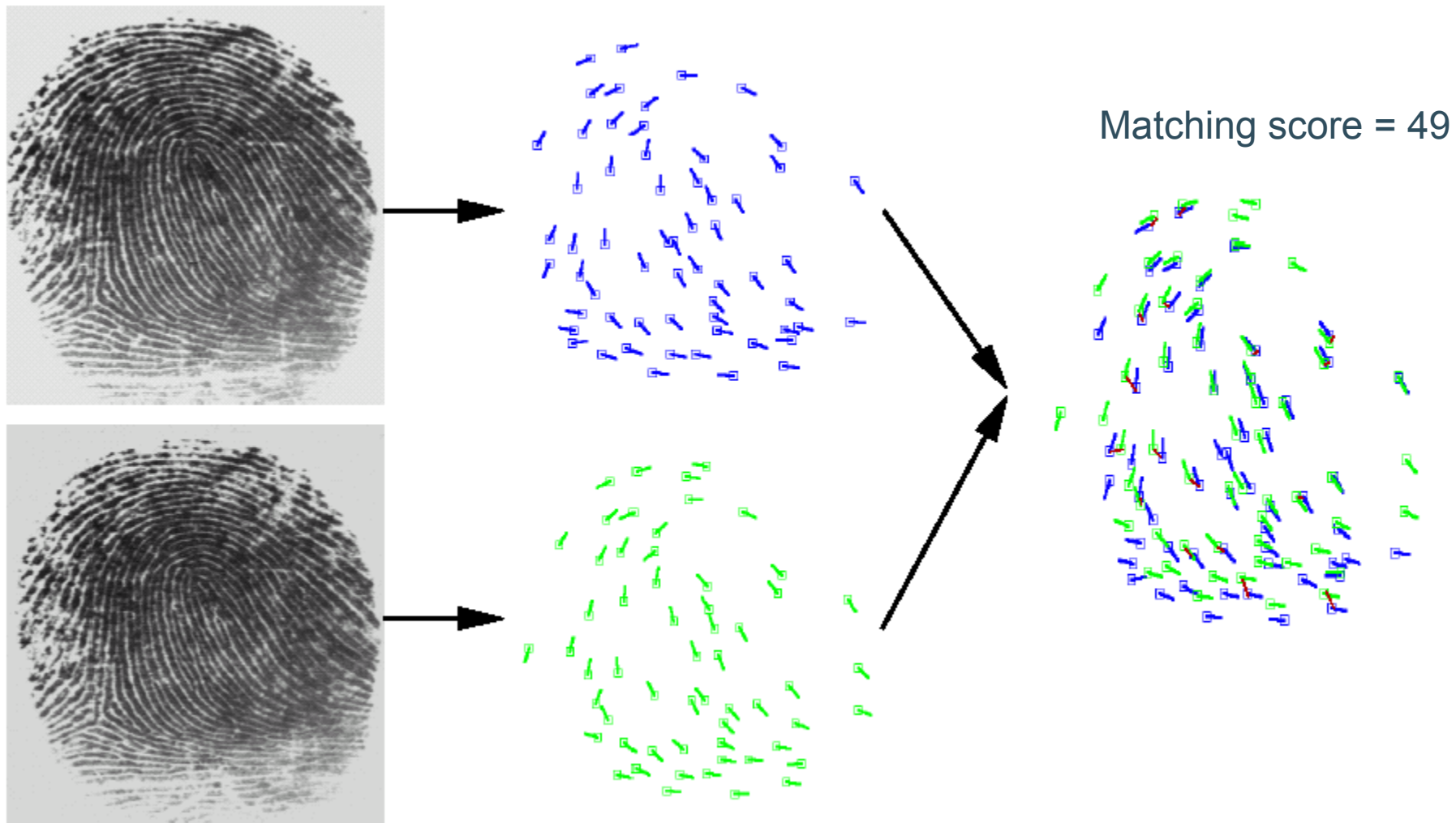
Elastic matching



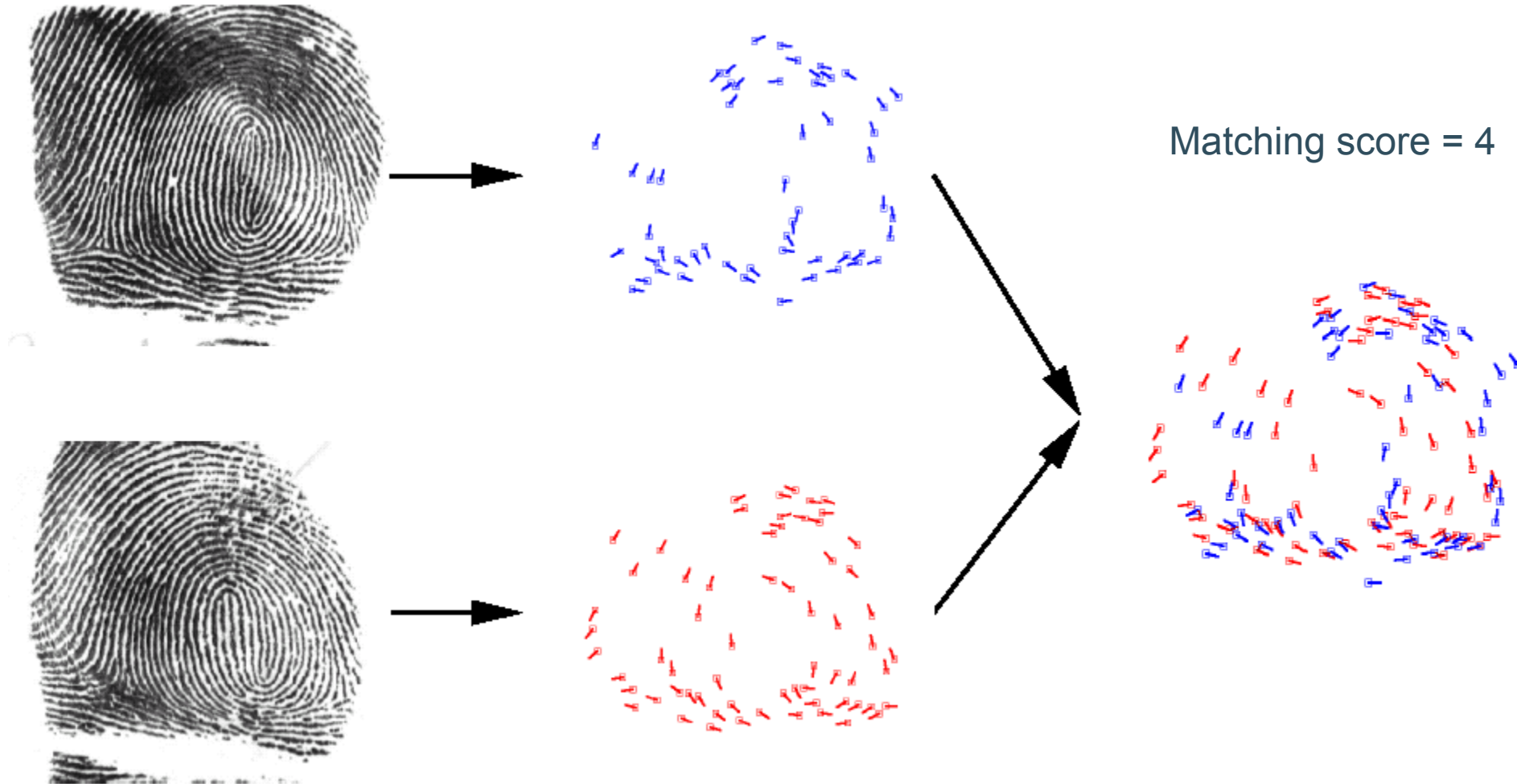
Matching: result



Matching same FP

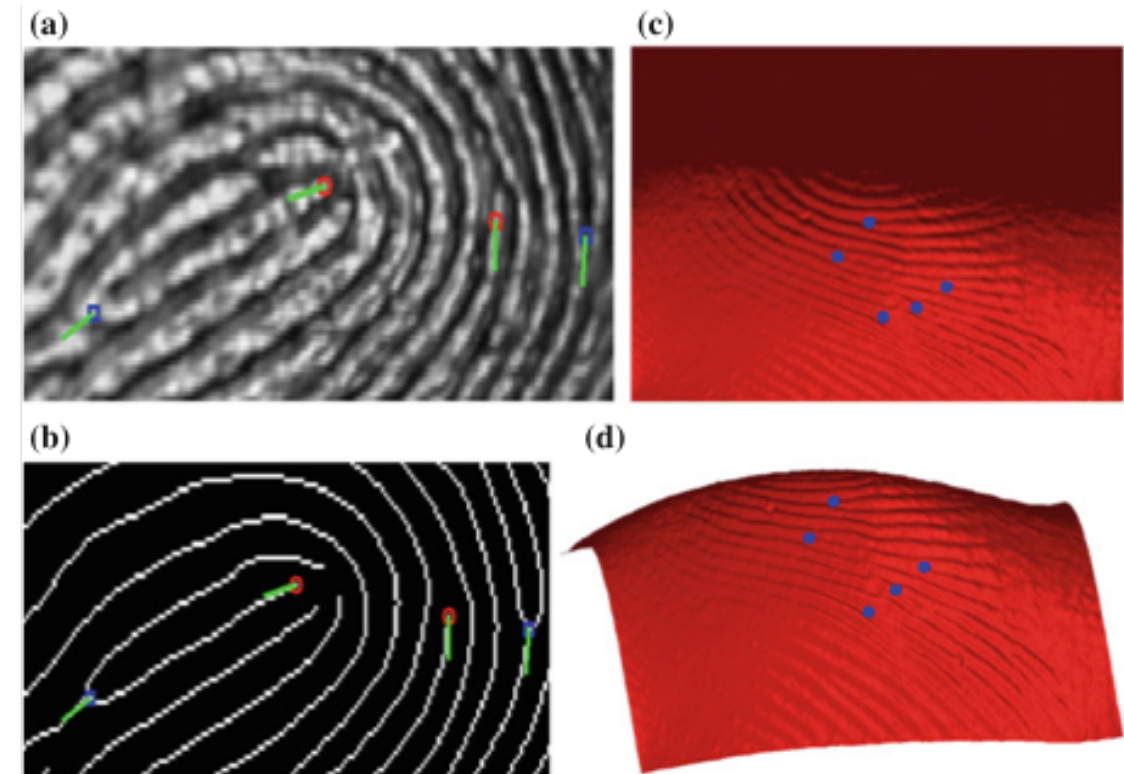
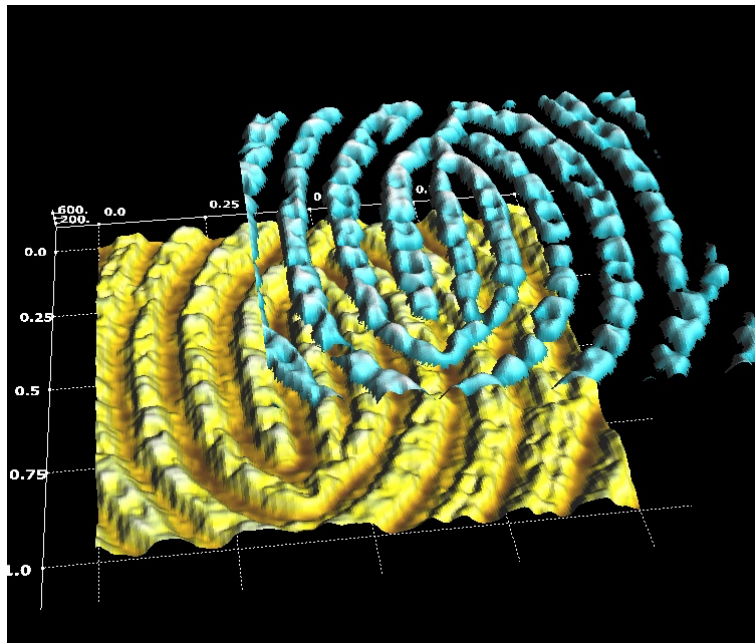


Matching different FPs



3D FP minutiae matching

- Extension of point matching to 3D



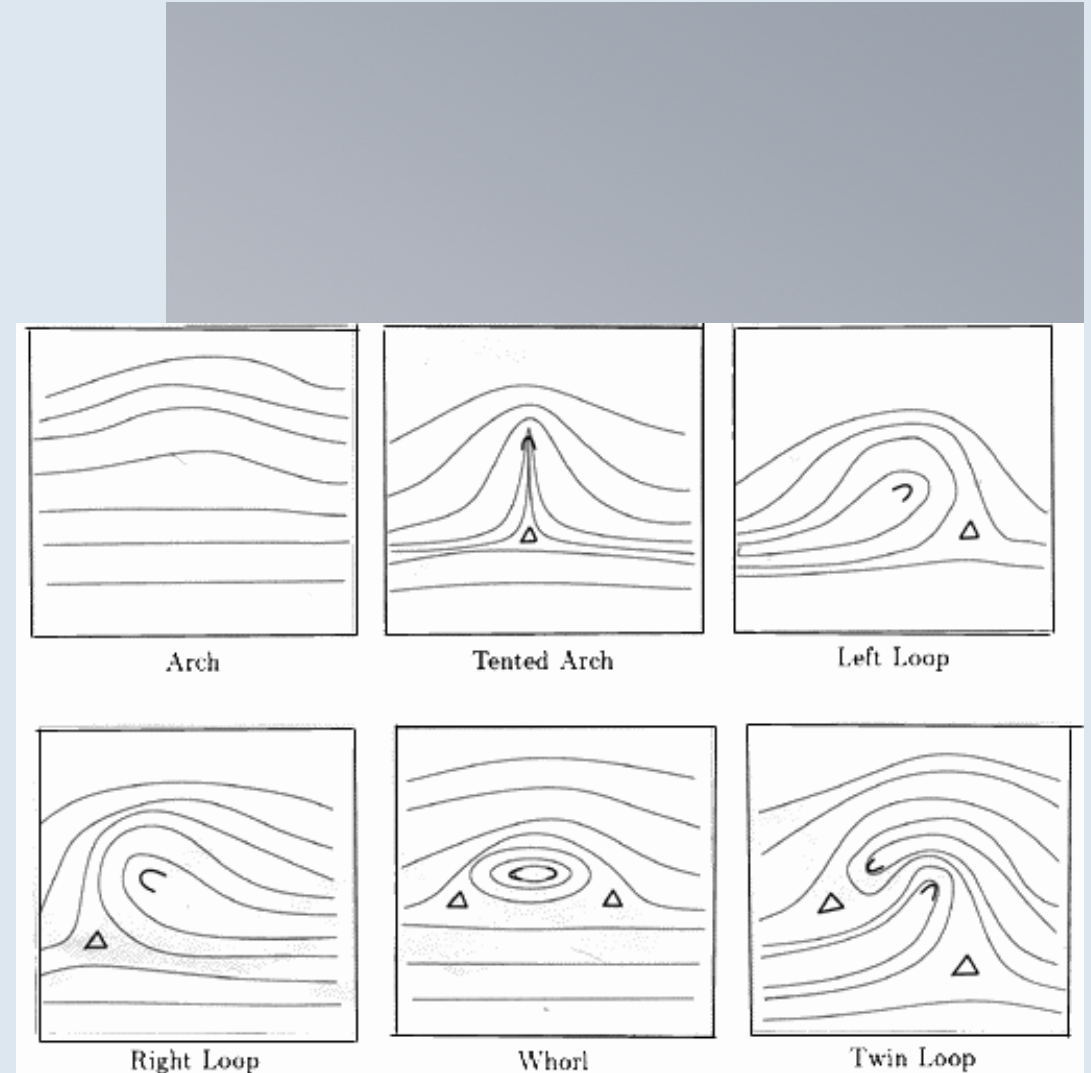
Global versus Local Minutiae Matching

- Local minutiae matching
 - comparing two fingerprints according to local minutiae structures only
 - local structures are characterized by attributes that are invariant with respect to global transformation (e.g., translation, rotation, etc.) and therefore are suitable for matching without any a priori global alignment.
- Matching fingerprints based only on local minutiae arrangements relaxes global spatial relationships which are highly distinctive and therefore reduce the amount of information available for discriminating fingerprints.
- Global versus local matching trade-off:
 - simplicity, low computational complexity, and high distortion-tolerance (local matching)
 - high distinctiveness (global matching).

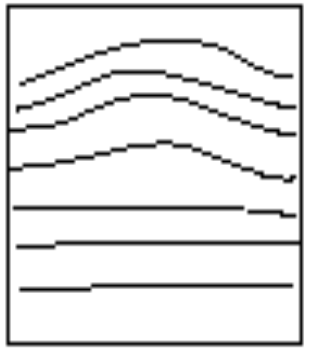
Global versus Local Minutiae Matching

- The benefits of both local and global matching can be obtained by implementing **hybrid** strategies that **perform a local structure matching followed by a consolidation stage**.
- The local structure matching allows to quickly and robustly determine pairs of minutiae that match locally (i.e., whose neighbouring features are compatible) and derive from them one or more candidate alignments for T and I.
- The consolidation is aimed at verifying if and to what extent local matches hold at global level.
 - Hough
 - Ransac
- See assignment 2: minutiae-based fingerprint recognition

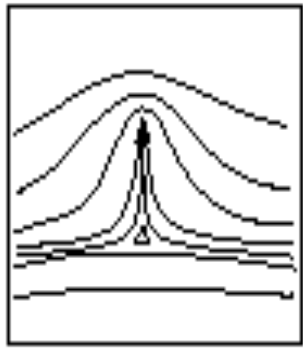
Fingerprint classification



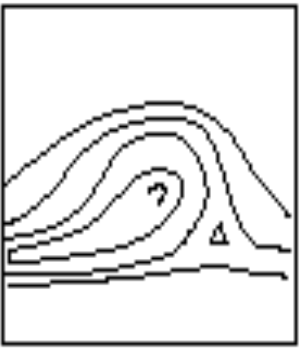
Fingerprint Classification



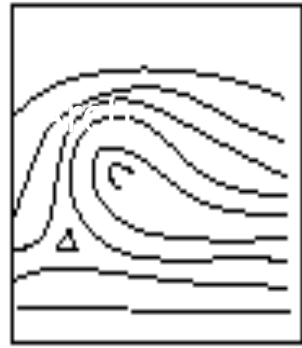
Arch



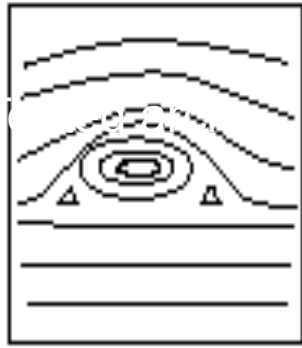
Tented Arch



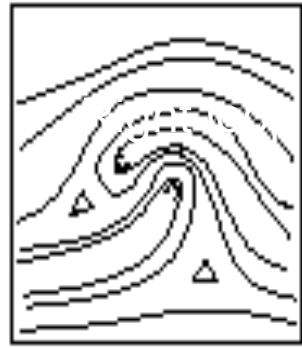
Left Loop



Right Loop



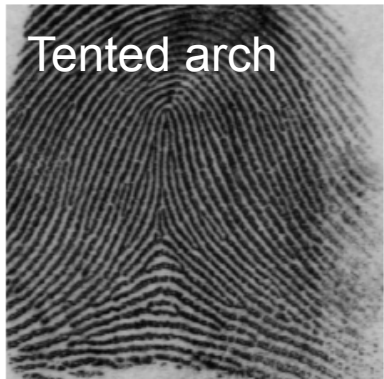
Whorl



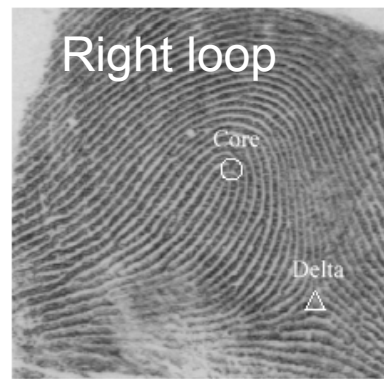
Twin Loop



Arch



Tented arch



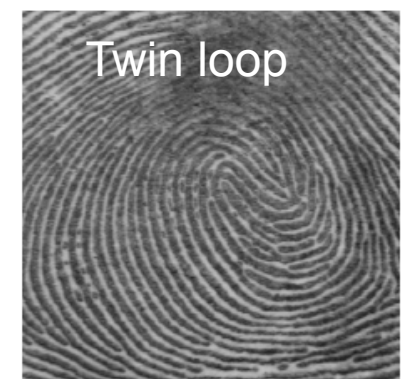
Right loop



Left loop



Whorl



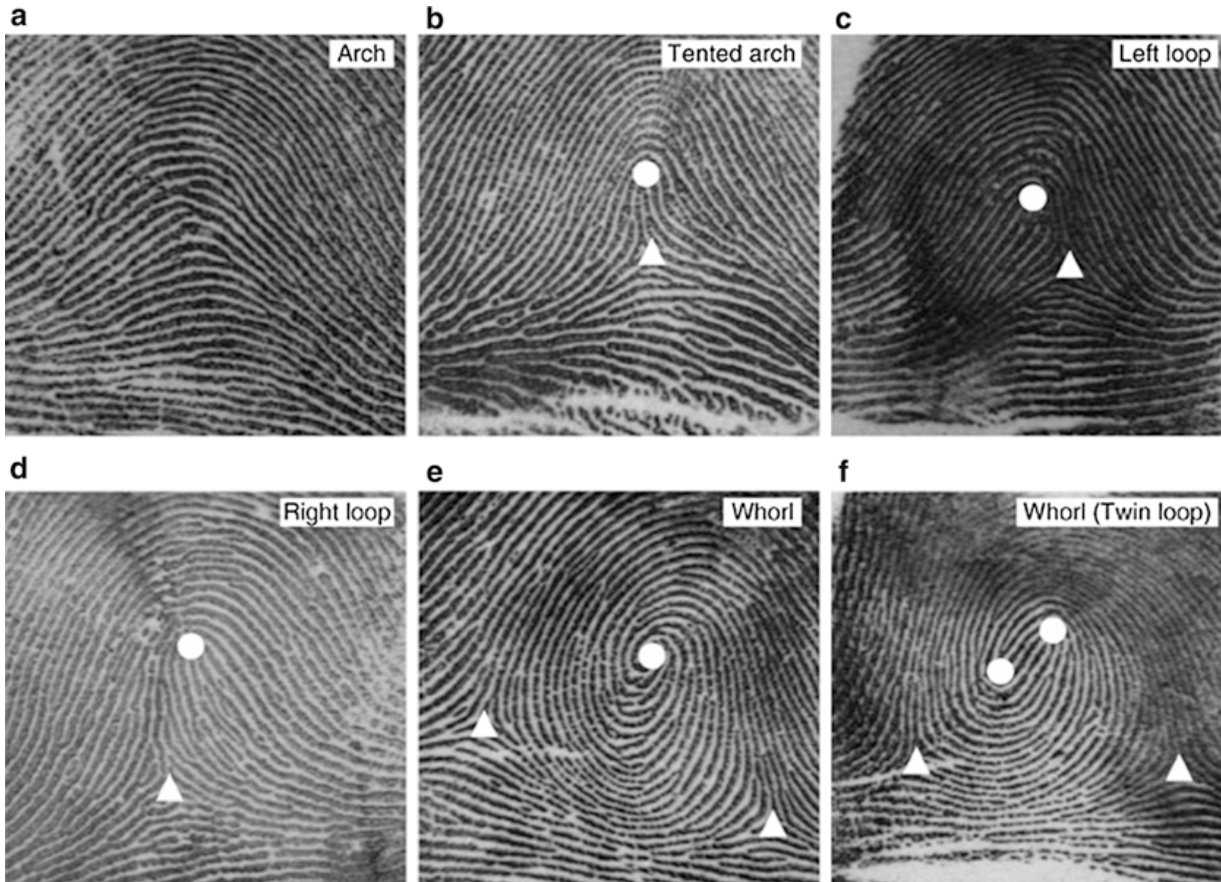
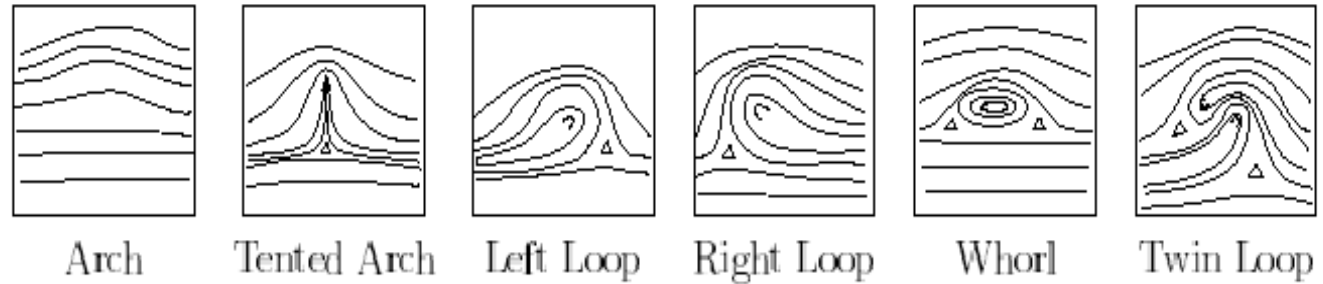
Twin loop

Left loop

Whorl

Twin loop

Fingerprint Classification

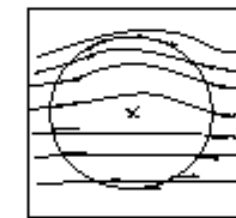


Core = topmost point in innermost ridge

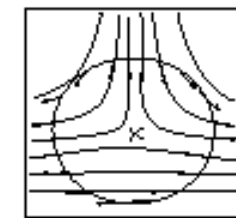
Delta = tri-radial point with three ridges radiating from it

Fingerprint Classification

- Direction field
- Smooth Direction field (till classification succeeds)
- Locate Singular Points:
Poincare Index = summing up the changes
in direction angle around a closed curve
around a point



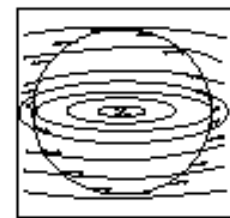
Ordinary point
 0°



Delta point
 -180°



Core point
 180°



Double-core point
 360°

Singular point detection

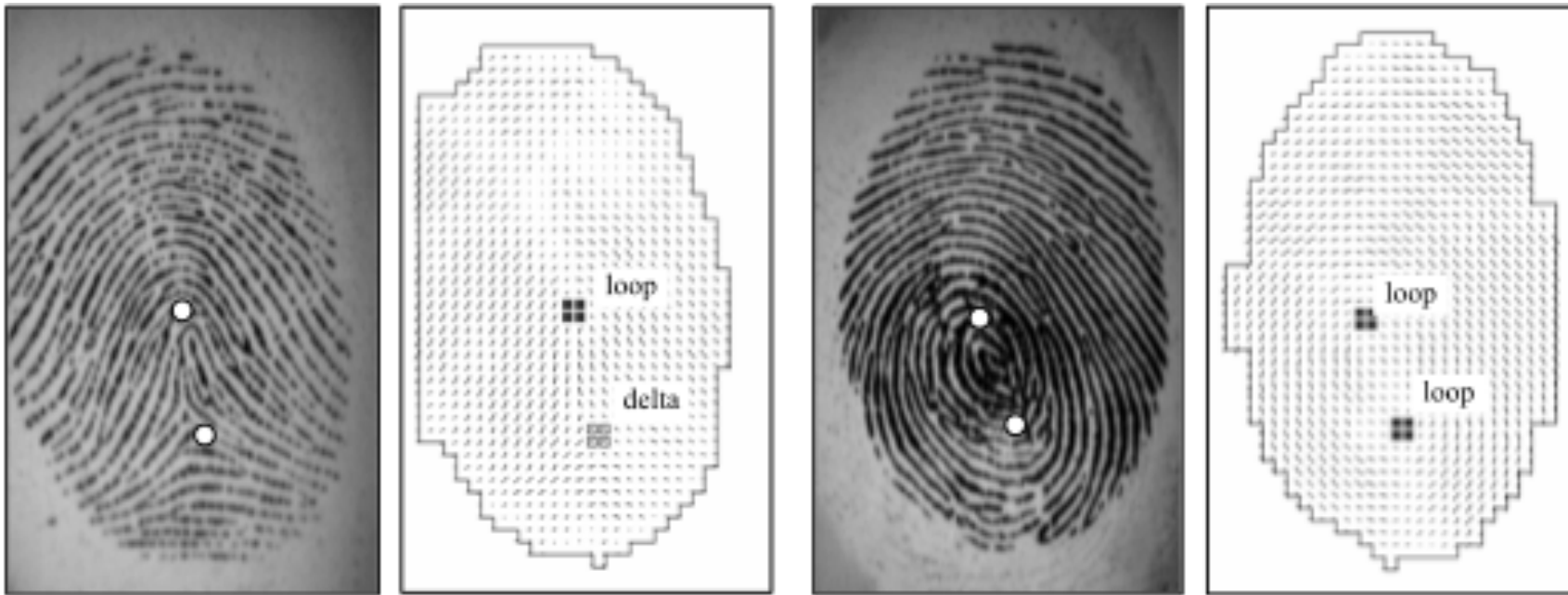
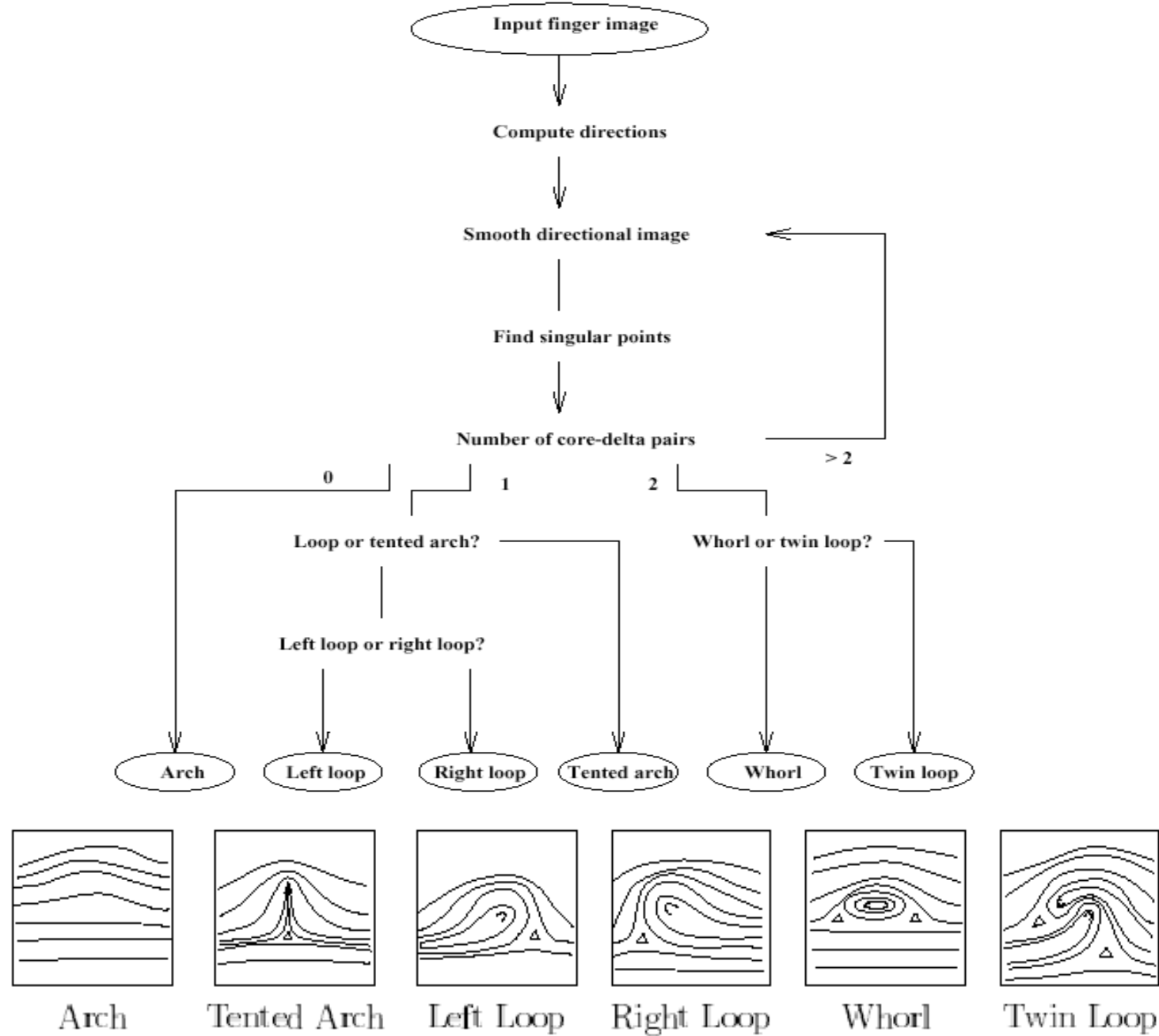
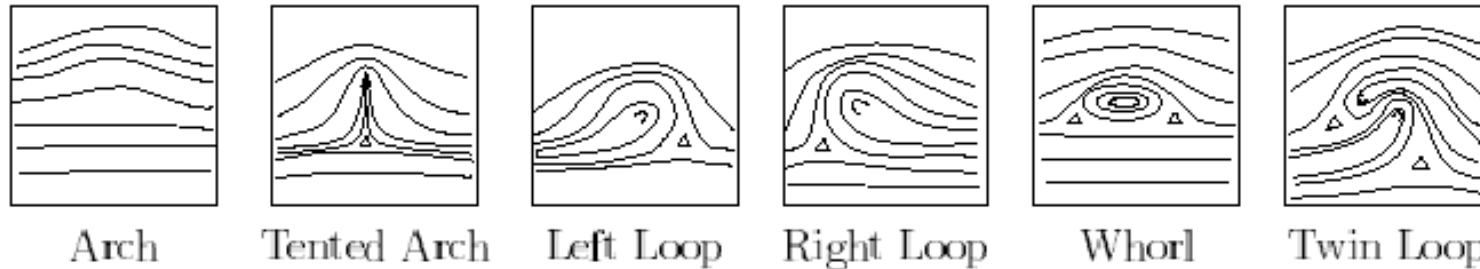


Figure 3.20. Singularity detection using Poincaré index. The elements whose Poincaré index is 180° (loop) or -180° (delta) are enclosed by small boxes. Usually, more than one point (four points in these examples) is found for each singular region: hence, the center of each singular region can be defined as the barycenter of the corresponding points. Note that the position of the loop singularities is slightly moved toward the borders because of the local smoothing of the orientation image.



Multilevel Classification and Matching

1. Determine Fingerprint Class (Arch, Loop, ...)



2. Constrain further using ridge density (between cores and deltas)
3. Perform Minutiae based matching

FP evaluation

Benchmarking

- A benchmark is defined by a **database** and an associated **testing protocol**.
- The protocol defines:
 - the subsets of images that can be used for training and testing,
 - the pair of images that have to be compared,
 - the performance metrics to be used and how they must be computed.
- Collecting fingerprint databases is expensive and prone to human errors.
- Using exactly the same benchmark is essential to compare the performance of different algorithms.

History of Fingerprint Benchmarking

- NIST (National Institute of Standards and Technology)
 - Good for FP classification and inked/latent FP
- Fingerprint Verification Competition (FVC)
 - FVC'2000
 - FVC'2002
 - FVC'2004
 - FVC'2006
 - FVC Ongoing
- NIST public Proprietary Fingerprint Test (I, II, III)

FVC'2000 Database

	Sensor Type	Image Size	Set A (w×d)	Set B (w×d)	Resolution
DB1	Low-cost Optical Sensor	300×300	100×8	10×8	500 dpi
DB2	Low-cost Capacitive Sensor	256×364	100×8	10×8	500 dpi
DB3	Optical Sensor	448×478	100×8	10×8	500 dpi
DB4	Synthetic Generator	240×320	100×8	10×8	About 500 dpi

Table II. The four FVC2000 databases.

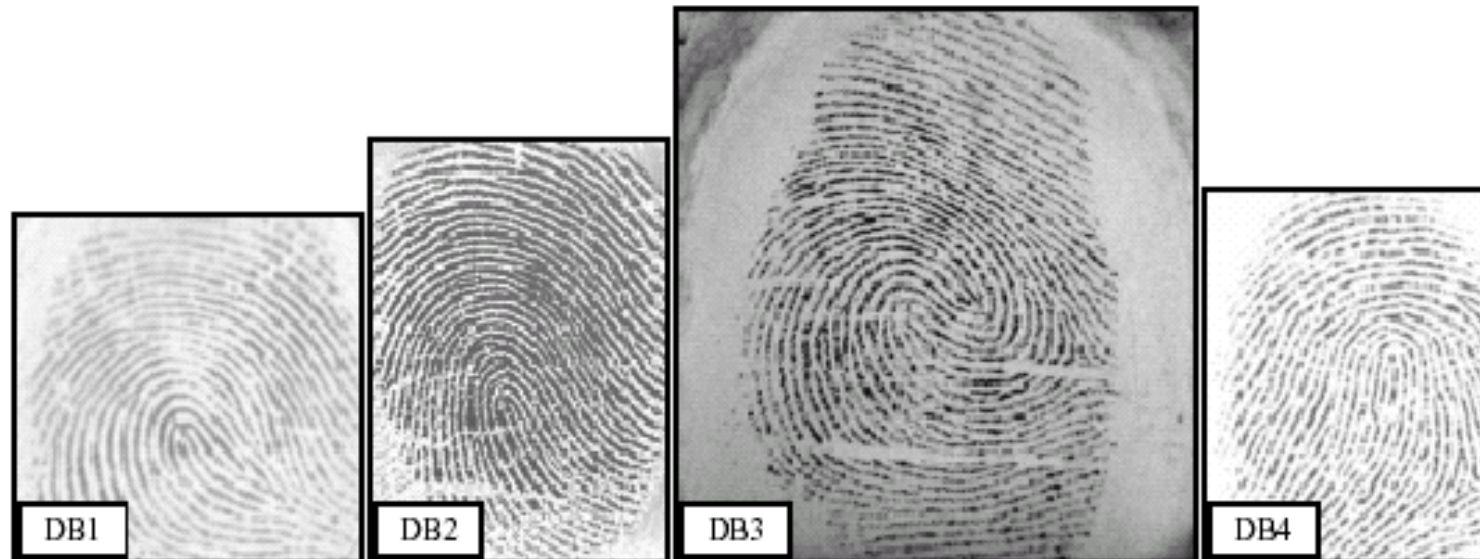


Figure 1. Sample images taken from DB1, DB2, DB3 and DB4. In order to show the different image size of each database, the four images are reported at the same scale factor.

Competition	Number of databases	Size of each Database: A - Evaluation set B - Trainin set	Notes
FVC2000 Maio et al. (2002a)	4	A: 100×8 B: 10×8	<ul style="list-style-type: none"> - Volunteers are mainly unhabituated students. - Two sessions, no quality check. - Low/Medium difficulty (DB1, DB2, DB4); Medium/High difficulty (DB3).
FVC2002 Maio et al. (2002b)	4	A: 100×8 B: 10×8	<ul style="list-style-type: none"> - Volunteers are mainly unhabituated students. - Three sessions, no quality check. - Voluntarily exaggerated perturbations: displacement, rotation, wetness and dryness. - Low difficulty (DB1, DB2, DB3, DB4).
FVC2004 Maio et al. (2004) Cappelli et al. (2006)	4	A: 100×8 B: 10×8	<ul style="list-style-type: none"> - Volunteers are mainly unhabituated students. - Three sessions, no quality check. - Voluntarily exaggerated perturbations: distortion, wetness and dryness. - Medium difficulty (DB1, DB2, DB3, DB4).
FVC2006 BioLab (2007)	4	A: 140×12 B: 10×12	<ul style="list-style-type: none"> - Heterogeneous population also includes unhabituated manual workers and elderly people. No quality check. - The final datasets were selected from a larger database by choosing the most difficult fingerprints according to a quality index. - High difficulty (DB1), Medium difficulty (DB3), Low difficulty (DB2, DB4).

	DB1	DB2	DB3	DB4
FVC2000	2.30%	1.39%	4.34%	3.38%
FVC2002	0.20%	0.17%	0.63%	0.16%
FVC2004	1.61%	2.32%	1.34%	0.81%
FVC2006	5.88%	0.05%	1.59%	0.39%

Table 4.3. Average accuracy (EER) of the three best performing algorithms over the different FVC databases. A direct comparison across the different competitions is not possible due to the use of databases of unequal difficulty.

Table 1.2 Summary of contact-based fingerprint image databases in public domain

Impression type	Name of database	No. of subjects	No. of images	Image resolution
Latent	NIST Special Database 27-latent	258	2580	800 × 768
	IIIT-D Multi-sensor Optical and Latent Fingerprint (MOLF)-DB4	100	4000	Variable
	IIIT-D Multi-sensor Optical and Latent Fingerprint (MOLF)-DB5	100	1600	1924 × 1232
	NIST Special Database 10-plain	N/A	5520	832 × 768
	NIST Special Database 14-plain	13,500	27,000	N/A
Rolled	NIST Special Database 27-rolled	258	2580	800 × 768
	NIST Special Database 29-rolled	216	2160	N/A
	CASIA-Fingerprint V5	500	20,000	328 × 356
	CASIA Fingerprint Image Database for Testing Version 1.0	500	20,000	328 × 356
	NIST Special Database 300	888	8871	N/A
	IIIT-D Multi-sensor Optical and Latent Fingerprint (MOLF)-DB1	100	4000	352 × 544
	IIIT-D Multi-sensor Optical and Latent Fingerprint (MOLF)-DB2	100	4000	258 × 336
	IIIT-D Multi-sensor Optical and Latent Fingerprint (MOLF)-DB3	100	1200	1600 × 1500
	IIIT-D Multi-sensor Optical and Latent Fingerprint (MOLF)-DB3_A	100	4000	variable
	FVC2000-DB1	N/A	880	300 × 300
	FVC2000-DB2	N/A	880	256 × 364
	FVC2000-DB3	N/A	880	448 × 478

Table 1.2 (continued)

Impression type	Name of database	No. of subjects	No. of images	Image resolution
Flat	FVC2000-DB4	N/A	880	240 × 320
	FVC2002-DB1	N/A	880	388 × 374
	FVC2002-DB2	N/A	880	296 × 560
	FVC2002-DB3	N/A	880	300 × 300
	FVC2002-DB4	N/A	880	288 × 384
	FVC2004-DB1	N/A	880	640 × 480
	FVC2004-DB2	N/A	880	328 × 364
	FVC2004-DB4	N/A	880	288 × 384
	FVC2006-DB1	N/A	1800	96 × 96
	FVC2006-DB2	N/A	1800	400 × 560
	FVC2006-DB4	N/A	1800	288 × 384
	NIST Special Database 29-plain	216	2160	N/A
	NIST Special Database 34—Plain and Rolled fingerprints	10	N/A	N/A
	NIST Special Database 300	888	8787	N/A

Common mistakes in evaluating performance

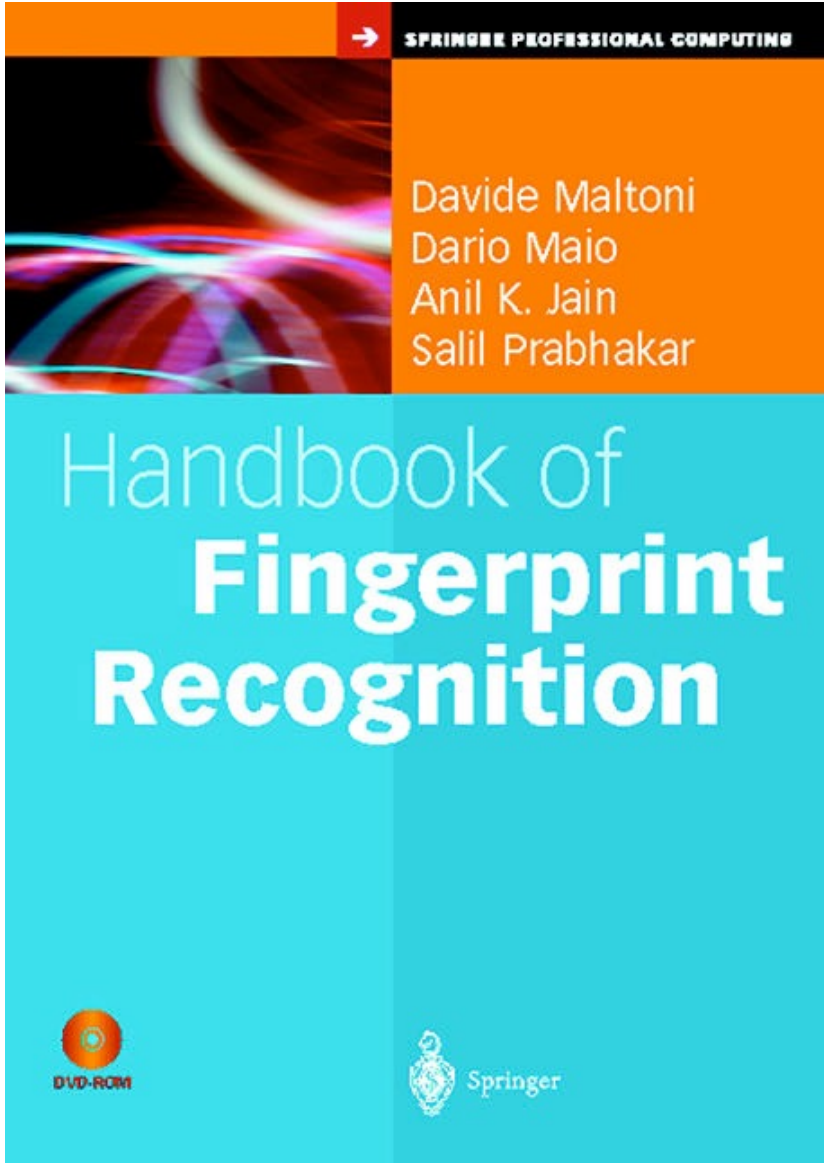
- Avoid using the same dataset for training, validating, and testing an algorithm.
- Do not compute performance on a very small dataset, and in particular abstain from claiming that a system has a very low error rate when the errors have been measured over a small dataset; if possible, report statistical significance of the results (e.g., confidence intervals).
- Avoid “cleaning” the database by removing samples that are either “rejected” or mis-classified by the system; in principle, by iteratively removing the fastidious samples, one could reach any desired level of accuracy.
- Do not conclude that the accuracy of a system is better than that of a competing system when they were evaluated over different datasets.
- Do not hide the weak points of an algorithm, but document its failures.

What is the best algorithm for matching fingerprints?

- The performance of a fingerprint recognition method involves **a trade-off** among different indicators:
 - accuracy (e.g., FMR and FNMR), efficiency (enrolment time, verification time), scalability to 1:N identification, template size, memory requirement, and so on.
- Different applications have **different performance requirements**.
 - For example, an application may prefer a fingerprint matching algorithm that is lower in accuracy but has a small template size over an algorithm that is more accurate but requires a large template size; specific constraints are also imposed by system security related issues).
- Since results on FVC benchmarks are often reported as FMR/FNMR values of the entire fingerprint recognition system developed, it is practically impossible to understand if an advancement in performance is due to a specific matching technique or is in large part due to a minor change in an existing feature extraction method.
- The only way to objectively compare fingerprint matchers is to start from the same set of features (i.e., the set of minutiae for minutiae based matchers). FVC-onGoing (2009) is being organized with such an aim.

To minutiae or not-minutiae?

- Most of the fingerprint matching approaches introduced in the last 4 decades are minutiae- based.
- One of the reasons to expect minutiae-based algorithms to perform well is the sheer amount of research done on this approach.
- Non-minutiae features are now receiving substantial interest: new methods based on local texture, ridge geometry, ridge spatial relationship and pores have been proposed in conjunction with minutiae matching.
- The integration of approaches relying on different features seems to be the most promising way to significantly improve the accuracy of fingerprint recognition systems.
- Global (and rigid) minutiae matching which was the main approach in the past, is being often replaced by two-phase approaches, that initially matches local portions of the fingerprint (e.g., local minutiae structures) and then consolidates the matching at global level. This allows a reduction in the computational complexity, and if the consolidation stage is designed appropriately, it also reduces the adverse effects of distortion. However, robust alignment remains a difficult task in fingerprints as compared to other biometrics such as iris or face.
- The world-wide large scale deployment of fingerprint systems demands a new generation of accurate and highly interoperable algorithms; therefore the development of minutiae-only matching algorithms (i.e., compliant with ISO/IEC 19794–2 (2005) and its future evolution) will not be abandoned for a long time.



FP relevance

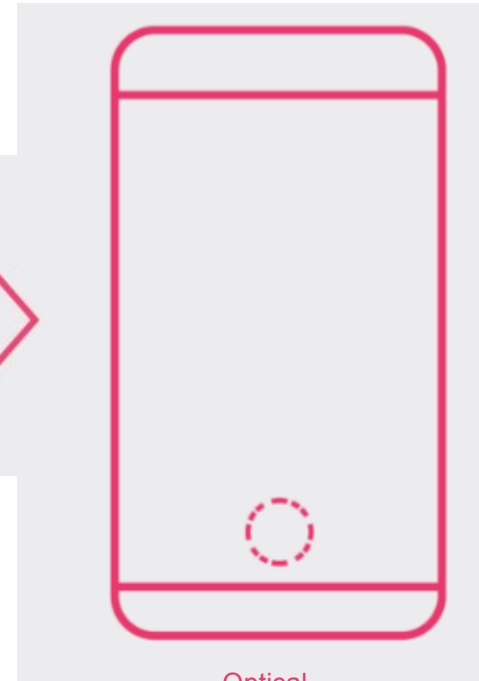
Research & Development Projects

Dedicated sensor



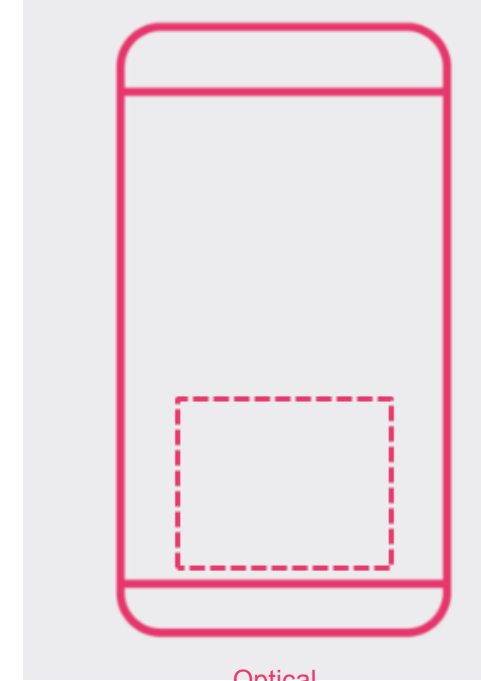
Available since 2014

Hot zone under-display



Ambition to enter the growing under-display market

Large area under-display



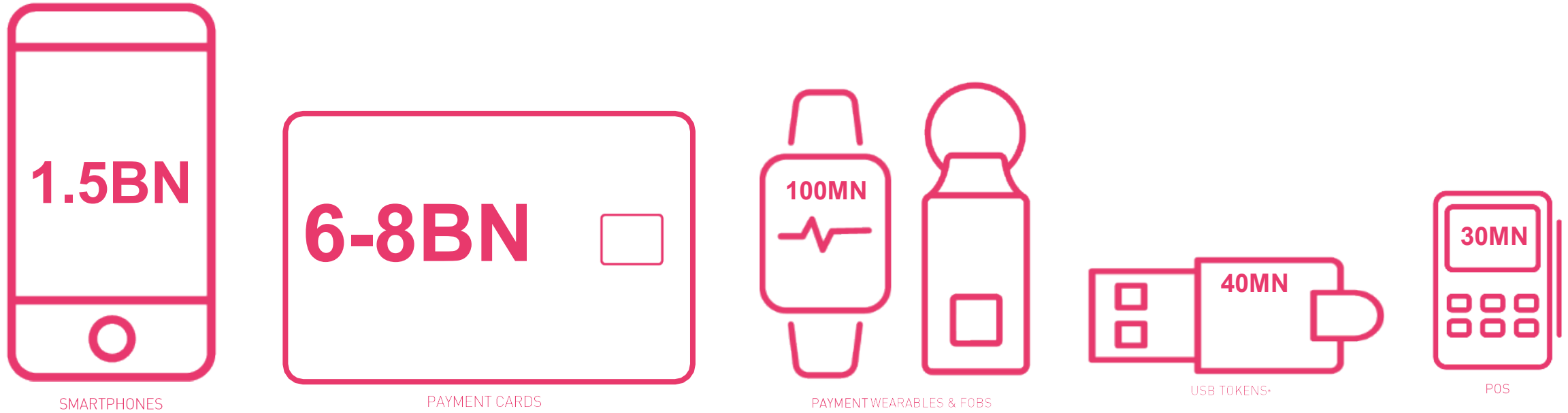
Under development

Full under-display



Under development

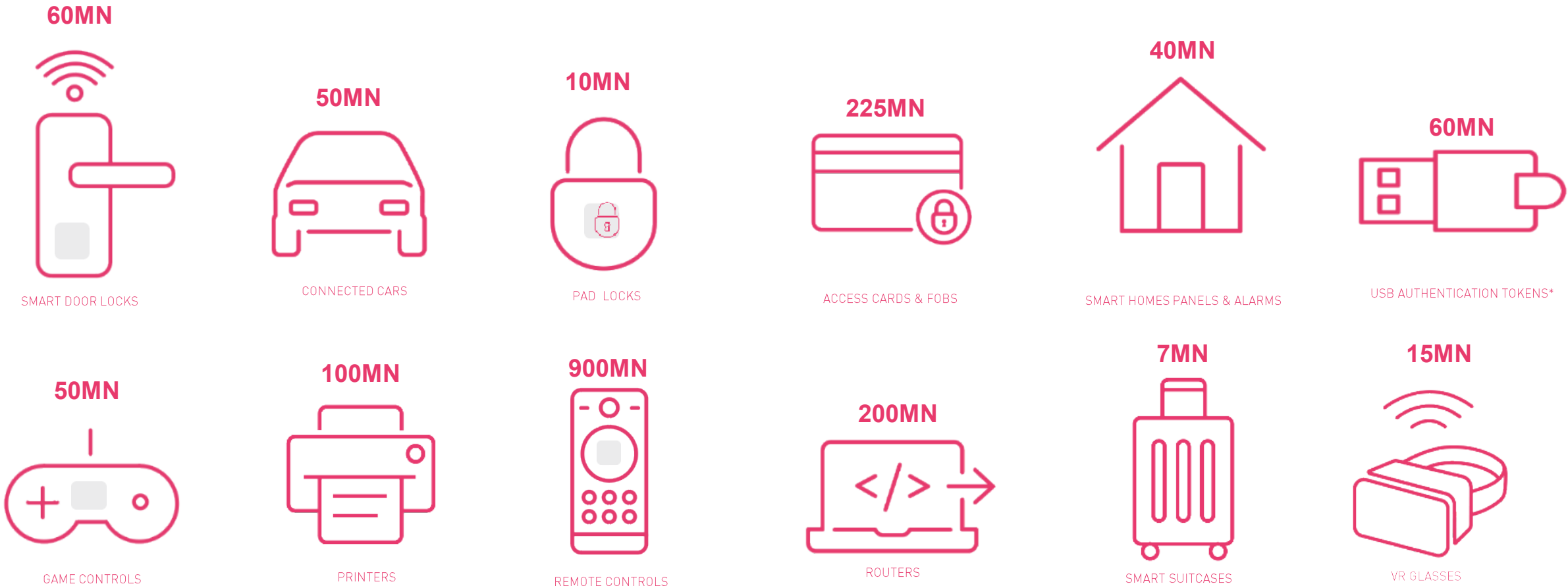
Market potential for personal payment devices



Fingerprints™ estimates on shipments based on various industry sources

* Some of these tokens can be used for cryptocurrency, as well as authentication of online payment but more logical access

Market potential for personal Access devices

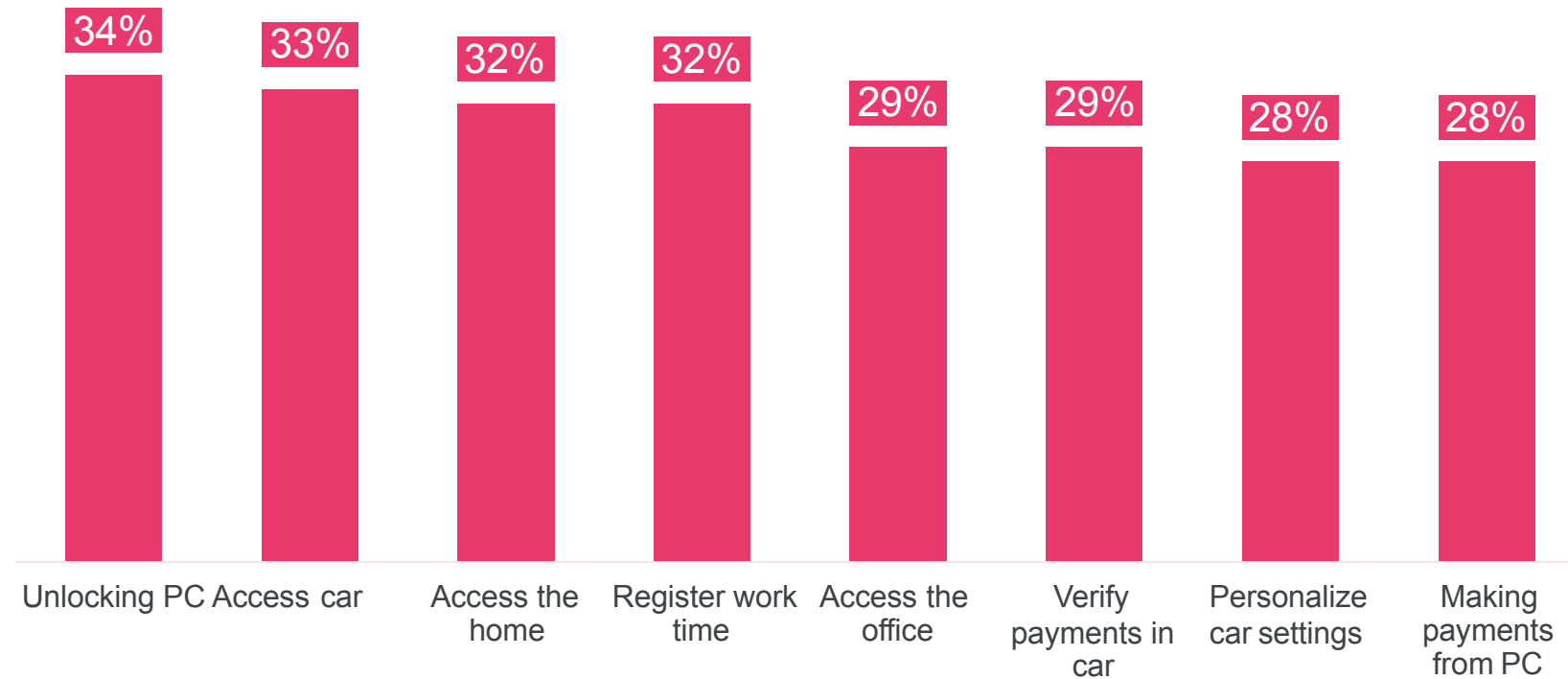


Fingerprints™ estimates on shipments based on various industry sources

* Used for logical access and access to e.g. cryptocurrency

CONSUMERS WANT BIOMETRICS *TO ACCESS THEIR THINGS!*

CONVENIENT - NO NEED TO BRING KEY
OR REMEMBER PIN OR PASSWORD
HIGHER SECURITY
MODERN



From what you know today, for what type of bank cardholders would you provide fingerprint recognition cards

SOURCE Fingerprints™ in collaboration with Kantar TNS. Base: 4,000 online consumers in China, India, UK, USA.